

1 Lecture 17. Instability and Buckling

1.1 Introduction

The *structural instability*, or stability loss, is listed in Lecture 14 as one of the possible *failure modes* characterizing a civil structure. By contrast with the material failure, extensively studied in the previous lectures, which is predicted using the equations of motion written on the initial, undeformed configuration, the prediction of the instability requires the equation of motion to be formulated on the deformed configuration of the structure. Consequently, it can be concluded that the structural instability is primarily due to geometry of the deformation. Since the deformed configuration is not known in advanced, obtaining a solution of the equations of motion is not a trivial task and frequently encounter mathematical difficulties. The generality of the motion equations are often reduced in the engineering practice to static equilibrium equations, by accepting the quasi-static nature of the loading and considering a slow application. Altrue, the *dynamic method* provides a general definition of the instability phenomenon, the *static method*, a *more simpler method*, is able to correctly obtain results for the case of *conservative forces*. Mane of the static loads considered in the structural investigations are of this nature. The classical theory of structural stability refers to the investigation of the elastic buckling of columns and frames, an extremely important subject for any structural practitioner. The inelastic behavior, in the classical sense, extends the elastic behavior of the material over the proportionality limit, complicating somehow the theoretical approach. Over the years the stability study developed in mane directions covering not only columns and frames, but all sorts of structural components as: plates, shells and three-dimensional bodies. The material behavior considered addressed also more complicated, but more closely related to reality, constitutive laws as: viscoelastic, visco-elasto-plastic and recently the theory of damage.

The subjects treated in this lecture, intend to familiarize the novice student of *Mechanics of Materials* with the instability phenomenon (definition, assumptions, limitations), by insisting first on the *elastic behavior of the column* and later commenting on its inelastic behavior. If someone is interesting to extend his/hers knowledge base to the instability of more complicated material behavior or structural geometry, a very extensive technical literature is available in English and Roumanian languages. Some of these remarkable textbooks and handbooks are listed in the reference section of this testbook.

1.2 Stability of Equilibrium. Definition.

The study of the deformable body, in general, and of the linear beam, in particular, required always the *equilibrium* and function of the aborted subject some form of *equilibrium equations* are written (global equilibrium, part equilibrium, infinitesimal equilibrium etc.). A new concept related with the equilibrium, the *stability of equilibrium*, is introduced by analyzing the equilibrium of a rigid sphere, as pictured in Figure 17.1, on three different surfaces.

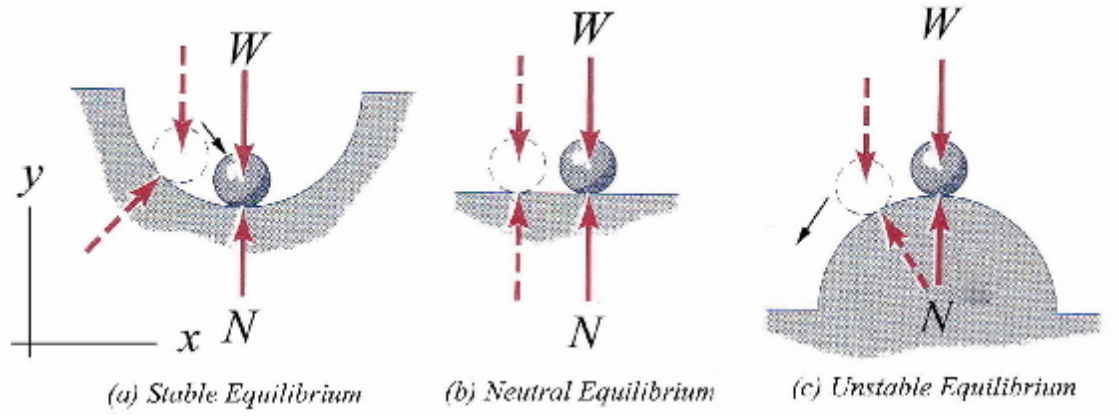


Figure 17.1 Stability of Equilibrium

In all three *configurations* (a), (b) and (c), the sphere is in equilibrium and consequently, the equilibrium equations are satisfied:

$$\sum F_x = 0 \quad (1)$$

$$\sum F_y = W + N = 0 \quad (2)$$

$$\sum M = 0 \quad (3)$$

Despite the fact that the equilibrium is satisfied the *stability of the equilibrium* is different in all three configurations illustrated. In the *configuration (a)* any change of the sphere position in the neighborhood of the original position will be only temporary and the sphere will move back regaining the original position. This configuration is called *stable equilibrium*. Contrary, the *configuration (c)* is called *unstable equilibrium* and is characterized by a movement of the sphere away from its initial position. The *configuration (b)* is called *neutral equilibrium*, because the sphere has not any tendency to move from or toward its initial position.

The general definition of stability, due to the theoretical contribution of Lyapunov in 1892, is stated as: "a system is stable if a small change in its input leads to a small change in the response of the output". Translated in terms more appropriated for the structural engineering a *structure is stable if a finite change in the initial conditions (input) does not produced an infinite change in the solution (response)*. Otherwise, the structure is *unstable*. Mathematically, the definition stated above is expressed as:

Definition 1 *If for an arbitrary positive number ϵ there exists a positive number δ such that every solution $v(t)$, obtained from the integration of the equation of motion, with initial value $v(t = t_0) \leq \delta$ satisfies the inequalities $v(t) \leq \epsilon$ for all times $t > t_0$.*

The static equilibrium being a particular case of the equation of motion, the time variable t loses its meaning and consequently, the condition of stability refers exclusively to the position of the equilibrium, as exemplify in the cases illustrated in Figure 17.1.

1.3 Buckling and Stability of Simple Systems

In the attempt to extend the fundamental concept of the stability equilibrium to more complicated systems, the simple system illustrated in Figure 17.2, containing some elastic components, is considered. This mechanical system is comprised of two members: (a) a *rigid member AB* and (b) a *linear elastic rotational spring*. The elastic rotational spring is attached at end A of the rigid member and is characterized by a constant rigidity k_θ . The entire system is subjected to a vertical compressive force P acting at end B of the rigid member, along the longitudinal axis x , and is assumed to conserve its orientation.

Considering as *initial equilibrium configuration* the vertical position of the rigid member AB, as shown in Figure 17.2.a, the possible configurations of the equilibrium stability are studied. The initial equilibrium configuration of the system is disturbed by laterally displacing the end B of the rigid member AB. A *new equilibrium configuration* is found as shown in Figure 17.2.b.

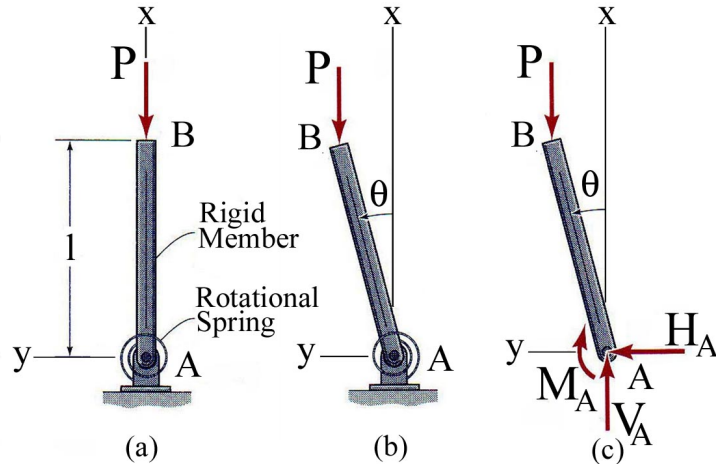


Figure 17.2 Column Buckling - Simple Example

The free-body diagram corresponding to the new equilibrium configuration is pictured in Figure 17.2.c. The equilibrium equations are:

$$\begin{aligned} \sum F_x &= 0 \rightarrow -P + V_A = 0 \rightarrow V_A = P \\ \sum F_y &= 0 \rightarrow H_A = 0 \\ \sum_A M &= 0 \rightarrow -P * l * \sin \theta + M_A = 0 \end{aligned} \quad (4)$$

The behavior of the linear elastic rotational spring during the deformation from the initial equilibrium configuration is characterized by the following relation:

$$M_A = k_\theta * \theta \quad (5)$$

Substituting equation (5) into the third equation of the equilibrium equations (4), this equation is recast as:

$$-P * l * \sin \theta + k_\theta * \theta = 0 \quad (6)$$

Consequently, the value of the load P , called *critical load* P_{cr} , required for the equilibrium expressed by equation (6) to exists, is calculated:

$$P = P_{cr} = \frac{k_\theta * \theta}{l * \sin \theta} \quad (7)$$

Conclusion 2 *The critical load P_{cr} depends on the variation of the rotation angle θ .*

Developing in power series the expression (7) and holding only the first three terms different than zero, the following approximation of the critical load P_{cr} is obtained:

$$P_{cr} \simeq \frac{1}{l}k_\theta + \frac{1}{6l}\theta^2 k_\theta + \frac{7}{360l}\theta^4 k_\theta \quad (8)$$

Since the initial equilibrium configuration, the vertical configuration, is represented by $\theta = 0$, the stability of the equilibrium is verify in the neighborhood of this equilibrium configuration and consequently, the critical load P_{cr} has a constant value:

$$P_{cr} = P_{cr}^0 = \frac{k_\theta}{l} = constant \quad (9)$$

By analogy with the equilibrium configurations of the sphere illustrated in Figure 17.1, the following equilibrium configurations are possible in the case of the simple mechanical system:

$$if \begin{cases} P < P_{cr}^0 \\ P = P_{cr}^0 \\ P > P_{cr}^0 \end{cases} \rightarrow \begin{matrix} \text{stable equilibrium} \\ \text{neutral equilibrium} \\ \text{unstable equilibrium} \end{matrix} \quad (10)$$

Similar conclusions are obtained if successive equilibrium configurations obtained varying the rotation angle θ are considered. The equation (10) can then be generalized for any rotation angle θ :

$$if \begin{cases} P < P_{cr}(\theta) \\ P = P_{cr}(\theta) \\ P > P_{cr}(\theta) \end{cases} \rightarrow \begin{matrix} \text{stable equilibrium} \\ \text{neutral equilibrium} \\ \text{unstable equilibrium} \end{matrix} \quad (11)$$

A suggestive graphical representation of the equilibrium stability, called the *equilibrium diagram*, is employed. *The plot represents the relation between the variation of the compressive load P and the lateral deflection of the system*, represented in this case by the rotation angle θ . The equilibrium diagram is illustrated in Figure 17.3.

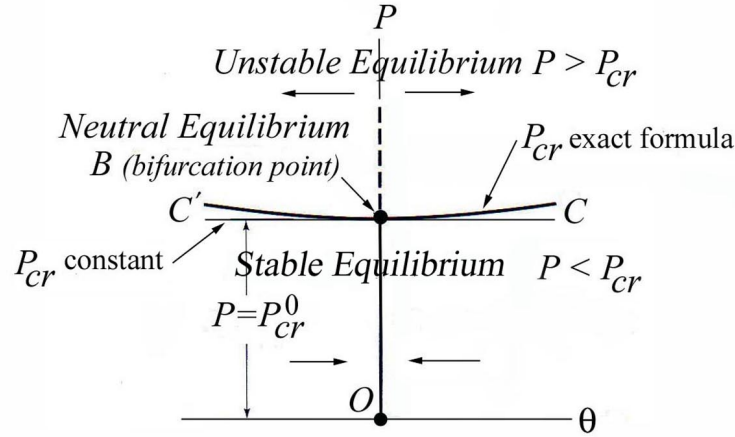


Figure 17.3 Equilibrium Diagram - Simple Example

Conclusion 3 (a) All three equilibrium configurations discussed above (stable, neutral and unstable) are easily identified in the equilibrium diagram. All tendencies of the system to move are indicated on Figure 7.3 with directional arrows;

(b) As long as $P < P_{cr}$ the equilibrium is stable and the system tends to return to its initial equilibrium position, the vertical position, described by $\theta = 0$;

(c) The neutral equilibrium is marked by the bifurcation point B and corresponds to $P = P_{cr}^0$;

(d). New equilibrium configurations are found along the curves BC and BC', constructed using the exact expression (7) of the critical load P_{cr} ;

(e). For values of the compressive force $P > P_{cr}$ any small lateral displacement will make the system unstable;

(f) The values of the critical load $P_{cr}(\theta)$ represents the frontier delineating the stable and unstable equilibrium configurations.

In the technical literature the *loss of stability* and the critical load P_{cr} are also called *buckling* and *buckling load*, respectively. For structural engineering the value of the first critical load P_{cr}^0 , corresponding to the first equilibrium configuration, is always important.

1.4 Buckling of Elastic Columns

By definition, in the American technical literature, a linear structural member located in a vertical position and loaded by a compressive axial force is called *column*. By its important structural role played in any civil structure, the behavior of the column subjected to a compressive force is an issue of importance. In this section problems related to the *elastic buckling* of the ideal linear column are presented and discussed.

1.4.1 The Ideal Pin-Ended Column. Euler Buckling Load.

The knowledge accumulated from the analysis of the rigid column shown in Figure 17.2 is extended to the study of the stability of the *elastic columns*. This study begins with the classical example of the *ideal pin-ended linear column* illustrated in Figure 17.4. This type of column is referred, in the technical literature, as *the Ideal Euler Column*.

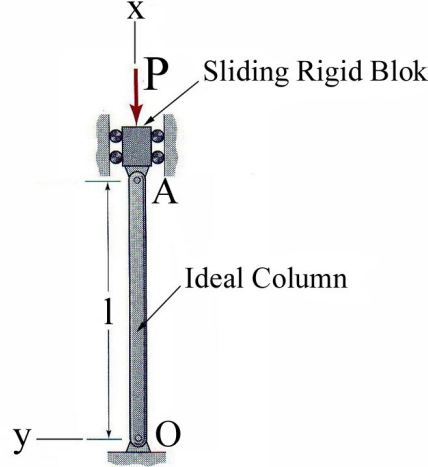


Figure 17.4 Ideal Pin-Ended Column

The column OA , a perfect straight beam developed without any imperfections along the x coordinate axis, is made of a *homogeneous linearly elastic material* (follows the Hook's constitutive law) and freely rotates at both ends, O and A , without friction. The axis x is passing through the centroids of *constant cross-section* of the column OA . Additionally, the cross-section is assumed to be symmetrical about the vertical plane xy of the column. The compressive force P is transferred to the column at end A through a sliding rigid bloc.

Conclusion 4 *Restricting the cross-section of the column to be constant and symmetrical about xy plane implies that the lateral deformation (buckling) of the column can manifest only in the symmetry plan Oxy . The buckling out side of the symmetry plane Oxy is restrained.*

As long the intensity of the compressive force P is less than the critical force P_{cr} , $P < P_{cr}$, the equilibrium configuration is a *straight line* and *the equilibrium is stable*. Consequently, as known from study of the axial deformation, *Lecture 5* of the first volume, the consequence of the applied compressive force P is an uniformly distributed normal stress σ_x acting on the column cross-section and a shortening Δ of the column length l :

$$\sigma_x = \frac{P}{A} \quad (12)$$

and

$$\Delta = \frac{P * L}{E * A} \quad (13)$$

where E is the elastic modulus of the material and A is the constant area of the column cross-section.

However, if the intensity of compressive force P is increased until the critical force P_{cr} is reached, $P = P_{cr}$, the equilibrium become *neutral equilibrium* and an additional configuration, a *buckled shape*, as shown in Figure 17.5, is possible. This value of force P corresponds to the bifurcation point on the equilibrium diagram.

Conclusion 5 *The concept of the existence at neutral equilibrium, the bifurcation point, of double configuration, straight and buckled, corresponding to the same compressive force $P = P_{cr}$ is very powerful theoretical concept extensively used in the theoretical derivations concerned with the stability of elastic columns.*

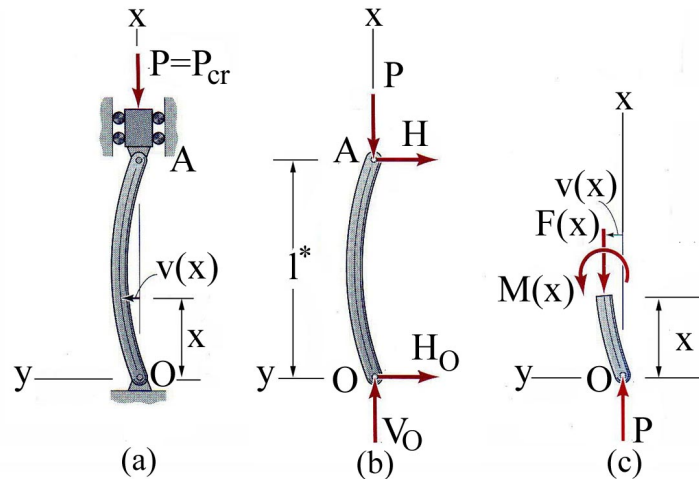


Figure 17.5 Ideal Pined Ended Column - Buckling Shape

The *critical compressive load* P_{cr} and the *buckled shape* of the column are determined using the *equilibrium on the deformed configuration* illustrated in Figure 17.5.c. This is a *static method of investigating the stability of the column* and is called the *Equilibrium or Bifurcation method*. The reactions pertinent to both column ends, shown in Figure 17.5.b, are obtained solving the the equilibrium equations as:

$$\begin{aligned} \sum F_x &= 0 \rightarrow -P + V_O = 0 \rightarrow V_O = P \\ \sum F_y &= 0 \rightarrow -H_O - H_A = 0 \rightarrow H_A = H_O = 0 \end{aligned} \quad (14)$$

The internal resultants, the axial force $F(x)$ and bending moment $M_z(x)$, acting on a cross-section located at distance x from the point O , are obtained writing the static equilibrium equations of the inferior part of the column, isolated from the entire length l , as shown in Figure 17.5.c:

$$\sum F_x = 0 \rightarrow -F(x) + P = 0 \quad (15)$$

$$\sum_O M_z = 0 \rightarrow -M_z(x) - F(x) * v(x) = 0 \quad (16)$$

Remark 6 *The negative sense of the bending moment $M_z(x)$ follows the beam convention described in the first volume.*

Solving the equations (15) and (16) the axial force $F(x)$ and the bending moment $M_z(x)$ in a cross-section are expressed as:

$$F(x) = P \quad (17)$$

$$M_z(x) = -P * v(x) \quad (18)$$

Considering valid the small deflection assumption, the functional relation between the bending moment $M_z(x)$ and the curvature $k(x)$ of the lateral deflection curve $v(x)$ considered during the study of the bending induced deflection remains valid:

$$k(x) = \frac{1}{\rho(x)} \simeq \frac{dv(x)^2}{dx^2} = \frac{M_z(x)}{E * I_z} \quad (19)$$

where E and I_z are the material elastic modulus and cross-section moment of inertia, respectively.

Substituting equation (18) into equation (19) the following *second-order homogeneous differential equation* is obtained:

$$E * I_z * v''(x) + P * v(x) = 0 \quad (20)$$

Dividing equation (20) by $E * I_z$, this is recast as:

$$v(x)'' + k^2 * v(x) = 0 \quad (21)$$

where:

$$k^2 = \frac{P}{E * I_z} \quad (22)$$

Conclusion 7 *The differential homogeneous equation (22) has constant coefficients due to the fact that the equilibrium corresponds to neutral equilibrium configuration,, the bifurcation point, where the compressive force $P = P_{cr}$ is constant.*

The general solution of equation (22) is:

$$v(x) = C_1 * \sin(k * x) + C_2 * \cos(k * x) \quad (23)$$

The integration constants C_1 and C_2 are obtained by applying the boundary conditions at both ends, O and A , of the column:

- at point O ($x = 0$):

$$v(x = 0) = 0 \rightarrow C_1 * \sin(k * 0) + C_2 * \cos(k * 0) = 0 \quad (24)$$

- at point A ($x = l$):

$$\begin{aligned} v(x = l) = 0 &\rightarrow v(x = l) = 0 \\ &\rightarrow C_1 * \sin(k * l) + C_2 * \cos(k * l) = 0 \end{aligned} \quad (25)$$

From equation (24) it results:

$$C_2 = 0 \quad (26)$$

Substituting $C_2 = 0$ into equation (25):

$$C_1 * \sin(k * l) = 0 \quad (27)$$

and consequently, two solutions are possible for C_1 :

$$(1) \text{ if } \sin(k * l) \neq 0 \text{ then } C_1 = 0 \quad (28)$$

or

$$(2) \text{ if } \sin(k * l) = 0 \text{ then } C_1 \neq 0 \quad (29)$$

Conclusion 8 (a) If solution (28), $C_1 = 0$, is true, it results that the deflection $v(x)$ is zero along the entire length of the column and the equilibrium is realized on the undeformed configuration;

(b) If solution (29), $C_1 \neq 0$, is true, then $\sin(k * l) = 0$, and the deflection $v(x) \neq 0$. In this case the equilibrium is realized on the undeformed configuration. The trigonometric equation $\sin(k * l) = 0$, (29), has a infinite number of solutions:

$$k = k_n = \frac{n * \pi}{l} \quad n = 1, 2, \dots \quad (30)$$

and for each value of n a new k_n is obtained. The magnitude of the integration constant C_1 remained undetermined, indicating that only the buckling shape is known. It is supposed that the value of C_1 is a small value in order to respect the small deformation assumption previously made. Finally, the deflection $v(x)$ is obtained substituting the expression of k_n into equation (23):

$$v(x) = v^n(x) = C_1 * \sin(k_n * x) = C_1 * \sin\left(\frac{n * \pi}{l} * x\right) \quad (31)$$

Each deflection curve $v_n(x)$ obtained by assigning $n = 1, 2, \dots$ is called buckling mode. The buckling modes represent a family of sinusoidal curves. From equation (22) the critical load P_{cr}^n corresponding to each buckling mode is calculated:

$$P_{cr}^n = E * I_z * k_n^2 = E * I_z * \left(\frac{n * \pi}{l} \right)^2 = E * I_z * \left(\frac{\pi}{l_b^n} \right)^2 \quad (32)$$

where

$$l_b^n = \frac{1}{n} * l \quad (33)$$

is called buckling length corresponding to the n -th buckling mode.

The first two buckling modes the corresponding critical loads and buckling length are:

$$\begin{aligned} n &= 1 \rightarrow v^1(x) = C_1 * \sin\left(\frac{1 * \pi}{l} * x\right) \\ &\rightarrow P_{cr}^1 = E * I_z * \left(\frac{\pi}{l}\right)^2 = E * I_z * \left(\frac{\pi}{l_f^1}\right)^2 \rightarrow l_f^1 = l \\ n &= 2 \rightarrow v^2(x) = C_1 * \sin\left(\frac{2 * \pi}{l} * x\right) \\ &\rightarrow P_{cr}^2 = E * I_z * \left(\frac{\pi}{\frac{1}{2}l}\right)^2 = E * I_z * \left(\frac{\pi}{l_f^2}\right)^2 \rightarrow l_f^2 = \frac{l}{2} \end{aligned} \quad (34)$$

where $l_f^1 = l$ and $l_f^2 = \frac{l}{2}$ are the buckling lengths corresponding to buckling modes 1 and 2, respectively.

The undeformed configuration and first two buckling modes are illustrated in Figure 17.6.

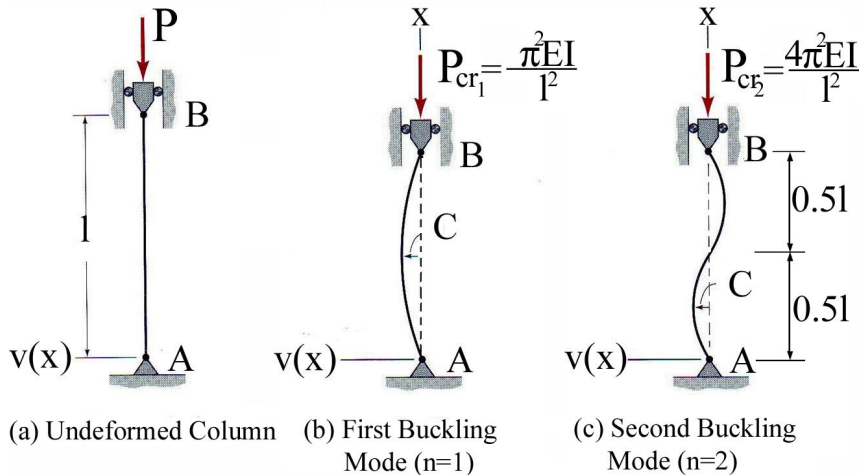


Figure 17.6 Ideal Pined-Ended Column - Buckling Modes

Remark 9 *Theoretically, a large number of buckling modes are possible to be obtained, but from practical point of view just the first buckling mode ($n = 1$), also called the fundamental buckling mode, and its corresponding critical load P_{cr}^1 are important. The first critical load, P_{cr}^1 , called Euler buckling load in recognition of the Swiss mathematician Leonhard Euler contribution to the stability problem, is denoted:*

$$P_{cr}^1 = E * I_z * \left(\frac{\pi}{l}\right)^2 \quad (35)$$

The normal stress σ_{cr} acting on the column cross-section when $F(x) = -P_{cr}$, called *Euler buckling stress*, is calculated from equation (35):

$$\sigma_{cr}(x) = \frac{F(x)}{A} = -\frac{P_{cr}}{A} = -\frac{E * I_z * \left(\frac{\pi}{l}\right)^2}{A} = \frac{E * \pi^2}{\left(\frac{l}{r_z}\right)^2} \quad (36)$$

where $(r_z)^2 = \frac{I_z}{A}$ is the gyration radius.

The ratio $\frac{l}{r_z}$, denoted λ , is called *slenderness*:

$$\lambda = \frac{l}{r_z} \quad (37)$$

Substituting the slenderness expression λ into equation (36) the critical normal stress σ_{cr} becomes:

$$\sigma_{cr} = \frac{E * \pi^2}{\lambda^2} \quad (38)$$

Geometrically, the variation of the critical normal stress σ_{cr} with the slenderness λ is a *hyperbola*, called *Euler's hyperbola*. The validity of the critical normal stress σ_{cr} formula (38) is restricted by the constitutive law considered employed, *the Hook's Law*, to an upper-bound value equal to the *proportionality stress limit* of the material σ_y^0 :

$$\sigma_{cr} = \frac{E * \pi^2}{\lambda^2} \leq \sigma_y^0 \quad (39)$$

The resulting slenderness limit λ_0 is obtained from the limit of inequality (39)

$$\lambda_0 = \pi * \sqrt{\frac{E}{\sigma_y^0}} \quad (40)$$

Remark 10 The expression (40) indicates that for a slenderness $\lambda \geq \lambda_0$ the critical normal stress is always $\sigma_{cr} \leq \sigma_y^0$. For structural steel ($E = 200\text{GPa}$, $\sigma_y^0 = 250\text{MPa}$) and aluminium ($E = 73\text{GPa}$, $\sigma_y^0 = 410\text{MPa}$) the slenderness limit λ_0 are 89 and 42, respectively. The variation of the critical stress $\sigma_{cr}(\lambda)$ with the slenderness λ is expressed as:

$$\sigma_{cr}(\lambda) = \begin{cases} \sigma_y^0 & \text{if } \lambda < \lambda_0 \\ \frac{E * \pi^2}{\lambda^2} & \text{if } \lambda \geq \lambda_0 \end{cases} \quad (41)$$

Remark 11 The variation of the Euler critical stress σ_{cr} for steel ($E = 200\text{GPa}$, $\sigma_y^0 = 250\text{MPa}$, $\lambda_0 = 89$) and aluminium ($E = 73\text{GPa}$, $\sigma_y^0 = 410\text{MPa}$, $\lambda_0 = 42$) function of the slenderness λ are illustrated in Figure 17.7

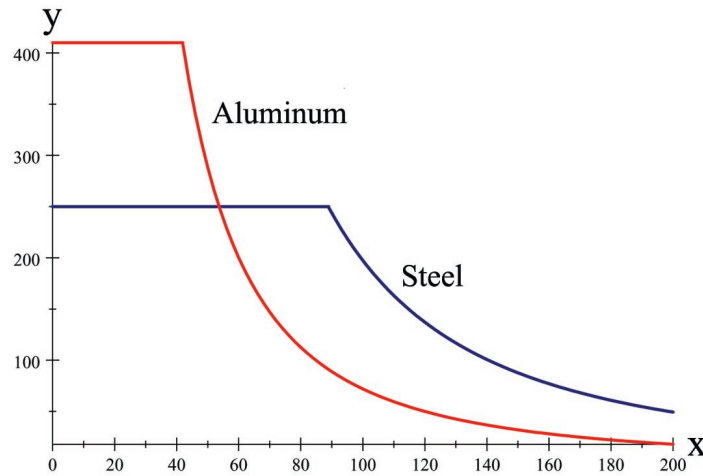


Figure 17.7 Ideal Pin-Ended Column - Critical Stress σ_{cr}

1.4.2 Buckling of Columns with Other Rigid Support Conditions

The methodology employed to determine the buckling modes and critical load of pin-ended column, namely *the static method*, can be extended to any type of column as long the buckling shape can be anticipated. In this section a general method of determining the buckling characteristics of a ideal linear column is introduced and then, applied to some of the most frequently encounter supporting conditions.

1.4.2.1 Differential Equations of Beam-Column. The Second Order Theory. The equilibrium equations considering the undeformed configuration, extensively employed, are referred as the *first order theory*. When the equilibrium equations are written considering the deformed configuration, the theoretical derivations are known as the *second order theory*.

An ideal linear column, subjected to an axial compressive force P and a transversal load $p_n(x)$, is considered. An infinitesimal element, of length dx , is isolated from this buckled column (the deformed configuration) and pictured in Figure 17.8.a

Remark 12 (a) Two sets of three cross-sectional resultants (axial force, shear force and bending moment) are defined: (1) a set composed of cross-sectional resultants $F(x) = -P$, $V(x)$ and $M(x)$ acting on the cross-section of the undeformed configuration and (2) a set comprised of cross-sectional resultants $F_d(x)$, $V_d(x)$ and $M(x)$ acting on the cross-section of the deformed configuration. Both sets, illustrated in figures 17.8.a and 17.8.b, respectively, are used in the following discussion. The relations between the two sets of axial and shear forces are obtained by projecting the first set of forces on the directions of the second set of forces:

$$F_d = -P * \cos \theta - V * \sin \theta \simeq -P - V * \theta \simeq -P - V * v' \quad (42)$$

$$V_d = -P * \sin \theta + V * \cos \theta \simeq -P * \theta + V \simeq -P * v' + V \quad (43)$$

Remark 13 where $\theta(x)$ is the rotation angle of the cross-section located at distance x from the origin and $\tan \theta \simeq \sin \theta = \frac{dv}{dx} = v'$ and $\cos \theta \simeq 1$ are approximations valid when the small displacement assumption is considered.

(b) The variable x , indicating the cross-section position along the column longitudinal axis is dropped from the following formulae for clarity of writing, but is always implied.

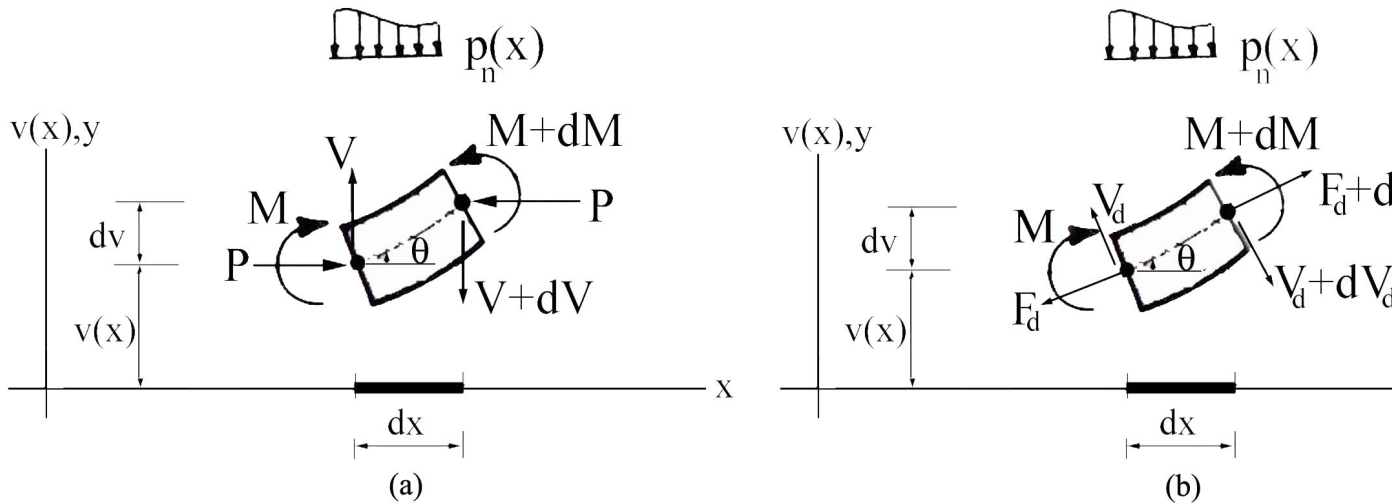


Figure 17.8 Equilibrium of the Infinitesimal Beam Element

First, the equilibrium of the infinitesimal element is written using the first set of cross-sectional resultants $F(x) = -P$, $V(x)$ and $M(x)$. The longitudinal force $F(x)$ is constant along the column length and equal with the compressive force P . For this reason only two equations are necessary to describe the equilibrium of the infinitesimal element dx :

$$\begin{aligned} \sum Y &= 0 \\ \rightarrow V - (V + dV) - p_n * dx &= 0 \end{aligned} \quad (44)$$

$$\begin{aligned} \sum M_{\text{right_section}} &= 0 \\ \rightarrow M - (M + dM) - P * dv + V * dx - p_n(x) * dx * \frac{dx}{2} &= 0 \end{aligned} \quad (45)$$

After algebraic manipulations and neglecting the product of infinitesimal quantities the following differential equations are obtained:

$$\frac{dV}{dx} = -p_n(x) \quad (46)$$

$$\frac{dM}{dx} + P * \frac{dv}{dx} - V = 0 \quad (47)$$

Remark 14 *The differential equation (47) differs from the differential equation established in Lecture 4 of the first volume, where the equilibrium on the undeformed configuration is considered, only by the existence of the term $P * \frac{dv}{dx}$. This term introduces the influence of the compressive force P .*

Substituting the expression of the shear force V obtained from equation (42) into equation (47) the differential relation between the bending moment M and the shear force V_d acting on the cross-section of the deformed configuration is obtained:

$$\begin{aligned} \frac{dM}{dx} + P * \frac{dv}{dx} - V_d - P * v' &= 0 \\ \rightarrow \frac{dM}{dx} &= V_d \end{aligned} \quad (48)$$

Remark 15 *The differential expression (48) indicates a functional similarity with the differential expression established from the equilibrium of the undeformed infinitesimal element.*

Considering equations (19) and (43), the dependence of the bending moment $M(x)$ and shear force $V(x)$ on the lateral displacement $v(x)$ is expressed:

$$M(x) = E * I_z * v''(x) \quad (49)$$

$$V(x) = V_d + P * v' = \frac{dM}{dx} + P * v' = E * I_z * v''' + P * v' \quad (50)$$

Differentiating once more equation (47), relatively to variable x , and then substituting equation (46) into it, the equation (47) becomes:

$$\frac{d^2 M}{dx^2} + P * \frac{d^2 v}{dx^2} + p_n(x) = 0 \quad (51)$$

Considering again valid the assumption of the small deformations, the moment-curvature relation (19) is substituted into equation (51):

$$E * I_z * \frac{d^4 v}{dx^4} + P * \frac{d^2 v}{dx^2} + p_n(x) = 0 \quad (52)$$

The equation (52) represents the *differential equation of the deflection curve $v(x)$ for an ideal column-beam subjected to a compressive force $P = \text{constant}$ and a transversal load $p_n(x)$* . The general solution is:

$$v(x) = v_0(x) + v_p(x) \quad (53)$$

where $v_0(x)$ and $v_p(x)$ are the solution of the *homogeneous differential equation* and the *particular* solution, respectively. The particular solution depends on the lateral load $p_n(x)$.

To determine the buckling behavior, the particular case $p_n(x) = 0$ is considered, and consequently, the differential equation (52) degenerates into a differential homogenous equation:

$$E * I_z * \frac{d^4 v}{dx^4} + P * \frac{d^2 v}{dx^2} = 0 \quad (54)$$

where $v(x) = v_0(x)$.

Denoting as before $k^2 = \frac{P}{E * I_z}$, the equation (54) is recast as:

$$\frac{d^4 v}{dx^4} + k^2 * \frac{d^2 v}{dx^2} = 0 \quad (55)$$

or

$$v^{IV} + k^2 * v'' = 0 \quad (56)$$

The solution of the homogenous differential equation (55) is:

$$v(x) = C_1 * \sin(k * x) + C_2 \cos(k * x) + C_3 * x + C_4 \quad (57)$$

where C_1 , C_2 , C_3 and C_4 are integration constants.

The expressions of the deflection curve $v(x)$, the first, second and third derivatives are obtained by successively differentiating expression (57):

$$\theta(x) \simeq v'(x) = \frac{d}{dx} v(x) = k * C_1 * \cos(k * x) - k * C_2 * \sin(k * x) + C_3 \quad (58)$$

$$v''(x) = \frac{d^2}{dx^2} v(x) = -k^2 * C_1 * \sin(k * x) - k^2 * C_2 * \cos(k * x) \quad (59)$$

$$v'''(x) = \frac{d^3}{dx^3} v(x) = -k^3 * C_1 * \cos(k * x) + k^3 * C_2 * \sin(k * x) \quad (60)$$

Substituting the above relations into (49) and (50):

$$M(x) = -k^2 * E * I_z * [C_1 * \sin(k * x) + C_2 * \cos(k * x)] \quad (61)$$

$$V(x) = E * I_z * [v''' + k^2 * v'] = E * I_z * k^2 * C_3 \quad (62)$$

The four integration constants, C_1, C_2, C_3 and C_4 , are determined recognizing the boundary conditions at the ends of the column. These conditions are of two kinds: (a) kinematic, v and θ , and (b) static, $M(x)$ and $V(x)$. The most usual encountered boundary conditions are:

$$\begin{array}{llll} \circ & \text{fixed end} & v & = 0 & \theta & = 0 \\ \circ & \text{pinned end} & v & = 0 & M & = 0 \\ \circ & \text{free end} & M & = 0 & V & = 0 \\ \circ & \text{fixed-sliding end} & \theta & = 0 & V & = 0 \end{array} \quad (63)$$

The *zero condition* expressed by equations (63) are obtained by particularizing the variable x to the position, $x = 0$ or $x = l$, of the boundaries in equations (58), (59), (49) and (50). Consequently, *a homogenous algebraic system of four equations containing the integration constants C_1, C_2, C_3 and C_4 as unknowns*, is obtained:

$$\Delta(k * l) * \tilde{C} = \tilde{0} \quad (64)$$

where $\tilde{C} = \begin{bmatrix} C_1 \\ C_2 \\ C_3 \\ C_4 \end{bmatrix}$ is the integration constants vector.

*For the homogenous algebraic system to have solutions outside of the trivial, zero, solution, the determinant of the matrix $\Delta(k * l)$ has to be equal to zero.*

$$\det [\Delta(k * l)] = 0 \quad (65)$$

The equation obtained by expanding the determinant is called the *characteristic equation*. Solving the characteristic equation (65) the buckling modes, buckling length and critical load are obtained. This exercise is practice in the following sections for a number of commonly encounter types of ideal column end restrains.

Remark 16 *Alltrue there are many equilibrium configurations and corresponding buckling modes, for structural engineers only the first buckling mode is of interest. In the following section only the first buckling mode and its corresponding characteristics, the buckling length and critical load, are calculated.*

1.4.2.2 Basic Assumptions Before a number of columns are investigated the main assumptions already employed, but losses between the lines, are emphasized. These assumptions are extremely important for a structural engineer because *they delimited the validity field of the developed formulae*. They are :

1. *The cross-section is constant along the entire length of the column and is symmetrical about the vertical plane xy of the column. The symmetry assumption is the grantor of the fact that buckling manifests only in the plane of symmetry xy ;*
2. *The column is an linear column characterized by a straight axis x and without any fabrication imperfections;*
3. *The material is elastic, linear and isotropic (Hook 's Law);*
4. *The small deformation assumption is valid and reflected in the proportionality relation between the cross-sectional bending moment $M(x)$ and the second derivative of the deflection $v(x)$ as: $M(x) = E * I_z * v''(x)$;*
5. *The compressive force P retains its vertical orientation during the deformation and at the bifurcation point (neutral equilibrium);*
6. *The influence of the shear force on the deflection is neglected;*
7. *The concept of the existence of two configurations, undeformed and deformed, corresponding to the same compressive force P_{cr} is valid. Without this concept the entire buckling calculations become obsolete.*

1.4.2.3 Column with One Fixed End Columns having one end fixed are relatively frequent encountered in structural engineering. Example of this type of ideal columns are illustrated in Figure 17.9. Function of the conditions characterizing the other end, the column is called: fixed-free (fig 17.9.a), fixed-fixed (fig 17.9.b) and fixed-pinned (fig 17.9.c).

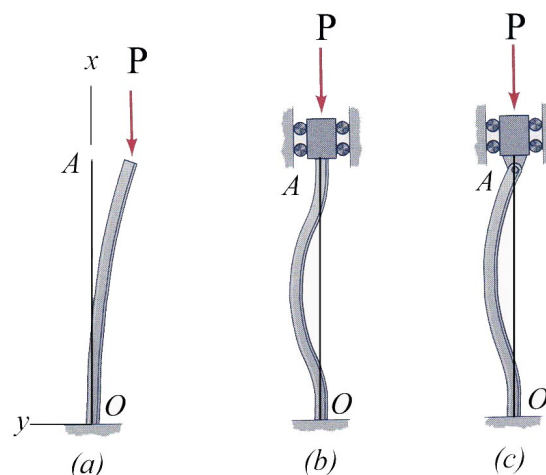


Figure 17.9 Ideal One Fixed End Column - Examples

The boundary conditions at the end $O(x = 0)$, the fixed end, are:

$$\begin{aligned} v(x = 0) = 0 &\rightarrow C_1 * \sin(k * 0) + C_2 \cos(k * 0) + C_3 * 0 + C_4 = 0 \\ &\rightarrow C_2 + C_4 = 0 \end{aligned} \quad (66)$$

$$\begin{aligned} \theta(x) = v'(x = 0) = 0 &\rightarrow k * C_1 * \cos(k * 0) - k * C_2 * \sin(k * 0) + C_3 = 0 \\ &\rightarrow k * C_1 + C_3 = 0 \end{aligned} \quad (67)$$

1.4.2.3.1 Fixed-Free Column (Figure 17.9.a) The boundary conditions at the end $A(x = l)$ are:

$$\begin{aligned} M(x = l) = 0 &\rightarrow E * I_z * v''(x = l) = 0 \rightarrow \\ &\rightarrow -k^2 * C_1 * \sin(k * l) - k^2 * C_2 * \cos(k * l) = 0 \end{aligned} \quad (68)$$

and

$$\begin{aligned} V(x = l) = 0 &\rightarrow E * I_z * v'''(x = l) + P * v'(x = l) = 0 \rightarrow \\ &\rightarrow k^2 * E * I_z * C_3 = 0 \end{aligned} \quad (69)$$

The algebraic homogeneous algebraic system (64) pertinent to this type of column is:

$$\begin{bmatrix} 0 & 1 & 0 & 1 \\ k & 0 & 1 & 0 \\ -k^2 * \sin(k * l) & -k^2 * \cos(k * l) & 0 & 0 \\ 0 & 0 & k^2 * E * I_z & 0 \end{bmatrix} \begin{bmatrix} C_1 \\ C_2 \\ C_3 \\ C_4 \end{bmatrix} = \begin{bmatrix} 0 \\ 0 \\ 0 \\ 0 \end{bmatrix} \quad (70)$$

The determinant of the matrix $\Delta(k)$ is:

$$\begin{aligned}
\det \Delta(k) &= \begin{vmatrix} 0 & 1 & 0 & 1 \\ k & 0 & 1 & 0 \\ -k^2 * \sin(k * l) & -k^2 * \cos(k * l) & 0 & 0 \\ 0 & 0 & k^2 * E * I_z & 0 \end{vmatrix} = \\
&= k^5 * E * I_z * \cos(k * l)
\end{aligned} \tag{71}$$

The resulting characteristic equation is:

$$k^5 * E * I_z * \cos(k * l) = 0 \tag{72}$$

The solution of the transcendental equation (72) is:

$$kl = \frac{\pi}{2} + n * \pi \quad n = 0, 1, 2, \dots \tag{73}$$

The solution obtained above can be also graphically found by plotting the variation of the left-side of equation (42):

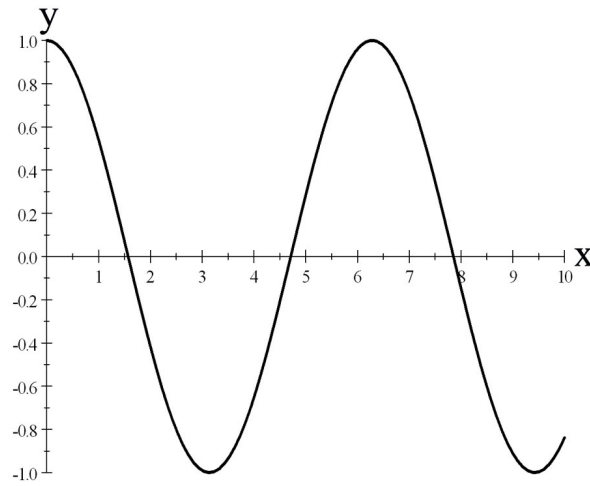


Figure 17.10 Fixed-Free Column - Solution

The first critical load P_{cr}^1 is obtained for $n = 0$:

$$\begin{aligned}
P_{cr}^1 &= E * I_z * k^2 = E * I_z * \left(\frac{\pi}{2 * l} \right)^2 = \\
&= \frac{E * I_z * \pi^2}{4 * l^2} = 0.25 * P_{cr}^E
\end{aligned} \tag{74}$$

where $P_{cr}^E = \frac{E * I_z * \pi^2}{l^2}$ is the first critical load of the *Ideal Euler Column*.

The buckling length l_b is:

$$l_b = 2 * l \quad (75)$$

Once the solution $k * l = \frac{\pi}{2}$ is known, the integration constants are calculated solving the homogeneous algebraic system (70)

$$\tilde{C} = \begin{bmatrix} C_1 \\ C_2 \\ C_3 \\ C_4 \end{bmatrix} = \begin{bmatrix} 0 \\ C_2 \\ 0 \\ -C_2 \end{bmatrix} \quad (76)$$

Remark 17 *The integration constant C_2 remained undetermined and consequently, only the shape of the deflection curve $v(x)$ is known.*

Substituting the integration constants vector \tilde{C} into expressions (57), (58) and (59), the deflection, rotation and bending moment are calculated:

$$v(x) = C_2 \left[\cos\left(\frac{\pi}{2 * l} * x\right) - 1 \right] \quad (77)$$

$$\theta(x) \simeq v'(x) = -\frac{\pi}{2 * l} * C_2 * \sin\left(\frac{\pi}{2 * l} * x\right) \quad (78)$$

$$M(x) = -E * I_z * C_2 * \left(\frac{\pi}{2 * l}\right)^2 * \cos\left(\frac{\pi}{2 * l} * x\right) \quad (79)$$

Conclusion 18 *The constant $C_2 \simeq 0$ must be different than zero for a deformed configuration to be possible $v(x) \simeq 0$.*

The shapes of the deflection curve $v(x)$ and bending moment $M(x)$ are plotted in Figure 17.11.

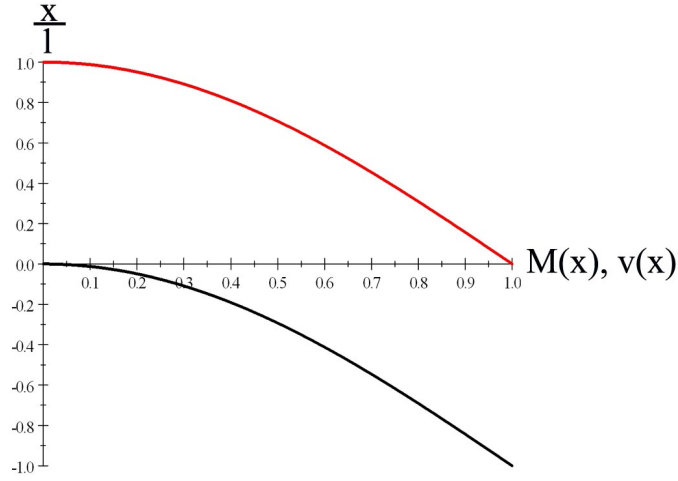


Figure 17.11 Fixed-Free Column - Shapes

1.4.2.3.2 Fixed-Fixed Column (Figure 17.9.b) The boundary conditions at the end A ($x = l$) are:

$$v(x = l) = C_1 * \sin(k * l) + C_2 \cos(k * l) + C_3 * l + C_4 = 0 \quad (80)$$

and

$$\theta(x) = v'(x = l) = k * C_1 * \cos(k * l) - k * C_2 * \sin(k * l) + C_3 = 0 \quad (81)$$

The algebraic homogeneous algebraic system (64) pertinent to this type of column is:

$$\begin{bmatrix} 0 & 1 & 0 & 1 \\ k & 0 & 1 & 0 \\ \sin(k * l) & \cos(k * l) & l & 1 \\ k * \cos(k * l) & -k * \sin(k * l) & 1 & 0 \end{bmatrix} \begin{bmatrix} C_1 \\ C_2 \\ C_3 \\ C_4 \end{bmatrix} = \begin{bmatrix} 0 \\ 0 \\ 0 \\ 0 \end{bmatrix} \quad (82)$$

The determinant of the matrix $\Delta(k)$ is:

$$\det \Delta(k) = \begin{vmatrix} 0 & 1 & 0 & 1 \\ k & 0 & 1 & 0 \\ \sin(k * l) & \cos(k * l) & l & 1 \\ k * \cos(k * l) & -k * \sin(k * l) & 1 & 0 \end{vmatrix} = \quad (83)$$

$$\begin{aligned} &= k - 2k \cos kl + k \cos^2 kl + k \sin^2 kl - k^2 l \sin kl = \\ &= k * (2 - 2 \cos kl - kl \sin kl) \end{aligned} \quad (84)$$

The resulting characteristic equation is:

$$2 - 2 \cos kl - kl \sin kl = 0 \quad (85)$$

The solution of the above characteristic equation can not be obtained analytically and the numerically solution is:

$$kl = 6.2832 = 2 * \pi \quad (86)$$

This solution can be also graphically obtained, by plotting the function located on the left-side of the characteristic equation. The plot is shown in Figure 17.12.

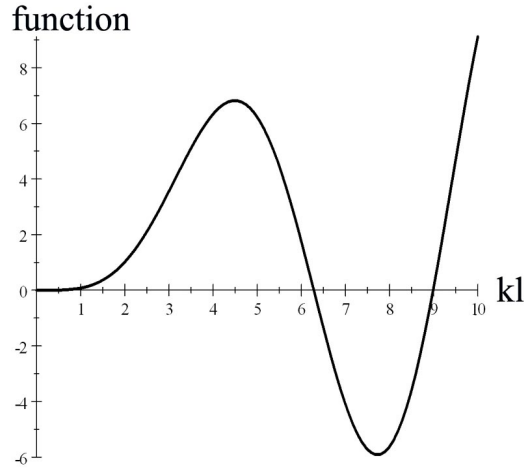


Figure 17.12 Fixed-Fixed Column -Solution

The first critical load P_{cr}^1 is calculated:

$$\begin{aligned} P_{cr}^1 &= E * I_z * k^2 = E * I_z * \left(\frac{2 * \pi}{l} \right)^2 = \\ &= 4 * \frac{E * I_z * \pi^2}{l^2} = 4 * P_{cr}^E \end{aligned} \quad (87)$$

where $P_{cr}^E = \frac{E * I_z * \pi^2}{l^2}$ is the first critical load of the *Ideal Euler Column*.

The buckling length l_b is:

$$l_b = 0.5 * l \quad (88)$$

Once the solution $k * l = 2 * \pi$ is known, the integration constants are calculated solving the homogeneous algebraic system (82):

$$\tilde{C} = \begin{bmatrix} C_1 \\ C_2 \\ C_3 \\ C_4 \end{bmatrix} = \begin{bmatrix} 0 \\ C_2 \\ 0 \\ -C_2 \end{bmatrix} \quad (89)$$

Remark 19 *The integration constant C_2 remained undetermined and consequently, only the shapes of the deflection curve is known.*

Substituting the integration constants vector \tilde{C} into expressions (57), (58) and (59), the deflection, rotation and bending moment are calculated:

$$v(x) = C_2 \left[\cos\left(\frac{2 * \pi}{l} * x\right) - 1 \right] \quad (90)$$

$$\theta(x) \simeq v'(x) = -\frac{2 * \pi}{l} * C_2 * \sin\left(\frac{2 * \pi}{l} * x\right) \quad (91)$$

$$M(x) = -E * I_z * C_2 * \left(\frac{2 * \pi}{l}\right)^2 * \cos\left(\frac{2 * \pi}{l} * x\right) \quad (92)$$

Conclusion 20 *The constant $C_2 \simeq 0$ must be different than zero for a deformed configuration to be possible $v(x) \simeq 0$.*

The shapes of the deflection curve $v(x)$ and bending moment $M(x)$ are plotted in Figure 17.13.

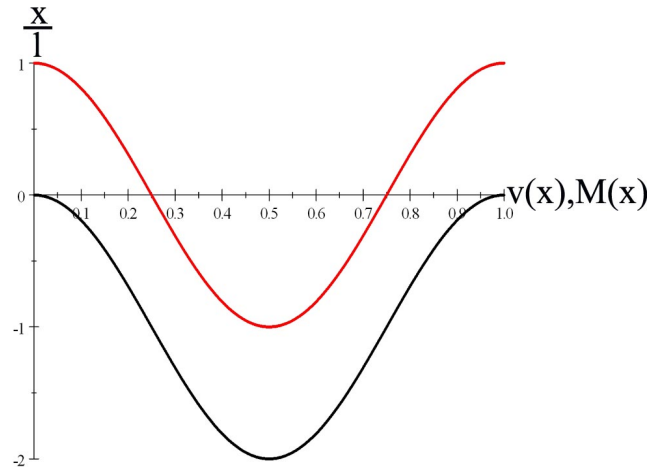


Figure 17.13 Fixed-Fixed Column - Shapes

The shape of the bending moment has two inflection points, the points where the moment is zero. The two locations are found:

$$\begin{aligned}
M(x) &= 0 \\
\rightarrow \cos\left(\frac{2 * \pi}{l} * x\right) &= 0 \\
\rightarrow \frac{2 * \pi}{l} * x &= \frac{\pi}{2} \text{ and } \frac{2 * \pi}{l} * x = \frac{\pi}{2} + \pi \\
\rightarrow x &= \frac{l}{4} \text{ and } x = \frac{3 * l}{4}
\end{aligned}$$

Conclusion 21 *The inflection points are located at $x = 0.25 * l$ and $x = 0.75 * l$. The distance between the two inflection points coincide with the buckling length $l_b = 0.5 * l$.*

1.4.2.3.3 Fixed-Pined Column (Figure 17.9.c) The boundary conditions at the end A ($x = l$) are:

$$\begin{aligned}
v(x = l) &= 0 \\
\rightarrow C_1 * \sin(k * l) + C_2 \cos(k * l) + C_3 * l + C_4 &= 0
\end{aligned} \tag{93}$$

and

$$\begin{aligned}
M(x = l) = 0 &\rightarrow -E * I_z * v''(x = l) = 0 \\
\rightarrow -k^2 * C_1 * \sin(k * l) - k^2 * C_2 * \cos(k * l) &= 0
\end{aligned} \tag{94}$$

The algebraic homogeneous algebraic system (64) pertinent to this type of column is:

$$\begin{bmatrix} 0 & 1 & 0 & 1 \\ k & 0 & 1 & 0 \\ \sin(k * l) & \cos(k * l) & l & 1 \\ -k^2 * \sin(k * l) & -k^2 * \cos(k * l) & 0 & 0 \end{bmatrix} \begin{bmatrix} C_1 \\ C_2 \\ C_3 \\ C_4 \end{bmatrix} = \begin{bmatrix} 0 \\ 0 \\ 0 \\ 0 \end{bmatrix} \tag{95}$$

The determinant of the matrix $\Delta(k)$ is:

$$\begin{aligned}
\det \Delta(k) &= \begin{vmatrix} 0 & 1 & 0 & 1 \\ k & 0 & 1 & 0 \\ \sin(k * l) & \cos(k * l) & l & 1 \\ -k^2 * \sin(k * l) & -k^2 * \cos(k * l) & 0 & 0 \end{vmatrix} = \\
&= k^2 \sin kl - k^3 l \cos kl
\end{aligned} \tag{96}$$

The resulting characteristic equation is:

$$\begin{aligned}
\sin kl - kl \cos kl &= 0 \\
\rightarrow \tan kl - kl &= 0
\end{aligned} \tag{97}$$

The solution of the above characteristic equation can not be obtained analytically. The numerical solution is:

$$kl = 4.4934 \tag{98}$$

This solution can be also graphically obtained, by plotting the function located on the left-side of the characteristic equation. The plot is shown in Figure 17.14.

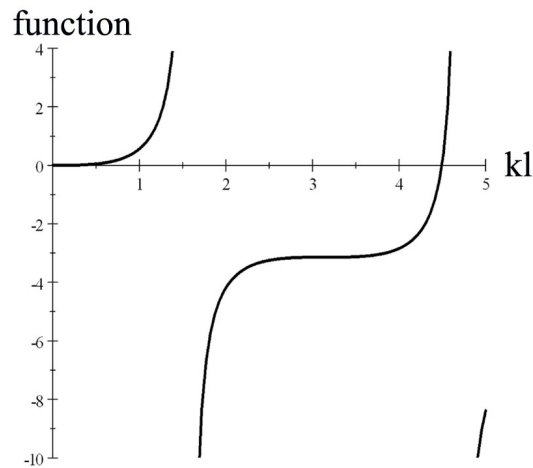


Figure 17.14 Fixed-Pined Column - Solution

The first critical load P_{cr}^1 is calculated:

$$\begin{aligned}
P_{cr}^1 &= E * I_z * k^2 = E * I_z * \left(\frac{4.4934}{l} \right)^2 = \\
&= E * I_z * \left(\frac{4.4934}{l} \right)^2 \frac{\pi^2}{\pi^2} = \frac{E * I_z * \pi^2}{\left(\frac{\pi}{4.4934} * l \right)^2} = \\
&= \frac{E * I_z * \pi^2}{(0.69916 * l)^2} = 2.0457 * P_{cr}^E
\end{aligned} \tag{99}$$

where $P_{cr}^E = \frac{E * I_z * \pi^2}{l^2}$ is the first critical load of the *Ideal Euler Column*.

The buckling length l_b is:

$$l_b = 0.699 \simeq 0.7 * l \tag{100}$$

Once the solution $k * l = 4.4934$ is known, the integration constants are calculated solving the homogeneous algebraic system (95):

$$\tilde{C} = \begin{bmatrix} C_1 \\ C_2 \\ C_3 \\ C_4 \end{bmatrix} = \begin{bmatrix} C_1 \\ -k * l * C_1 \\ -k * C_1 \\ k * l * C_1 \end{bmatrix} \tag{101}$$

Remark 22 *The integration constant C_1 remained undetermined and consequently, only the shapes of the deflection curve $v(x)$ is known.*

Substituting the integration constants vector \tilde{C} into expressions (57), (58) and (59), the deflection, rotation and bending moment are calculated:

$$v(x) = C_1 * \left[\sin\left(\frac{4.4934}{l} * x\right) - 4.4934 * \cos\left(\frac{4.4934}{l} * x\right) - \frac{4.4934}{l} * x + 4.4934 \right]$$

$$\theta(x) \simeq v'(x) = \frac{4.4934}{l} * C_1 * \left[\cos\left(\frac{4.4934}{l} * x\right) + 4.4934 * \sin\left(\frac{4.4934}{l} * x\right) - \frac{4.4934}{l} \right] \tag{102}$$

$$M(x) = -E * I_z * \left(\frac{4.4934}{l} \right)^2 * C_1 * \left[-\sin\left(\frac{4.4934}{l} * x\right) + 4.4934 * \cos\left(\frac{4.4934}{l} * x\right) \right] \tag{103}$$

Conclusion 23 *The constant $C_1 \simeq 0$ must be different than zero for a deformed configuration to be possible $v(x) \simeq 0$.*

The shapes of the deflection curve $v(x)$ and bending moment $M(x)$ are plotted in Figure 17.15.

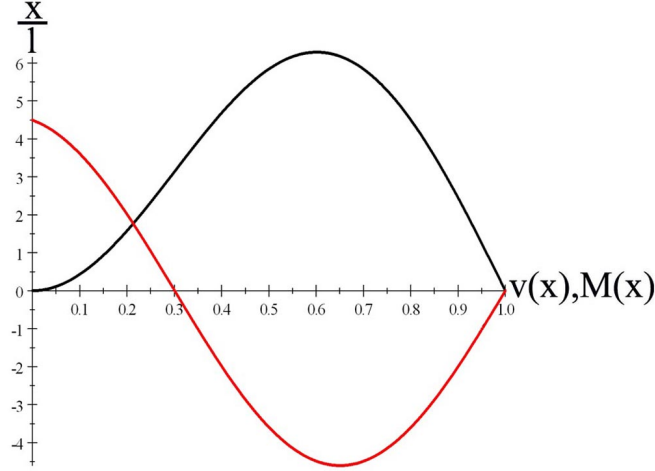


Figure 17.15 Fixed-Pined Column - Shapes

The shape of the bending moment has one inflection points, the point where the moment is zero. The two locations are found:

$$\begin{aligned}
 M(x) &= 0 \\
 \rightarrow -\sin\left(\frac{4.4934}{l} * x\right) + 4.4934 * \cos\left(\frac{4.4934}{l} * x\right) &= 0 \\
 \rightarrow \tan\left(\frac{4.4934}{l} * x\right) &= 4.4934 \\
 \rightarrow \frac{4.4934}{l} * x &= 1.3518 \text{ and } \frac{4.4934}{l} * x = 4.4934 \\
 \rightarrow x &= 0.30 * l \text{ and } x = l
 \end{aligned}$$

Conclusion 24 *The inflection points are located at $x = 0.30 * l$ and $x = l$. The distance between the two inflection points coincide with the buckling length $l_b = 0.7 * l$.*

1.4.2.3.4 Fixed-Sliding Fixed Column The boundary conditions at the end A ($x = l$) are:

$$\begin{aligned}
 \theta(x = l) &= v'(x = l) = 0 \\
 \rightarrow k * C_1 * \cos(k * l) - k * C_2 * \sin(k * l) + C_3 &= 0
 \end{aligned} \tag{104}$$

and

$$V(x = l) = 0 \rightarrow k^2 * E * I_z * C_3 = 0 \quad (105)$$

The algebraic homogeneous algebraic system (17.115) pertinent to this type of column is:

$$\begin{bmatrix} 0 & 1 & 0 & 1 \\ k & 0 & 1 & 0 \\ k * \cos(k * l) & -k * \sin(k * l) & 1 & 0 \\ 0 & 0 & k^2 * E * I_z & 0 \end{bmatrix} \begin{bmatrix} C_1 \\ C_2 \\ C_3 \\ C_4 \end{bmatrix} = \begin{bmatrix} 0 \\ 0 \\ 0 \\ 0 \end{bmatrix} \quad (106)$$

The determinant of the matrix $\Delta(k)$ is:

$$\begin{aligned} \det \Delta(k) &= \begin{vmatrix} 0 & 1 & 0 & 1 \\ k & 0 & 1 & 0 \\ k * \cos(k * l) & -k * \sin(k * l) & 1 & 0 \\ 0 & 0 & k^2 * E * I_z & 0 \end{vmatrix} = \\ &= k^4 E I_z \sin kl \end{aligned} \quad (107)$$

The resulting characteristic equation is:

$$\sin kl = 0 \quad (108)$$

The solution of the above characteristic equation is:

$$kl = \pi \quad (109)$$

This solution can be also graphically obtained, by plotting the function located on the left-side of the characteristic equation. The plot is shown in Figure 17.16.

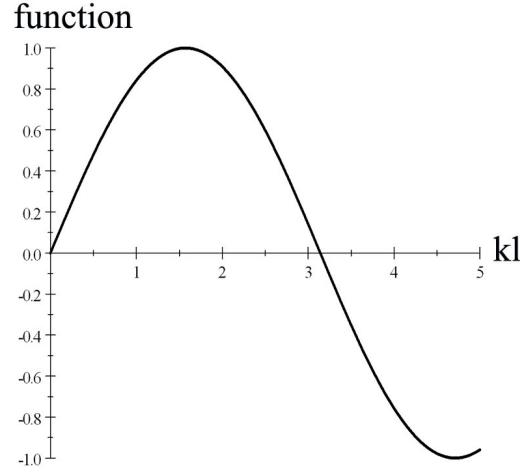


Figure 17.16 Fixed-Sliding Fixed Column - Solution

The first critical load P_{cr}^1 is calculated:

$$\begin{aligned} P_{cr}^1 &= E * I_z * k^2 = E * I_z * \left(\frac{\pi}{l}\right)^2 = \\ &= \frac{E * I_z * \pi^2}{l^2} = P_{cr}^E \end{aligned} \quad (110)$$

where $P_{cr}^E = \frac{E * I_z * \pi^2}{l^2}$ is the first critical load of the *Ideal Euler Column*.

The buckling length l_b is:

$$l_b = l \quad (111)$$

Once the solution $k * l = \pi$ is known, the integration constants are calculated solving the homogeneous algebraic system (95):

$$\tilde{C} = \begin{bmatrix} C_1 \\ C_2 \\ C_3 \\ C_4 \end{bmatrix} = \begin{bmatrix} 0 \\ C_2 \\ 0 \\ -C_2 \end{bmatrix} \quad (112)$$

Remark 25 The integration constant C_1 remained undetermined and consequently, only the shapes of the deflection curve $v(x)$ is known.

Substituting the integration constants vector \tilde{C} into expressions (57), (58) and (59), the deflection, rotation and bending moment are calculated:

$$v(x) = -C_2 * \left[\cos\left(\frac{\pi}{l} * x\right) - 1 \right]$$

$$\theta(x) \simeq v'(x) = C_2 * \frac{\pi}{l} * \sin\left(\frac{\pi}{l} * x\right) \quad (113)$$

$$M(x) = -E * I_z * \left(\frac{\pi}{l}\right)^2 * \cos\left(\frac{\pi}{l} * x\right) \quad (114)$$

Conclusion 26 *The constant $C_2 \simeq 0$ must be different than zero for a deformed configuration to be possible $v(x) \simeq 0$.*

The shapes of the deflection curve $v(x)$ and bending moment $M(x)$ are plotted in Figure 17.17.

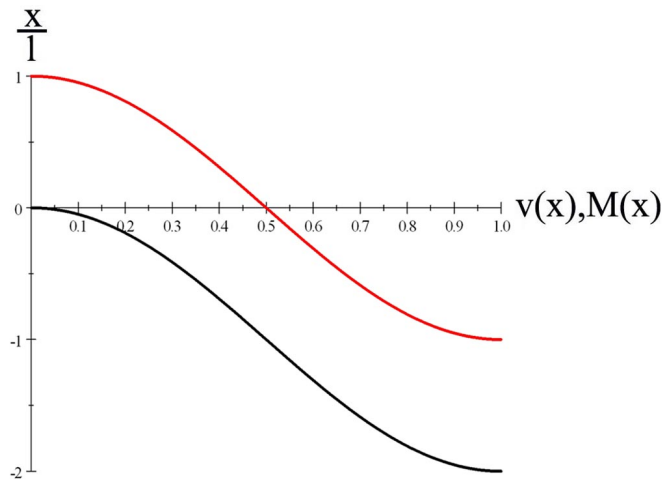


Figure 17.17 Ideal Fixed-Sliding Fixed Column - Shapes

The shape of the bending moment has one inflection points, the point where the moment is zero. The two locations are found:

$$\begin{aligned} M(x) &= 0 \\ \rightarrow \cos\left(\frac{\pi}{l} * x\right) &= 0 \\ \rightarrow x &= 0.50 * l \text{ and } x = 1.5 * l \end{aligned}$$

1.4.2.4 Column with OnePined End The boundary conditions at the end O , the hinged end, are:

$$\begin{aligned} v(x = 0) = 0 &\rightarrow C_1 * \sin(k * 0) + C_2 \cos(k * 0) + C_3 * 0 + C_4 = 0 \\ &\rightarrow C_2 + C_4 = 0 \end{aligned} \quad (115)$$

$$\begin{aligned} M(x = 0) = 0 &\rightarrow E * I_z * v''(x = 0) = 0 \\ &\rightarrow E * I_z * [-k^2 * C_1 * \sin(k * 0) - k^2 * C_2 * \cos(k * 0)] = 0 \\ &\rightarrow E * I_z * C_2 = 0 \rightarrow C_2 = 0 \end{aligned} \quad (116)$$

1.4.2.4.1 Pined-Pined Column (Euler's Column) The boundary conditions at the end A ($x = l$) are:

$$v(x = l) = C_1 * \sin(k * l) + C_2 \cos(k * l) + C_3 * l + C_4 = 0 \quad (117)$$

and

$$\begin{aligned} M(x = l) = 0 &\rightarrow E * I_z * v''(x = l) = 0 \\ &\rightarrow -k^2 * C_1 * \sin(k * l) - k^2 * C_2 * \cos(k * l) = 0 \end{aligned} \quad (118)$$

The algebraic homogeneous algebraic system pertinent to this type of column is:

$$\begin{bmatrix} 0 & 1 & 0 & 1 \\ 0 & 1 & 0 & 0 \\ \sin(k * l) & \cos(k * l) & l & 1 \\ -k^2 * \sin(k * l) & -k^2 * \cos(k * l) & 0 & 0 \end{bmatrix} \begin{bmatrix} C_1 \\ C_2 \\ C_3 \\ C_4 \end{bmatrix} = \begin{bmatrix} 0 \\ 0 \\ 0 \\ 0 \end{bmatrix} \quad (119)$$

The determinant of the matrix $\Delta(k)$ is:

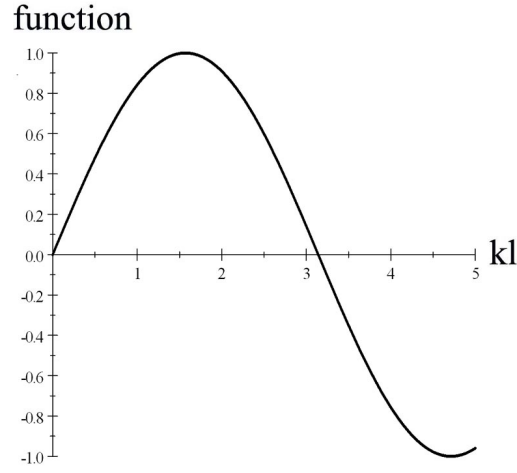


Figure 1: Figure 17.18 Pined-Pined Column - Solution

$$\det \Delta(k) = \begin{vmatrix} 0 & 1 & 0 & 1 \\ 0 & 1 & 0 & 0 \\ \sin(k * l) & \cos(k * l) & l & 1 \\ -k^2 * \sin(k * l) & -k^2 * \cos(k * l) & 0 & 0 \end{vmatrix} = \quad (120)$$

$$= k^2 l \sin kl$$

The resulting characteristic equation is:

$$\sin kl = 0 \quad (121)$$

The solution of the above characteristic equation is:

$$kl = \pi \quad (122)$$

This solution can be also graphically obtained, by plotting the function located on the left-side of the characteristic equation. The plot is shown in Figure 17.18.

The first critical load P_{cr}^1 is calculated:

$$\begin{aligned} P_{cr}^1 &= E * I_z * k^2 = E * I_z * \left(\frac{\pi}{l}\right)^2 = \\ &= \frac{E * I_z * \pi^2}{l^2} = P_{cr}^E \end{aligned} \quad (123)$$

where $P_{cr}^E = \frac{E * I_z * \pi^2}{l^2}$ is the first critical load of the *Ideal Euler Column*.

The buckling length l_b is:

$$l_b = l \quad (124)$$

Once the solution $k * l = \pi$ is known, the integration constants are calculated solving the homogeneous algebraic system (119):

$$\tilde{C} = \begin{bmatrix} C_1 \\ C_2 \\ C_3 \\ C_4 \end{bmatrix} = \begin{bmatrix} C_1 \\ 0 \\ 0 \\ 0 \end{bmatrix} \quad (125)$$

Remark 27 *The integration constant C_1 remained undetermined and consequently, only the shapes of the deflection curve $v(x)$ is known.*

Substituting the integration constants vector \tilde{C} into expressions (57), (58) and (59), the deflection, rotation and bending moment are calculated:

$$v(x) = C_1 * \sin(k * x) \quad (126)$$

$$\theta(x) \simeq v'(x) = C_1 * k * \cos(k * x) \quad (127)$$

$$M(x) = -E * I_z * C_1 * k^2 * \sin(k * x) \quad (128)$$

Conclusion 28 *The constant $C_1 \simeq 0$ must be different than zero for a deformed configuration to be possible $v(x) \simeq 0$.*

The shapes of the deflection curve $v(x)$ and bending moment $M(x)$ are plotted in Figure 17.19.

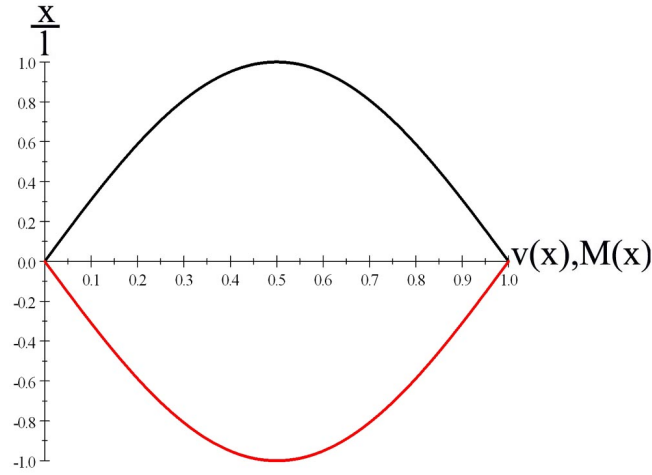


Figure 17.19 Pined-Pined Column - Shapes

The shape of the bending moment has one inflection points, the point where the moment is zero. The two locations are found:

$$\begin{aligned}
 M(x) &= 0 \\
 &\rightarrow \sin\left(\frac{\pi}{l} * x\right) = 0 \\
 &\rightarrow x = 0 \text{ and } x = l
 \end{aligned}$$

Conclusion 29 *The inflection points are located, as expected, at $x = 0$ and $x = l$. The distance between the two inflection points coincide with the buckling length $l_b = l$.*

1.4.2.4.2 Pined-Sliding Fixed Column The boundary conditions at the end A ($x = l$) are:

$$\theta(x = l) = v'(x = l) = 0 \quad (129)$$

$$\rightarrow k * C_1 * \cos(k * l) - k * C_2 * \sin(k * l) + C_3 = 0$$

$$\rightarrow C_1 * \cos(k * l) - C_2 * \sin(k * l) + C_3 = 0 \quad (130)$$

and

$$\begin{aligned}
 V(x = l) = 0 &\rightarrow E * I_z * v^{III}(x = l) + P * v'(x = l) = 0 \rightarrow \\
 &\rightarrow k^2 * E * I_z * C_3 = 0 \rightarrow k^2 * C_3 = 0
 \end{aligned}$$

The algebraic homogeneous algebraic system pertinent to this type of column is:

$$\begin{bmatrix} 0 & 1 & 0 & 1 \\ 0 & 1 & 0 & 0 \\ \cos(k * l) & -\sin(k * l) & 1 & 0 \\ 0 & 0 & k^2 & 0 \end{bmatrix} \begin{bmatrix} C_1 \\ C_2 \\ C_3 \\ C_4 \end{bmatrix} = \begin{bmatrix} 0 \\ 0 \\ 0 \\ 0 \end{bmatrix} \quad (131)$$

The determinant of the matrix $\Delta(k)$ is:

$$\begin{aligned} \det \Delta(k) &= \begin{vmatrix} 0 & 1 & 0 & 1 \\ 0 & 1 & 0 & 0 \\ \cos(k * l) & -\sin(k * l) & 1 & 0 \\ 0 & 0 & k^2 & 0 \end{vmatrix} = \\ &= k^2 \cos kl \end{aligned} \quad (132)$$

The resulting characteristic equation is:

$$\cos kl = 0 \quad (133)$$

The solution of the above characteristic equation is:

$$kl = \frac{\pi}{2} \quad (134)$$

This solution can be also graphically obtained, by plotting the function located on the left-side of the characteristic equation. The plot is shown in Figure 17.20.

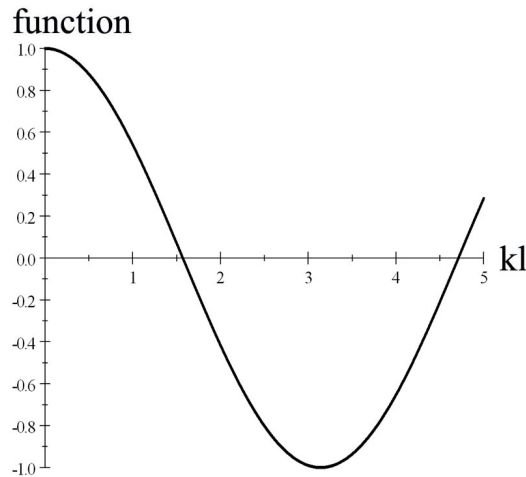


Figure 17.20 Pined-Sliding Fixed Column - Solution

The first critical load P_{cr}^1 is calculated:

$$\begin{aligned} P_{cr}^1 &= E * I_z * k^2 = E * I_z * \left(\frac{\pi}{2 * l} \right)^2 = \\ &= \frac{E * I_z * \pi^2}{(2 * l)^2} = 0.25 * P_{cr}^E \end{aligned} \quad (135)$$

where $P_{cr}^E = \frac{E * I_z * \pi^2}{l^2}$ is the first critical load of the *Ideal Euler Column*.

The buckling length l_b is:

$$l_b = 2 * l \quad (136)$$

Once the solution $k * l = \pi$ is known, the integration constants are calculated solving the homogeneous algebraic system (119):

$$\tilde{C} = \begin{bmatrix} C_1 \\ C_2 \\ C_3 \\ C_4 \end{bmatrix} = \begin{bmatrix} C_1 \\ 0 \\ 0 \\ 0 \end{bmatrix} \quad (137)$$

Remark 30 *The integration constant C_1 remained undetermined and consequently, only the shapes of the deflection curve $v(x)$ is known.*

Substituting the integration constants vector \tilde{C} into expressions (57), (58) and (59), the deflection, rotation and bending moment are calculated:

$$v(x) = C_1 * \sin\left(\frac{\pi}{2 * l} * x\right) \quad (138)$$

$$\theta(x) \simeq v'(x) = C_1 * k * \cos\left(\frac{\pi}{2 * l} * x\right) \quad (139)$$

$$M(x) = -E * I_z * C_1 * k^2 * \sin\left(\frac{\pi}{2 * l} * x\right) \quad (140)$$

Conclusion 31 *The constant $C_1 \simeq 0$ must be different than zero for a deformed configuration to be possible $v(x) \simeq 0$.*

The shapes of the deflection curve $v(x)$ and bending moment $M(x)$ are plotted in Figure 17.21.

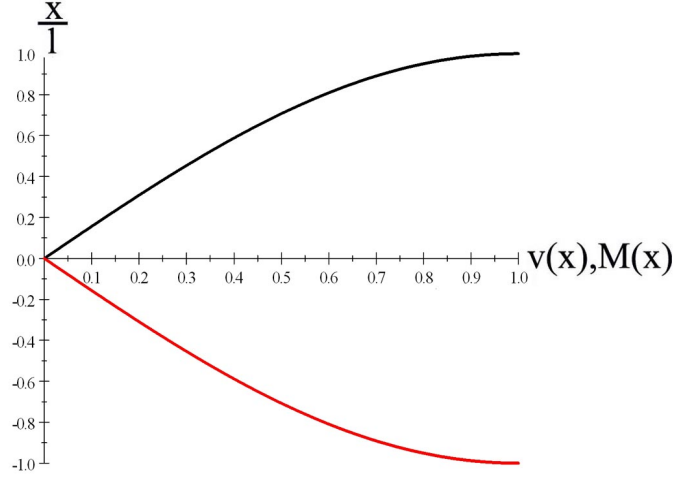


Figure 17.21 Pined-Sliding Fixed Column - Shapes

The shape of the bending moment has one inflection points, the point where the moment is zero. The two locations are found:

$$\begin{aligned} M(x) &= 0 \\ \rightarrow \sin\left(\frac{\pi}{2 * l} * x\right) &= 0 \\ \rightarrow x &= 0 \text{ and } x = 2 * l \end{aligned}$$

Conclusion 32 *The inflection points are located, as expected, at $x = 0$ and $x = 2 * l$. The distance between the two inflection points coincide with the buckling length $l_b = 2 * l$.*

1.4.2.4.3 Pined-Fixed Column The boundary conditions at the end A ($x = l$) are:

$$v(x = l) = 0 \rightarrow C_1 * \sin(k * l) + C_2 \cos(k * l) + C_3 * l + C_4 = 0 \quad (141)$$

and

$$\begin{aligned} \theta(x = l) = v'(x = l) &= 0 \\ \rightarrow k * C_1 * \cos(k * l) - k * C_2 * \sin(k * l) + C_3 &= 0 \end{aligned} \quad (142)$$

The algebraic homogeneous algebraic system pertinent to this type of column is:

$$\begin{bmatrix} 0 & 1 & 0 & 1 \\ 0 & 1 & 0 & 0 \\ \sin(k * l) & \cos(k * l) & l & 1 \\ k * \cos(k * l) & -k * \sin(k * l) & 1 & 0 \end{bmatrix} \begin{bmatrix} C_1 \\ C_2 \\ C_3 \\ C_4 \end{bmatrix} = \begin{bmatrix} 0 \\ 0 \\ 0 \\ 0 \end{bmatrix} \quad (143)$$

The determinant of the matrix $\Delta(k)$ is:

$$\begin{aligned} \det \Delta(k) &= \begin{vmatrix} 0 & 1 & 0 & 1 \\ 0 & 1 & 0 & 0 \\ \sin(k * l) & \cos(k * l) & l & 1 \\ k * \cos(k * l) & -k * \sin(k * l) & 1 & 0 \end{vmatrix} = \\ &= \sin kl - kl \cos kl \end{aligned} \quad (144)$$

The resulting characteristic equation is:

$$\sin kl - kl \cos kl = 0 \quad (145)$$

$$\rightarrow \tan kl - kl = 0 \quad (146)$$

The solution of the above characteristic equation is obtained numerically:

$$kl = 4.4934 \quad (147)$$

This solution can also be graphically obtained, by plotting the function located on the left-side of the characteristic equation. The plot is shown in Figure 17.22.

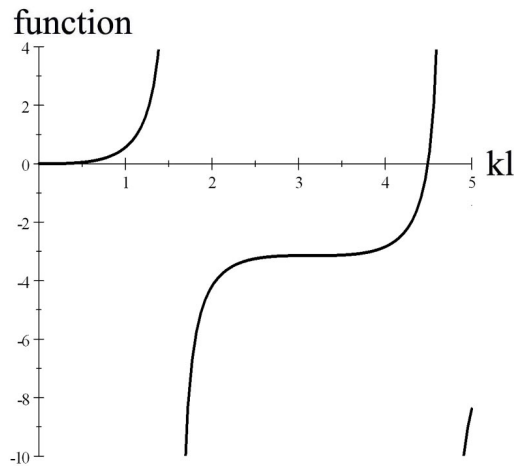


Figure 17.22 Pined-Fixed Column - Solution

The first critical load P_{cr}^1 is calculated:

$$\begin{aligned} P_{cr}^1 &= E * I_z * k^2 = E * I_z * \left(\frac{4.4934}{l} \right)^2 = \\ &= \left(\frac{4.4934}{\pi} \right)^2 * \frac{E * I_z * \pi^2}{l^2} = 2.046 * P_{cr}^E \end{aligned} \quad (148)$$

where $P_{cr}^E = \frac{E * I_z * \pi^2}{l^2}$ is the first critical load of the *Ideal Euler Column*.

The buckling length l_b is:

$$l_b = 0.699 * l \simeq 0.7 * l \quad (149)$$

Once the solution $k * l = \pi$ is known, the integration constants are calculated solving the homogeneous algebraic system (143):

$$\tilde{C} = \begin{bmatrix} C_1 \\ C_2 \\ C_3 \\ C_4 \end{bmatrix} = \begin{bmatrix} C_1 \\ 0 \\ -\frac{\sin 4.4934}{l} * C_1 \\ 0 \end{bmatrix} \quad (150)$$

Remark 33 *The integration constant C_1 remained undetermined and consequently, only the shapes of the deflection curve $v(x)$ is known.*

Substituting the integration constants vector \tilde{C} into expressions (57), (58) and (59), the deflection, rotation and bending moment are calculated:

$$v(x) = C_1 * \left[\sin\left(\frac{4.4934}{l} * x\right) - x * \frac{\sin 4.4934}{l} \right] \quad (151)$$

$$\theta(x) \simeq v'(x) = C_1 * \frac{4.4934}{l} * \left[\cos\left(\frac{4.4934}{l} * x\right) - 1 \right] \quad (152)$$

$$M(x) = E * I_z * C_1 * \left(\frac{4.4934}{l} \right)^2 * \sin\left(\frac{4.4934}{l} * x\right) \quad (153)$$

Conclusion 34 *The constant $C_1 \simeq 0$ must be different than zero for a deformed configuration to be possible $v(x) \simeq 0$.*

The shapes of the deflection curve $v(x)$ and bending moment $M(x)$ are plotted in Figure 17.23.

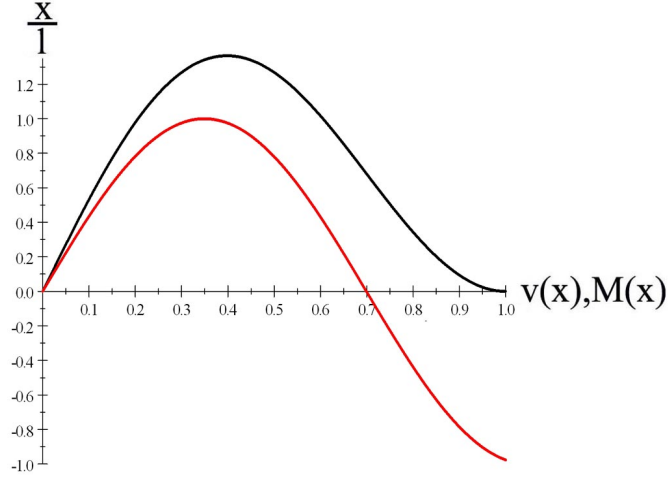


Figure 17.23 Pined-Fixed Column - Shapes

The shape of the bending moment has one inflection points, the point where the moment is zero. The two locations are found:

$$\begin{aligned}
 M(x) &= 0 \\
 \rightarrow \sin\left(\frac{4.4934}{l} * x\right) &= 0 \\
 \rightarrow x = 0 \text{ and } x = 0.69916l &\simeq 0.7 * l
 \end{aligned}$$

Conclusion 35 *The inflection points are located, as expected, at $x = 0$ and $x = 0.7 * l$. The distance between the two inflection points coincide with the buckling length $l_b = 0.7 * l$.*

1.4.3 Buckling of Columns with Linear Elastic Restrained Ends

A special type of columns are those characterized by elastically restrained ends. This type of columns provide a simplified way of analyzing the buckling of columns which are part of an ensemble of elastic structural elements, by isolating the column and representing the surrounding structure by elastic springs located at the ends. The methodology used is identical with that used in the previous section. From the multitude of possibilities only two cases are in-depth considered: *the hinged-pined column with rotational elastic spring (Figure 17.24.a)* and *the fixed-free column with horizontal elastic spring (Figure 17.24.b)*. Any other alternative can be analyzed in a similar manner. The last example (Figure 17.24.c) is a general case which can be used to analyze any combination of elastic linear restrained ends.

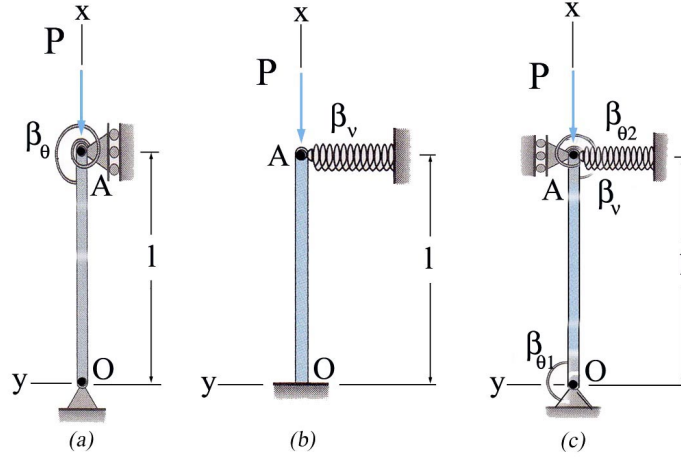


Figure 17.24 Type of Columns with Linear Elastic Restrained Ends

1.4.3.1 pin-ended Column with Rotational Elastic Spring (Figure 17.24.a)

The column considered for investigation is shown in Figure 17.24.a The rotational spring restrains the rotation θ about z axis at the end A and is characterized by a linear spring constant β_θ . The boundary conditions are:

- at the hinged end O ($x = 0$)

$$v(x = 0) = 0 \rightarrow C_1 * \sin(k * 0) + C_2 \cos(k * 0) + C_3 * 0 + C_4 = 0 \rightarrow \quad (154)$$

$$\rightarrow C_2 + C_4 = 0 \quad (155)$$

$$M(x = 0) = 0 \rightarrow \quad (156)$$

$$\rightarrow E * I_z * v''(x = 0) = 0 \rightarrow v''(x = 0) = 0 \rightarrow \quad (157)$$

$$\rightarrow [-k^2 * C_1 * \sin(k * 0) - k^2 * C_2 * \cos(k * 0)] = 0 \rightarrow \quad (158)$$

$$\rightarrow C_2 = 0$$

- at the pinned end A ($x = l$)

$$v(x = l) = 0 \rightarrow C_1 * \sin(k * l) + C_2 \cos(k * l) + C_3 * l + C_4 = 0 \quad (159)$$

$$-M(x = l) = M_{spring}$$

$$\rightarrow -E * I_z * v''(x = l) = \beta_\theta * v'(x = l) \rightarrow$$

$$\rightarrow -E * I_z * [-k^2 * C_1 * \sin(k * l) - k^2 * C_2 * \cos(k * l)] = \beta_\theta * [k * C_1 * \cos(k * l) - k * C_2 * \sin(k * l)]$$

$$\rightarrow [k^2 * E * I_z * \sin(k * l) - k * \beta_\theta * \cos(k * l)] C_1 + [k * \beta_\theta * \sin(k * l) + k^2 * E * I_z * \cos(k * l)] C_2 = 0$$

Remark 36 The $(-)$ minus sign in front of $M(x = l)$ is due to the positive moment convention used.

The determinant $\Delta(k)$ of the integration constants is:

$$\begin{aligned} \Delta(k) &= \begin{bmatrix} 0 & 1 & 0 & 1 \\ 0 & 1 & 0 & 0 \\ \sin(k * l) & \cos(k * l) & l & 1 \\ k^2 E I_z \sin kl - k \beta_\theta \cos kl & k \beta_\theta \sin kl + k^2 E I_z \cos kl & -\beta_\theta & 0 \end{bmatrix} = \quad (161) \\ &= k * l * \beta_\theta * \cos(k * l) - \beta_\theta * \sin(k * l) - k^2 * l * E * I_z * \sin(k * l) \end{aligned}$$

The resulting characteristic equation is:

$$\begin{aligned} k * l * \beta_\theta * \cos(k * l) - \beta_\theta * \sin(k * l) - k^2 * l * E * I_z * \sin(k * l) &= 0 \rightarrow \quad (162) \\ \beta_\theta * [k * l * \cos(k * l) - \sin(k * l)] - k^2 * l * E * I_z * \sin(k * l) &= 0 \rightarrow \\ \beta_\theta * [k * l * \cos(k * l) - \sin(k * l)] - k^2 * l * E * I_z * \sin(k * l) &= 0 \end{aligned}$$

If the rotational spring constant β_θ is expressed as:

$$\beta_\theta = \alpha * \frac{E * I_z}{l} \quad (163)$$

where α is a positive real constant varying in the interval $(0.. \infty)$, the characteristic equation.(162) becomes:

$$\begin{aligned} \alpha * \frac{E * I_z}{l} * [k * l * \cos(k * l) - \sin(k * l)] - k^2 * l * E * I_z * \sin(k * l) &= 0 \rightarrow (164) \\ \alpha * [k * l * \cos(k * l) - \sin(k * l)] - k^2 * l^2 * \sin(k * l) &= 0 \end{aligned}$$

The equation (164) indicates a dependency of the product $k * l$ on the real constant α . The analytical solution of the equation (??) is an impossibility and consequently, the graphical method is employed. The functional relation $\alpha - kl$, expressed by equation (164), is implicitly plotted in Figure 17.25 for α values varying in the interval 0 to $\infty \simeq .1000$.

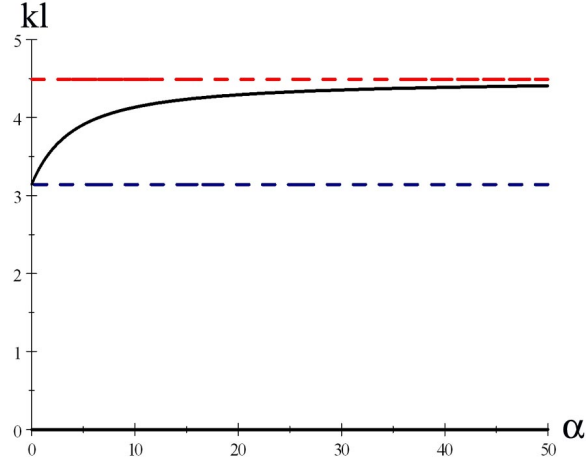


Figure 17.25

Remark 37 Analyzing the graph pictured in Figure 17.25 results:

- (a) the functional relation $\alpha - kl$ is a continuum increasing function, tending asymptotically at $k * l = 4.49$;
- (b) solving equation (164) for $\alpha = 0$ the solution $k * l = \pi$ is found, a value corresponding to hinged-pinned column;
- (c) solving equation (164) for $\alpha = \infty$ the solution $k * l = 4.493$ is found, a value corresponding to hinged-fixed column;

For a specified α value, using the graph shown in Figure 17.25, the corresponding $k * l$ is found:

$$k * l = \text{number} \quad (165)$$

The minimum critical load is calculated, as usual, as:

$$\begin{aligned} P_{cr} &= E * I_z * k^2 = E * I_z * \frac{\text{number}^2}{l^2} * \frac{\pi^2}{\pi^2} = \\ &= \frac{E * I_z * \pi^2}{\left(\frac{\pi * l}{\text{number}}\right)^2} = \frac{E * I_z * \pi^2}{l_b^2} \end{aligned} \quad (166)$$

where the buckling length l_b is obtained as:

$$l_b = \frac{\pi * l}{\text{number}} \quad (167)$$

The numerical value of $number \in [\pi, 4.493]$, in conformity with the plot shown in Figure 17.25, and consequently, the ratio $\frac{l_b}{l} \in [1, 0.7]$. The variation of the ratio $\frac{l_b}{l}$ is shown in Figure 17.26

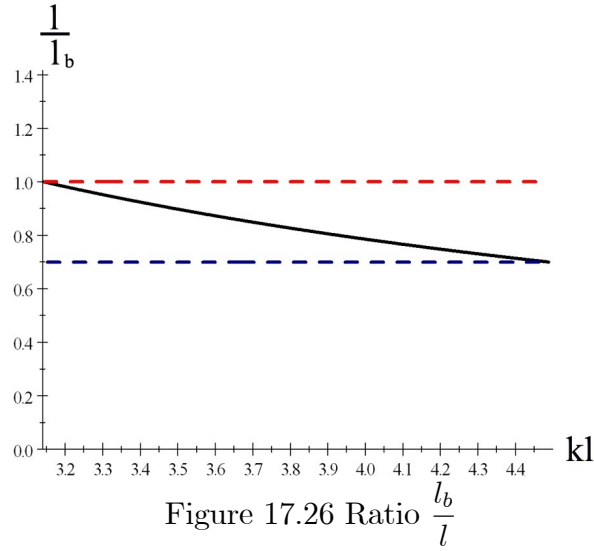


Figure 17.26 Ratio $\frac{l_b}{l}$

1.4.3.2 Fixed-Free Column with Horizontal Elastic Spring (Figure 17.24.b)

The second example of a column with elastic restrains is the fixed-free column with a horizontal linear elastic spring attached at the end A of the column as shown in Figure 17.24.b. The horizontal linear spring is characterized by a elastic spring constant β_v . The integration constants are obtained imposing the boundary conditions:

- at the fixed end, point O ($x = 0$):

$$\begin{aligned} v(x = 0) = 0 &\rightarrow C_1 * \sin(k * 0) + C_2 \cos(k * 0) + C_3 * 0 + C_4 = 0 \rightarrow (168) \\ &\rightarrow C_2 + C_4 = 0 \end{aligned}$$

$$\theta(x = 0) = 0 \rightarrow k * C_1 * \cos(k * 0) - k * C_2 * \sin(k * 0) + C_3 = 0 \rightarrow (169)$$

$$\rightarrow k * C_1 + C_3 = 0 \quad (170)$$

- at the end A ($x = l$), where the horizontal linear spring impedes on the horizontal displacement:

$$\begin{aligned}
-M(x = l) = 0 &\rightarrow -E * I_z * v''(x = l) = 0 \rightarrow v''(x = l) = 0 \\
&\rightarrow -k^2 * C_1 * \sin(k * l) - k^2 * C_2 * \cos(k * l) = 0 \rightarrow \\
&\rightarrow k^2 * C_1 * \sin(k * l) + k^2 * C_2 * \cos(k * l) = 0
\end{aligned} \tag{171}$$

$$\begin{aligned}
-V(x = l) &= \beta_v * v(x = l) \\
&\rightarrow -[E * I_z * v^{III}(x = l) + P * v'(x = l)] = \beta_v * v(x = l) \rightarrow \\
&\rightarrow -k^2 * E * I_z * C_3 = \beta_v [C_1 * \sin(k * l) + C_2 * \cos(k * l) + C_3 * l + C_4] \\
&\rightarrow \beta_v * \sin(k * l) * C_1 + \beta_v * \cos(k * l) * C_2 + (E * I_z * k^2 + l * \beta_v) * C_3 + \beta_v * C_4 = 0
\end{aligned} \tag{172}$$

The determinant $\Delta(k)$ is:

$$\begin{aligned}
\Delta(k) &= \begin{bmatrix} 0 & 1 & 0 & 1 \\ k & 0 & 1 & 0 \\ k^2 * \sin(k * l) & k^2 * \cos(k * l) & 0 & 0 \\ \beta_v * \sin(k * l) & \beta_v * \cos(k * l) & E * I_z * k^2 + l * \beta_v & \beta_v \end{bmatrix} = \\
&= k^2 * \beta_v * \sin(k * l) - k^3 * l * \beta_v * \cos(k * l) - k^5 * E * I_z * \cos(k * l)
\end{aligned} \tag{173}$$

The resulting characteristic equation is:

$$\begin{aligned}
k^2 * \beta_v * \sin(k * l) - k^3 * l * \beta_v * \cos(k * l) - k^5 * E * I_z * \cos(k * l) &= 0 \rightarrow \\
\beta_v * \sin(k * l) - k * l * \beta_v * \cos(k * l) - k^3 * E * I_z * \cos(k * l) &= 0 \rightarrow \\
\beta_v * [\sin(k * l) - k * l * \cos(k * l)] - k^3 * E * I_z * \cos(k * l) &= 0
\end{aligned} \tag{174}$$

If the rotational spring constant β_v is expressed as:

$$\beta_\theta = \alpha * \frac{E * I_z}{l^3} \tag{175}$$

where α is a positive real constant varying in the interval $(0.. \infty)$, the characteristic equation.(174) becomes:

$$\alpha * [\sin(k * l) - k * l * \cos(k * l)] - k^3 * l^3 * \cos(k * l) = 0 \quad (176)$$

Equation (176) indicates a dependency of the product $k * l$ on the real constant α . The equation (??) does not have a analytical solution and consequently, the graphical method is employed. The functional relation $\alpha - kl$, expressed by equation (176), is implicitly plotted in Figure 17.27 for $\alpha \in [0, \infty \simeq .1000]$.

Remark 38 (a) solving equation (176) for $\alpha = 0$ results a value $k * l = \frac{\pi}{2} = 1.5708$;

(b) solving equation (176) for $\alpha = 1000$ results a value $k * l = 4.493$;

(c) the variation of the $k * l$ as function of α has a linear aspect, starting at 4.712 for $\alpha = 0.001$ and tending towards 4.493 for $\alpha = 1000$. A discontinuity point is found at $\alpha = 0$. The starting value of the linear graph $k * l = 4.712$ corresponds to the second root of the equation (176) when $\alpha = 0$.

(d) The variation of $k * l$ is very limited and can be conservatively represented by the value $(k * l)_{\min} = 4.493$ for all values of α , with the exception of discontinuity point $\alpha = 0$. This finding indicates that the smallest elastic restraining of the cantilever tip will drastically increase the value of $k * l$, which in return reduces the buckling length l_b .

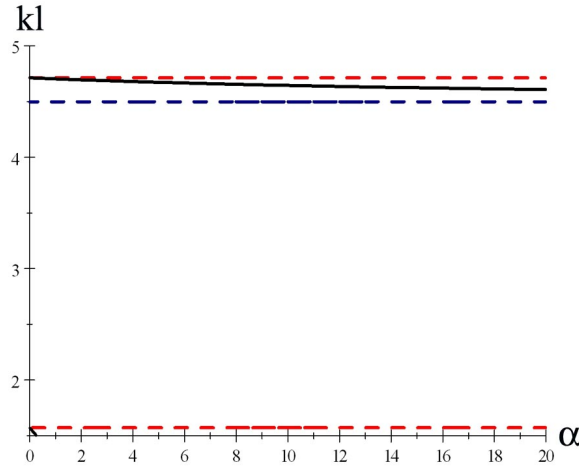


Figure 17.27

The minimum critical load P_{cr}^{\min} is calculated:

$$\begin{aligned} P_{cr}^{\min} &= E * I_z * k^2 = E * I_z * \frac{4.493^2}{l^2} * \frac{\pi^2}{\pi^2} = \\ &= \frac{E * I_z * \pi^2}{\left(\frac{\pi * l}{4.493}\right)^2} = \frac{E * I_z * \pi^2}{(l_b^{\max})^2} \quad \text{for } \alpha = [0.01, \infty] \end{aligned} \quad (177)$$

where the buckling length l_b^{\max} is obtained as:

$$l_b^{\max} = \frac{\pi * l}{4.493} = 0.7 * l \quad \text{for } \alpha = [0.01, \infty] \quad (178)$$

1.4.3.3 A General Case of Elastic Elastic Restraints (Figure 17.24.c) A more general case of column with linear elastic restraints located at the ends is illustrated in Figure 17.24.c. The end O ($x = 0$) is hinged, but its rotation is impeded by an elastic linear rotational spring, characterized by a spring constant $\beta_{\theta 1}$. The other end, the point A ($x = l$), has its lateral displacement and rotation restrained by two linear elastic springs, a horizontal disposed spring of rigidity β_v and a rotational spring of rigidity $\beta_{\theta 2}$. The integration constants are determined imposing the boundary conditions:

- at the hinged end O ($x = 0$) :

$$\begin{aligned} v(x = 0) = 0 &\rightarrow C_1 * \sin(k * 0) + C_2 \cos(k * 0) + C_3 * 0 + C_4 = 0 \rightarrow \\ &\rightarrow C_2 + C_4 = 0 \end{aligned} \quad (179)$$

$$M(x = 0) = M_{spring1}$$

$$\begin{aligned} &\rightarrow E * I_z * v''(x = 0) = \beta_{\theta 1} * v'(x = 0) \rightarrow \\ &\rightarrow E * I_z * [-k^2 * C_1 * \sin(k * 0) - k^2 * C_2 * \cos(k * 0)] = \beta_{\theta 1} * [k * C_1 * \cos(k * 0) - k * C_2 * \sin(k * 0)] \\ &\rightarrow E * I_z * [-k^2 * C_2] = \beta_{\theta 1} * [k * C_1 + C_3] \rightarrow \\ &\rightarrow \beta_{\theta 1} * k * C_1 + E * I_z * k^2 * C_2 + \beta_{\theta 1} * C_3 = 0 \end{aligned}$$

- at the pinned end A ($x = l$)

$$\begin{aligned} -V(x = l) &= \beta_{v2} * v(x = l) \quad (181) \\ &\rightarrow -[E * I_z * v'''(x = l) + P * v'(x = l)] = \beta_{v2} * v(x = l) \rightarrow \\ &\rightarrow -k^2 * E * I_z * C_3 = \beta_{v2} * [C_1 * \sin(k * l) + C_2 \cos(k * l) + C_3 * l + C_4] \\ &\rightarrow \beta_{v2} * \sin(k * l) * C_1 + \beta_{v2} * \cos(k * l) * C_2 + (E * I_z * k^2 + l * \beta_{v2}) * C_3 + \beta_{v2} * C_4 = 0 \end{aligned}$$

$$-M(x = l) = M_{spring}$$

$$\begin{aligned} &\rightarrow -E * I_z * v''(x = l) = \beta_{\theta 2} * v'(x = l) \rightarrow \\ &\rightarrow -E * I_z * [-k^2 * C_1 * \sin(k * l) - k^2 * C_2 * \cos(k * l)] = \beta_{\theta 2} * [k * C_1 * \cos(k * l) - k * C_2 * \sin(k * l)] \\ &\rightarrow [k^2 * E * I_z * \sin(k * l) - k * \beta_{\theta 2} * \cos(k * l)] C_1 + [k^2 * E * I_z * \cos(k * l) + k * \beta_{\theta 2} * \sin(k * l)] C_2 = 0 \end{aligned}$$

Remark 39 The $(-)$ minus sign in front of $M(x = l)$ and $-V(x = l)$ are due to the positive moment and shear force convention used.

The determinant $\Delta(k)$ of the integration constants is:

$$\Delta(k) = \begin{bmatrix} 0 & 1 & 0 & 1 \\ \beta_1 * k & E * I_z * k^2 & \beta_1 & 0 \\ \beta_v * \sin(k * l) & -\beta_v * \cos(k * l) & E * I_z * k^2 + l * \beta_v & \beta_v \\ k^2 E I_z \sin kl - k \beta_2 \cos kl & k^2 E I_z \cos kl + k \beta_2 \sin kl & -\beta_2 & 0 \end{bmatrix} = \quad (1)$$

$$k^5 * \beta_1 * E^2 I_z^2 \cos kl - k \beta_1 \beta_2 \beta_v - k^6 E^3 I_z^3 \sin kl + k^5 \beta_2 E^2 I_z^2 \cos kl + k \beta_1 \beta_2 \beta_v \cos^2 kl -$$

$$-k \beta_1 \beta_2 \beta_v \sin^2 kl - k^4 l \beta_v E^2 I_z^2 \sin kl + k^2 l \beta_1 \beta_2 \beta_v \sin kl + k^4 \beta_1 \beta_2 E I_z \sin kl - k^2 \beta_1 \beta_v E I_z \sin kl$$

$$-k^2 \beta_2 \beta_v E I_z \sin kl - 2k^2 \beta_1 \beta_v E I_z \cos kl \sin kl + k^3 l \beta_1 \beta_v E I_z \cos kl + k^3 l \beta_2 \beta_v E I_z \cos kl$$

After algebraic manipulation the characteristic equation is:

$$(-\sin kl) k^5 + (\alpha_1 \cos kl + \alpha_2 \cos kl) k^4 + (\alpha_1 \alpha_2 \sin kl - l \alpha_v \sin kl) k^3 + (l \alpha_1 \alpha_v \cos kl + l \alpha_2 \alpha_v \cos kl$$

$$+ (l \alpha_1 \alpha_2 \alpha_v \sin kl - \alpha_2 \alpha_v \sin kl - 2 \alpha_1 \alpha_v \cos kl \sin kl - \alpha_1 \alpha_v \sin kl) k + (\alpha_1 \alpha_2 \alpha_v \cos^2 kl - \alpha_1 \alpha_2 \alpha_v \sin^2 kl)$$

$$= 0$$

where $\alpha_1 = \frac{\beta_1}{E * I_z}$, $\alpha_2 = \frac{\beta_2}{E * I_z}$ and $\alpha_v = \frac{\beta_v}{E * I_z}$ are the *rigidity coefficients*. of the linear elastic springs.

Remark 40 (a) A variation of the rigidity coefficient from 0 to 10 practically covers the range from absence of the spring to a rigid connection;

(b) The determinant (183) and the characteristic equation (183) can be particularized function of the particular conditions existing at the ends of the column.

1.5 Limitations of the Linear Elastic Stability. Discussions

The stability (buckling) of the columns, characterized by rigid or elastic end restraints and subjected to a compressive axial load, is based on the *seven basic assumptions* acknowledged at the beginning of the previous section. These assumptions, commonly used in the structural engineering evaluation, bring the advantage of reducing the mathematical complexity, but obviously induced limitations of the derived formulae. In this section some of these assumptions are relaxed and the validity range of the previously derived formulae is established.

1.5.1 Initial Curvature. Imperfections in Columns.

In the engineering practice, the assumption of perfect linearity of the column central line is often violated, due to the existence of the *initial imperfection* resulting from the fabrication process of the material employed. In this case the column has an *initial crookedness* $v_0(x)$ a function, in general, difficult to anticipate. Just to emphasize the effect of the initial crookedness on the behavior of a Euler ideal hinged-pinned column, a sinusoidal representation for $v_0(x)$ is assumed as:

$$v_0(x) = \delta * \sin(\beta * x) \quad (185)$$

where $\beta = n * \frac{\pi}{l}$ and δ are two constants and l is the length of the column.

The total lateral displacement $v(x)$ of the buckled column is expressed as:

$$v(x) = w(x) + v_0(x) \quad (186)$$

where $w(x)$ is the lateral displacement measured from the initial position $v_0(x)$ to the final position $v(x)$.

In the absence of the transversal load the differential equation (55) retains its validity, but has to be applied in a slightly different form, as:

$$w^{IV} + k^2 * v'' = 0 \quad (187)$$

Remark 41 *Following the derivation of the differential equation (55) results that the forth order derivative of $v(x)$ represents in fact the second order derivative of the bending moment M . Because the bending moment is produced by change in curvature only the lateral displacement $w(x)$ participate, and consequently, only the forth order derivative of the $w(x)$ appears in the first term of the equation (187).*

Substituting equation (186) into equation (187) a new *non-homogeneous forth order ordinary differential equation* is obtained:

$$w^{IV} + k^2 * w'' = -k^2 * v_0'' = -k^2 * \beta^2 * \delta * \sin(\beta * x) \quad (188)$$

The solution of the differential equation (188) is obtained as:

$$w(x) = w_0(x) + w_p(x) \quad (189)$$

where $w_0(x)$ and $w_p(x)$ are the solutions of the homogeneous and particular solutions of the differential equation (189), respectively.

The homogeneous solution, similar to solution (57), is:

$$w_0(x) = C_1 * \sin(k * x) + C_2 \cos(k * x) + C_3 * x + C_4 \quad (190)$$

The particular solution $w_p(x)$ is expressed in a similar manner to $v_0(x)$ as:

$$w_p(x) = \alpha * \sin(\beta * x) \quad (191)$$

where α is an unknown constant, remaining to be determined.

The particular solution $w_p(x)$ must verify the equation (188):

$$\alpha * \beta^4 * \sin(\beta * x) - \alpha * k^2 * \beta^2 * \sin(\beta * x) = k^2 * \beta^2 * \delta * \sin(\beta * x) \quad (192)$$

and after algebraic manipulations the constant α is obtained as:

$$\alpha = \frac{k^2}{\beta^2 - k^2} * \delta \quad (193)$$

Consequently, in accordance to equation (186) the general solution $v(x)$ is calculated:

$$\begin{aligned} v(x) &= w(x) + w_0(x) = w_0(x) + w_p(x) + w_0(x) = \\ &= C_1 * \sin(k * x) + C_2 \cos(k * x) + C_3 * x + C_4 + \frac{k^2}{\beta^2 - k^2} * \delta * \sin(\beta * x) + \delta * \sin(\beta * x) = \\ &= C_1 * \sin(k * x) + C_2 \cos(k * x) + C_3 * x + C_4 + \left(\frac{k^2}{\beta^2 - k^2} + 1\right) * \delta * \sin(\beta * x) = \\ &= C_1 * \sin(k * x) + C_2 \cos(k * x) + C_3 * x + C_4 + \frac{\beta^2}{\beta^2 - k^2} * \delta * \sin(\beta * x) \end{aligned} \quad (194)$$

where the relative displacement $w(x)$ is:

$$w(x) = C_1 * \sin(k * x) + C_2 \cos(k * x) + C_3 * x + C_4 + \frac{k^2}{\beta^2 - k^2} * \delta * \sin(\beta * x) \quad (195)$$

The integration constants, C_1 , C_2 , C_3 and C_4 , are determined by imposing the boundary conditions at the ends of the column. The boundary conditions at point A, the hinged end, located at $(x = 0)$ are:

$$\begin{aligned} v(x = 0) = 0 &\rightarrow C_1 * \sin(k * 0) + C_2 \cos(k * 0) + C_3 * 0 + C_4 + \frac{\beta^2}{\beta^2 - k^2} * \delta * \sin(\beta * 0) = 0 \\ &\rightarrow C_2 + C_4 = 0 \end{aligned} \quad (196)$$

$$\begin{aligned} M(x = 0) = 0 &\rightarrow E * I_z * w''(x = 0) = 0 \rightarrow w''(x = 0) = 0 \rightarrow \\ &\rightarrow -k^2 * C_1 * \sin(k * 0) - k^2 * C_2 \cos(k * 0) - \frac{\beta^2 * k^2}{\beta^2 - k^2} * \delta * \sin(\beta * 0) = 0 \rightarrow \\ &\rightarrow C_2 = 0 \end{aligned} \quad (197)$$

The boundary conditions at end B, located at $(x = l)$, are:

$$v(x = l) = 0 \rightarrow C_1 * \sin(k * l) + C_2 \cos(k * l) + C_3 * l + C_4 + \frac{\beta^2}{\beta^2 - k^2} * \delta * \sin(\beta * l) = 0 \quad (198)$$

$$\begin{aligned} M(x = l) = 0 &\rightarrow E * I_z * w''(x = l) = 0 \rightarrow w''(x = l) = 0 \rightarrow \\ &\rightarrow -k^2 * C_1 * \sin(k * l) - k^2 * C_2 \cos(k * l) - \frac{\beta^2 * k^2}{\beta^2 - k^2} * \delta * \sin(\beta * l) = 0 \rightarrow \\ &\rightarrow C_1 * \sin(k * l) + C_2 \cos(k * l) + \frac{\beta^2}{\beta^2 - k^2} * \delta * \sin(\beta * l) = 0 \end{aligned} \quad (199)$$

The equations (196) through (199) are forming an algebraic system matricially expressed as:

$$\begin{bmatrix} 0 & 1 & 0 & 1 \\ 0 & 1 & 0 & 0 \\ \sin(k * l) & \cos(k * l) & l & 1 \\ \sin(k * l) & \cos(k * l) & 0 & 0 \end{bmatrix} \begin{bmatrix} C_1 \\ C_2 \\ C_3 \\ C_4 \end{bmatrix} = \begin{bmatrix} 0 \\ 0 \\ -\frac{\beta^2}{\beta^2 - k^2} * \delta * \sin(\beta * l) \\ -\frac{\beta^2}{\beta^2 - k^2} * \delta * \sin(\beta * l) \end{bmatrix} \quad (200)$$

Solving the algebraic system (200) the following solutions are obtained:

$$\begin{bmatrix} C_1 \\ C_2 \\ C_3 \\ C_4 \end{bmatrix} = -\frac{\beta^2}{\beta^2 - k^2} * \delta * \sin(\beta * l) * \begin{bmatrix} \frac{1}{\sin(k * l)} \\ 0 \\ 0 \\ 0 \end{bmatrix} \quad (201)$$

The final expressions of the lateral displacement $v(x)$ and bending moment $M(x)$ are then calculated:

$$\begin{aligned} v(x) &= C_1 * \sin(k * x) + C_2 \cos(k * x) + C_3 * x + C_4 + \frac{\beta^2}{\beta^2 - k^2} * \delta * \sin(\beta * x) \quad (202) \\ &= -\frac{\beta^2}{\beta^2 - k^2} * \delta * \sin(\beta * l) * \frac{1}{\sin(k * l)} * \sin(k * x) + \frac{\beta^2}{\beta^2 - k^2} * \delta * \sin(\beta * x) = \\ &= \frac{\beta^2}{\beta^2 - k^2} * \delta * \left[\sin(\beta * x) - \frac{\sin(\beta * l)}{\sin(k * l)} * \sin(k * x) \right] = \\ &= \frac{1}{1 - \frac{k^2}{\beta^2}} * \delta * \left[\sin(\beta * x) - \frac{\sin(\beta * l)}{\sin(k * l)} * \sin(k * x) \right] = \\ &= \frac{1}{1 - \frac{P}{n^2 * P_{cr}}} * \delta * \left[\sin(n * \frac{\pi}{l} * x) - \frac{\sin(n * \pi)}{\sin(k * l)} * \sin(k * x) \right] \end{aligned}$$

and

$$\begin{aligned}
M(x) &= E * I_z * w''(x) = \\
&= E * I_z * [-k^2 * C_1 * \sin(k * x) - k^2 * C_2 \cos(k * x) - \frac{\beta^2 * k^2}{\beta^2 - k^2} * \delta * \sin(\beta * x)] = \\
&= -E * I_z * k^2 * [-\frac{\beta^2}{\beta^2 - k^2} * \delta * \sin(\beta * l) * \frac{1}{\sin(k * l)} * \sin(k * x) + \frac{\beta^2}{\beta^2 - k^2} * \delta * \sin(\beta * x)] = \\
&= E * I_z * k^2 * \frac{\beta^2}{\beta^2 - k^2} * \delta * [\frac{\sin(\beta * l)}{\sin(k * l)} * \sin(k * x) - \sin(\beta * x)] = \\
&= P * \frac{\beta^2}{\beta^2 - k^2} * \delta * [\frac{\sin(\beta * l)}{\sin(k * l)} * \sin(k * x) - \sin(\beta * x)] = \\
&= -\frac{P}{1 - \frac{P}{n^2 * P_{cr}}} * \delta * [\sin(n * \frac{\pi}{l} * x) - \frac{\sin(n * \pi)}{\sin(k * l)} * \sin(k * x)] = \\
&= -P * v(x)
\end{aligned} \tag{203}$$

Remark 42 From equations (202) and (203) results that the maximum bending moment M_{\max} and the total displacement v_{\max} are realized in the same cross-section.

Considering $n \geq 1$ and is an integer number ($n = 1, 2, 3 \dots$), the total displacement and the bending moment functions became:

$$v(x) = \frac{1}{1 - \frac{P}{n^2 * P_{cr}}} * \delta * [\sin(n * \frac{\pi}{l} * x) - \frac{\sin(n * \pi)}{\sin(k * l)} * \sin(k * x)] \tag{204}$$

$$= \frac{1}{1 - \frac{P}{n^2 * P_{cr}}} * \delta * \sin(n * \frac{\pi}{l} * x) \tag{205}$$

and

$$M(x) = -P * v(x) = -\frac{P}{1 - \frac{P}{n^2 * P_{cr}}} * \delta * \sin(n * \frac{\pi}{l} * x) \tag{206}$$

Remark 43 It can be noted that the initial imperfection has zero values at both ends of the column and consequently $\sin(n * \pi) = 0$.

The maximum values of both functions, $v(x)$ and $M(x)$, is realized for when $\cos(n * \frac{\pi}{l} * x) = 0$ and, consequently, at location $x = \frac{l}{2 * n}$. The following maximum values are calculated:

$$v_{\max} = \frac{1}{1 - \frac{P}{n^2 * P_{cr}}} * \delta \quad (207)$$

and

$$M_{\max} = \frac{P}{1 - \frac{P}{n^2 * P_{cr}}} * \delta \quad (208)$$

Then, the maximum normal stress σ_x^{\max} is obtained:

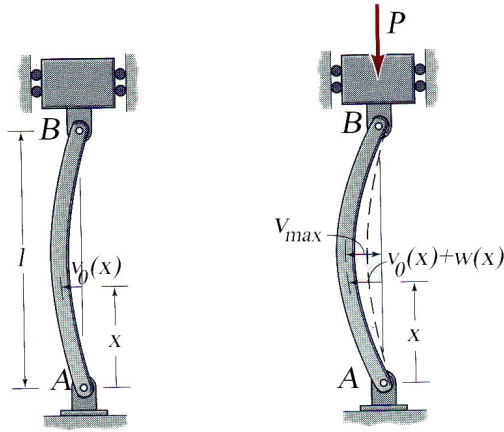
$$\begin{aligned} \sigma_x^{\max} &= \frac{P}{A} + \frac{M_{\max}}{I_z} * y_{\max} = \frac{P}{A} + \frac{P * \delta}{A * r_z^2 * (1 - \frac{P}{n^2 * P_{cr}})} * y_{\max} = \\ &= \frac{P}{A} * (1 + \frac{\delta}{r_z^2 * (1 - \frac{P}{n^2 * P_{cr}})} * y_{\max}) = \frac{P}{A} * (1 + \frac{\gamma}{(1 - \frac{P}{n^2 * P_{cr}})}) = \\ &= \sigma_c * (1 + \frac{\gamma}{(1 - \frac{P}{n^2 * P_{cr}})}) \end{aligned} \quad (209)$$

where $\gamma = \frac{\delta}{r_z^2} * y_{\max}$ is called the *imperfection ratio* and $\sigma_c = \frac{P}{A}$ is the compressive normal stress.

Considering that $\sigma_x^{\max} = \sigma_y^0$ (the proportionality limit stress) a family of normalized curves representing the ratio $y = \frac{\sigma_c}{\sigma_y^0}$ can be calculated function of the ratios $\gamma = \frac{\delta}{r_z^2} * y_{\max}$ and $x = \frac{P}{P_{cr}}$:

$$y = \frac{1}{1 + \frac{\gamma}{1 - \frac{1}{n^2} * x}} \quad (210)$$

The case corresponding to $n = 1$ is pictured in Figure 17.28.



(a) Undeformed Shape (b) Deformed Shape

Figure 17.28 Column with Initial Imperfections

The normalized curves $y = \frac{\sigma_c}{\sigma_y^0}$ corresponding to five values of the imperfection ratio $\gamma \in (0, 0.1, 0.5, 1, 2)$ and $0 \leq x = \frac{P}{P_{cr}} \leq 1$ are shown in Figure 17.29.

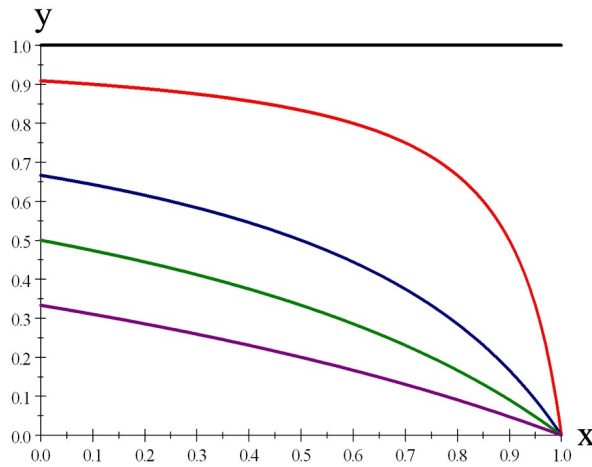
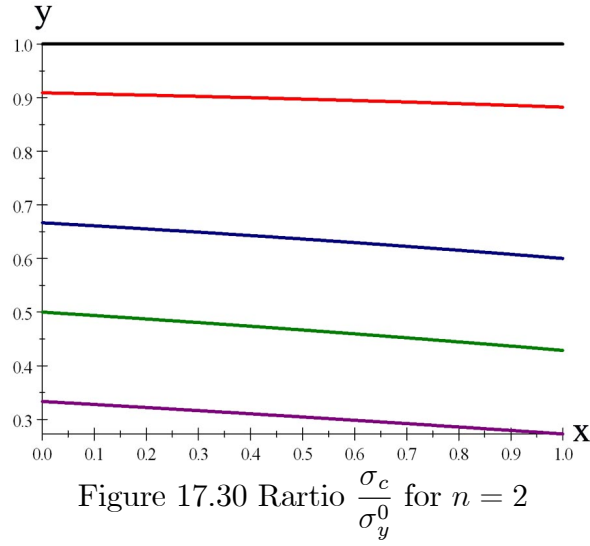
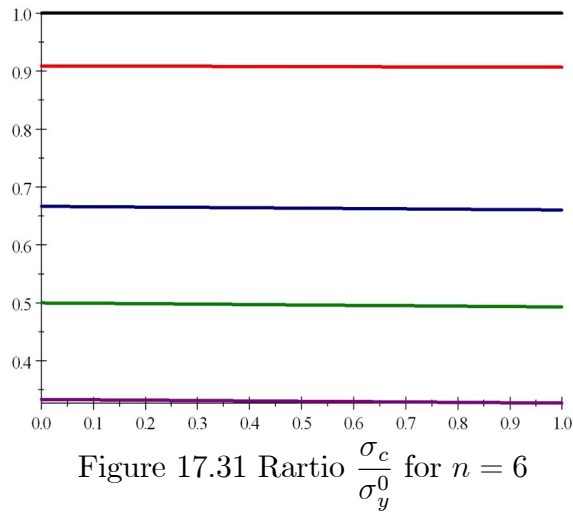


Figure 17.29 Ratio $\frac{\sigma_c}{\sigma_y^0}$ for $n = 1$

For the case when $n = 2$ a similar family of curves $\frac{\sigma_c}{\sigma_y^0}$ corresponding to $\gamma \in (0, 0.1, 0.5, 1, 2)$ and $0 \leq x = \frac{P}{P_{cr}} \leq 1$ are plotted in Figure 17.30



For a more realistic case, $n = 6$, a similar family of curves $\frac{\sigma_c}{\sigma_y^0}$ for $\gamma \in (0, 0.1, 0.5, 1, 2)$ and $0 \leq x = \frac{P}{P_{cr}} \leq 1$ are plotted in Figure 17.31.



For comparison the variation of the ratio $y = \frac{\sigma_c}{\sigma_y^0}$ is plotted in Figure 17.32 for values of $n = (1, 2, 3, 4, 5)$ and an imperfection ratio $\gamma = 0.5$.

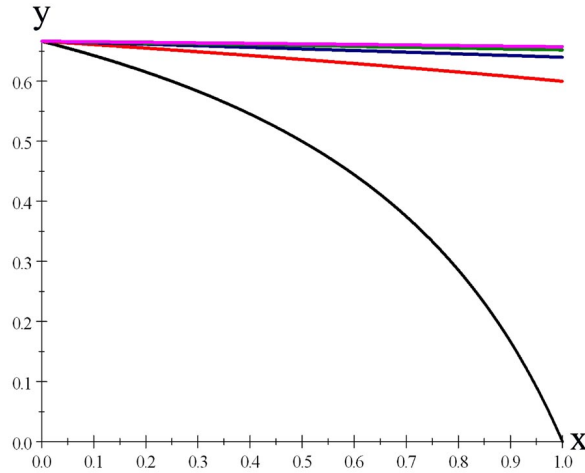


Figure 17.32 Ratio $\frac{\sigma_c}{\sigma_y^0}$ for $\gamma = 0.5$

Remark 44 (a) Starting at $n = 2$ the ratio $y = \frac{\sigma_c}{\sigma_y^0}$ has a linear aspect and tends towards an uniform limit $\frac{1}{1 + \gamma}$, which is 0.667 for the case plotted in Figure 17.21;

(b) The case $n = 2$ is an upper bound for the other cases.

The above calculations were derived for the *pin-ended Ideal Column*, but similar derivations can be conducted for other types of boundary conditions.

1.5.2 Effects of Shear Deformation on the Critical Load Calculation

In the classical buckling theory the influence of the shear force is neglected by accepting the valability of the Bernoulli-Euler deformation model. All the buckling cases investigated so far in the present lecture are using this assumption. In the technical literature the shear force influence on the lateral deformation of a beam is known as the *Timoshenko beam model*. This mathematical model, introduced by *Stephan Timoshenko*, relaxes the Bernoulli-Euler assumption, the supposed normality of the cross-section on the deflection curve after the lateral deformation of the beam appears, and consequently, the slope θ of the deflection curve is different of the rotation angle ϕ characterizing the rotation of the cross-section.

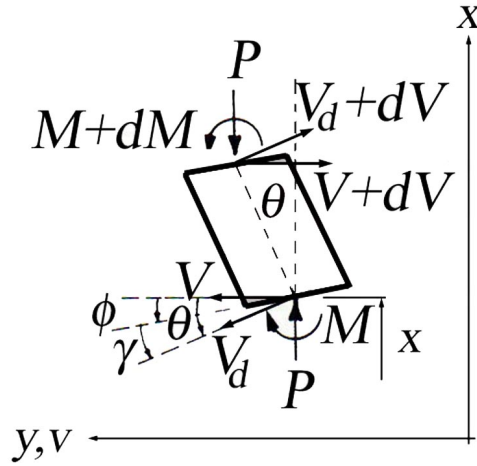


Figure 17.33 Shear Deformation

As shown in Figure 17.33, the difference between the two angles, θ and ϕ , is the rotation angle γ induced by the shear force V_d acting on the cross-section of the deformed shape configuration. Consequently, the following angular relation holds:

$$\theta = \phi + \gamma \quad (211)$$

The rotation angle of the cross-section, ϕ , due exclusively to the action of the bending moment $M(x)$, is expressed, as before, as:

$$\frac{1}{\rho} = \frac{d\phi}{dx} = \frac{M}{EI_z} \quad (212)$$

The rotation angle γ , induced by the shear force V_d , is obtained considering the linear relation expressed by *Hook's Law* :

$$\gamma = \frac{\tau}{G} \quad (213)$$

where τ and G are the shear stress and material shear modulus in a point of the cross-section, respectively.

The shear stress τ varies on the cross-section accordingly to the *Jurawski's Formula*, from zero value at the exterior fibers to a maximum value at the neutral axis, and in accordance with equation (213), the shear strain γ follows a similar distribution. The angle γ is then approximated by an average value representative of the entire cross-section as:

$$\gamma = \frac{1}{G} * \frac{V_d}{m * A} = \frac{V_d}{G * A_V} \quad (214)$$

where the shear transferring area A_V is defined as a percentage of the entire cross-section area A :

$$A_V = m * A \quad (215)$$

and m is the shear correction factor accounting for the non-uniform distribution of the shear stress on the cross-section.

The most frequent used shear correction factors m are:

- 0.83 for rectangular cross-section;
- 0.90 for circular cross-section;
- 0.606 for thin-walled tube cross-section;
- $\frac{A_{web}}{A}$ for I-type cross-section.

Employing the differential relation between the shear force V_d and the bending moment M , given by the equilibrium equation (48), the equation (214) is recasted as:

$$\gamma = -\frac{1}{G * A_V} * \frac{dM}{dx} \quad (216)$$

Substituting equation (216) into equation (211) and considering the validity of the "small deformation" assumption ($\theta \simeq \frac{dv}{dx}$), a differential relation is obtained:

$$\frac{dv}{dx} = \phi - \frac{1}{G * A_V} * \frac{dM}{dx} \quad (217)$$

Differentiating again the above obtained equation:

$$\frac{d^2v}{dx^2} = \frac{d\phi}{dx} - \frac{1}{G * A_V} * \frac{d^2M}{dx^2} \quad (218)$$

and then substituting equation (212) into it, a differential relation between the deflection curve $v(x)$ and the bending moment $M(x)$ is obtained:

$$\frac{d^2v}{dx^2} = \frac{M}{EI_z} - \frac{1}{G * A_V} * \frac{d^2M}{dx^2} \quad (219)$$

Remark 45 (a) The equation (219) is similar to the second order differential equation derived in Volume I to calculate the deflection of the beams subjected to transversal loads. The difference of the two formulae is the second term of the right side of the equation (219), term accounting for the influence of the shear force on the deflection;

(b) In order for the differential equation to be solved the variation of the bending moment $M(x)$ along the entire length l of the beam has to be known, a case valid for determinate columns only. To extend the validity of the formulation to the undetermined type of columns a differential relation between loads and deflection has to be derived.

1.5.2.1 pin-ended Column For the classical case of the *Ideal Euler Column*, the pin-ended column, the bending moment $M(x)$ is expressed from the equilibrium as:

$$M(x) = -P * v(x) \quad (220)$$

Substituting equation (?? into differential equation (219):

$$\frac{d^2v}{dx^2} = \frac{-P}{EI_z} * v + \frac{P}{G * A_V} * \frac{d^2v}{dx^2} \quad (221)$$

and after algebraic manipulations the following differential relation is obtained:

$$v'' + \frac{P}{(1 - \frac{P}{G * A_V})EI_z} * v = 0 \quad (222)$$

The differential equation (222) is recasted in a format identical with that equation (21):

$$v'' + k_m^2 * v = 0 \quad (223)$$

where

$$k_m^2 = \frac{P}{(1 - \frac{P}{G * A_V}) * E * I_z} = \frac{P}{\beta * E * I_z} \quad (224)$$

Remark 46 The difference between the expression of the parameter k^2 and k_m^2 used in equations (21) and (224), respectively, is the correction factor β introducing the influence of the shear force.

$$\beta = 1 - \frac{P}{G * A_V} \quad (225)$$

The solution of the differential equation (223) is:

$$v(x) = C_1 * \sin(k_m * x) + C_2 * \cos(k_m * x) \quad (226)$$

where C_1 and C_2 are integration constants determined imposing the boundary conditions.

The hinged-pined *Ideal Euler Column* is characterized by the following boundary conditions

$$(a) \text{ at } x = 0 \rightarrow v(x = 0) = 0$$

$$C_1 * \sin(k_m * 0) + C_2 * \cos(k_m * 0) = 0 \quad \rightarrow C_2 = 0 \quad (227)$$

$$(b) \text{ at } x = l \rightarrow v(x = l) = 0$$

$$\begin{aligned} C_1 * \sin(k_m * l) &= 0 \rightarrow \\ \sin(k_m * l) &= 0 \text{ and } C_1 \neq 0 \rightarrow \end{aligned} \quad (228)$$

From equation results:

$$k_m * l = n * \pi \quad n = 1, 2, \dots \text{and } C_1 \neq 0 \quad (229)$$

Substituting equation (229) into equation (224) and solving for P the expression of the critical load P_{cr} is calculated:

$$\begin{aligned} k_m^2 &= \left(\frac{n * \pi}{l}\right)^2 \rightarrow \frac{P_{cr}^m}{\left(1 - \frac{P_{cr}^m}{G * A_V}\right) * E * I_z} = \left(\frac{n * \pi}{l}\right)^2 \rightarrow \\ P_{cr}^m &= \left(1 - \frac{P_{cr}^m}{G * A_V}\right) * \frac{n^2 * \pi^2 * E * I_z}{l^2} \rightarrow \\ P_{cr}^m &= \left(1 - \frac{P_{cr}^m}{G * A_V}\right) * n^2 * P_{cr}^E \end{aligned} \quad (230)$$

where

$$P_{cr}^E = \frac{\pi^2 * E * I_z}{l^2} \quad (231)$$

is the critical axial load calculated when the shear force influence is neglected.

The expression of the critical load P_{cr}^m is then calculated:

$$P_{cr}^m = \frac{n^2}{1 + n^2 * \frac{P_{cr}^E}{G * A_V}} * P_{cr}^E = \frac{1}{\frac{1}{n^2} + \frac{P_{cr}^E}{G * A_V}} * P_{cr}^E \quad (232)$$

The critical normal stress σ_{cr}^m existing on the cross-section before the bifurcation point is:

$$\begin{aligned} \sigma_{cr}^m &= \frac{P_{cr}^m}{A} = \frac{n^2}{1 + n^2 * \frac{P_{cr}^E}{G * A_V}} * \sigma_{cr}^E = \frac{n^2}{1 + \frac{n^2 * \frac{\pi^2 * E * I_z}{l^2}}{G * A_V}} * \frac{\pi^2 * E}{\lambda^2} = \\ &= \frac{n^2}{1 + \frac{n^2 * \pi^2 * E * I_z}{l^2 * G * A_V}} * \frac{\pi^2 * E}{\lambda^2} = \frac{n^2}{1 + \frac{n^2 * \pi^2 * E * r_z^2 * A}{l^2 * G * m * A}} * \frac{\pi^2 * E}{\lambda^2} = \\ &= \frac{n^2}{1 + \frac{n^2 * \pi^2 * 2 * (1 + \nu) * G}{m * \frac{l^2}{r_z^2} * G}} * \frac{\pi^2 * E}{\lambda^2} = \frac{n^2}{1 + \frac{2 * n^2 * (1 + \nu) * \pi^2}{m * \lambda^2}} * \frac{\pi^2 * E}{\lambda^2} = \\ &= \frac{n^2 * \pi^2 * E}{\lambda^2 * (1 + \frac{2 * n^2 * (1 + \nu) * \pi^2}{m * \lambda^2})} = \frac{\pi^2 * E}{\lambda^2 * (\frac{1}{n^2} + \frac{2 * (1 + \nu) * \pi^2}{m * \lambda^2})} = \frac{\sigma_{cr}^E}{\frac{1}{n^2} + \frac{2 * (1 + \nu) * \pi^2}{m * \lambda^2}} \end{aligned} \quad (233)$$

where ν is the *Poisson's ratio*.

Remark 47 Analyzing equation (232) and (233) is found that the smallest values, the engineering interest values, are obtained for $n = 1$:

$$P_{cr}^m = \frac{1}{1 + \frac{P_{cr}^E}{G * A_V}} * P_{cr}^E \quad (234)$$

and

$$\begin{aligned} \sigma_{cr}^m &= \frac{1}{1 + \frac{2 * (1 + \nu) * \pi^2}{m * \lambda^2}} * \sigma_{cr}^E = \frac{\pi^2 * E}{\lambda^2 * (1 + \frac{2 * (1 + \nu) * \pi^2}{m * \lambda^2})} = \\ &= \frac{\pi^2 * E}{\lambda_m^2} \end{aligned} \quad (235)$$

where λ_m is the *transformed slenderness*:

$$\lambda_m = \sqrt{\lambda^2 * (1 + \frac{2 * (1 + \nu) * \pi^2}{m * \lambda^2})} = \lambda * \sqrt{1 + \frac{2 * (1 + \nu) * \pi^2}{m * \lambda^2}} \quad (236)$$

The expression of the critical stress σ_{cr}^m is limited by the extent of the elastic range to σ_y^0 :

$$\sigma_{cr}^m = \frac{\pi^2 * E}{\lambda_m^2} \leq \sigma_y^0 \quad (237)$$

The slenderness limit λ_{m0} is obtained from the limit of equation (237):

$$\lambda_{m0} = \pi * \sqrt{\frac{E}{\sigma_y^0}} \quad (238)$$

Remark 48 (a) The expression (238) indicates that for a slenderness $\lambda \geq \lambda_{m0}$ the critical normal stress $\sigma_{cr}^m \leq \sigma_y^0$. For structural steel ($E = 200\text{GPa}$, $\sigma_y^0 = 250\text{MPa}$, $\nu = 0.3$) and aluminium ($E = 73\text{GPa}$, $\sigma_y^0 = 410\text{MPa}$, $\nu = 0.33$) the transformed slenderness limit λ_{m0} are 89 and 42, respectively. Employing relation (236) the corresponding λ values are calculated:

- for steel $\lambda = 88.781 - 88.856$ when m varies from 0.66 to 1.00, respectively;

- for aluminum $\lambda = 41.524 - 41.686$ when m varies from 0.66 to 1.00, respectively

The above calculated values indicate a negligible error of $\frac{88.781}{89} = 0.99754$ and $\frac{41.524}{42} = 0.98867$ when the slenderness limit λ_0 is used instead of λ_{m0} . The variation of ratio $\frac{\lambda_m}{\lambda} = \sqrt{1 + \frac{2 * (1 + \nu) * \pi^2}{m * \lambda^2}}$ for $\nu = 0.3$ and $m = 0.66$ is shown in Figure 17.34.

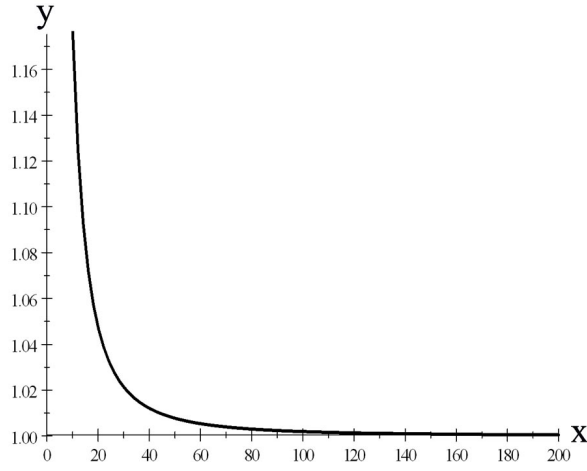


Figure 17.34 Ratio $\frac{\lambda_m}{\lambda}$

Surveying the graph, it can be concluded that for the elastic range limited between slenderness values $\lambda_{m0} \leq \lambda \leq 200$ the ratio $\frac{\lambda_m}{\lambda} \simeq 1.00$.

(b) The variation of the critical stress σ_{cr}^m with the slenderness λ_m is expressed as:

$$\sigma_{cr}(\lambda) = \begin{cases} \sigma_y & \text{if } \lambda < \lambda_{m0} \\ \frac{E\pi^2}{\lambda_{m0}^2} & \text{if } \lambda \geq \lambda_{m0} \end{cases} \quad (239)$$

Remark 49 Considering that the ratio $\frac{\lambda_m}{\lambda} \simeq 1.00$ the variation of critical normal stress $\sigma_{cr}^m(\lambda_m)$ is similar with the critical normal stress $\sigma_{cr}(\lambda)$ shown in Figure 17.7.

(d) The critical load P_{cr}^m , calculated when the influence of the shear force is considered, is smaller than the critical force P_{cr}^E , calculated neglecting the shear force influence:

$$P_{cr}^m < P_{cr}^E \quad (240)$$

For the compact cross-sections discussed above, characterized by with m varying between 0.67 and 1, the critical load P_{cr}^m is well approximated by the critical load P_{cr} :

$$P_{cr}^m = \sigma_{cr}^m * A \simeq \sigma_{cr} * A = P_{cr}^E \quad (241)$$

The situation changes for the case of built-up cross-sections.

1.5.2.2 Other Rigid End Conditions To obtain expression of critical load P_{cr}^m pertinent to other types of rigid end conditions, where the function of the bending moment $M(x)$ is not known in advance, a more involved theoretical approach, some how similar

to the one used in the absence of the shear force, must be used. The know function of the transversal load $p_n(x)$ has to be used instead of the bending moment $M(x)$.

Two unknown functions, the displacement $v(x)$ and rotation angle of the cross-section $\phi(x)$, have to be expressed relatively to the variation of the transversal loading force $p_n(x)$. *Because the bending moment is not related any more directly to the second derivative of the deflection $v(x)$, bboth functions, $v(x)$ and $\phi(x)$, are necessary to correctly express the static and kinematic boundary conditions.* Consequently, a system of two differential equations has to be obtained.

The first differential equation of the system is obtained by twice differentiating equation (212) and then successively employing the equilibrium equations, (47) and (46):

$$\begin{aligned}\frac{d^2}{dx^2}\left(\frac{d\phi}{dx}\right) &= \frac{d^2}{dx^2}\left(\frac{M}{E * I_z}\right) \rightarrow \frac{d^3\phi}{dx^3} = \frac{1}{E * I_z} * \frac{d^2M}{dx^2} \rightarrow \\ \frac{d^3\phi}{dx^3} &= \frac{1}{E * I_z} * \frac{d}{dx}\left(V - P * \frac{dv}{dx}\right) \rightarrow \frac{d^3\phi}{dx^3} = \frac{1}{E * I_z} * \left(\frac{dV}{dx} - P * \frac{d^2v}{dx^2}\right) \rightarrow \\ \frac{d^3\phi}{dx^3} &= \frac{1}{E * I_z} * (-p_n(x) - P * \frac{d^2v}{dx^2}) \rightarrow E * I_z * \phi''' + P * v'' = -p_n(x)\end{aligned}\quad (242)$$

The second differential of the system is obtained by differentiating equation (212) and then substituting it into equations (217):

$$\begin{aligned}\frac{d}{dx}\left(\frac{d\phi}{dx}\right) &= \frac{d}{dx}\left(\frac{M}{E * I_z}\right) \rightarrow \frac{d^2\phi}{dx^2} = \frac{1}{E * I_z} * \frac{dM}{dx} \rightarrow \\ \frac{dv}{dx} &= \phi - \frac{1}{G * A_V} * \frac{dM}{dx} \rightarrow \frac{dv}{dx} = \phi - \frac{E * I_z}{G * A_V} * \frac{d^2\phi}{dx^2} \rightarrow \\ \frac{E * I_z}{G * A_V} * \phi'' + v' - \phi &= 0 \rightarrow E * I_z * \phi'' + G * A_V * (v' - \phi) = 0\end{aligned}\quad (243)$$

In the absence of the lateral loading $p_n(x) = 0$ the differential equations (242) and (243) represent a *differential homogeneous ordinary system with constant coefficients*. *The differential system is recasted as:*

$$\begin{aligned}\phi''' + \frac{P}{E * I_z} * v'' &= 0 \\ \phi'' + \frac{G * A_V}{E * I_z} * (v' - \phi) &= 0\end{aligned}\quad (244)$$

The solutions of the differential system (244) are expressed as:

$$\begin{aligned} v(x) &= A * \exp(\eta * x) \\ \phi(x) &= B * \exp(\eta * x) \end{aligned} \quad (245)$$

where η , A and B are integration constants.

The solutions (245) have to verify the differential equations (244) and consequently, by substituting them back into equations (244), the following system is obtained:

$$\begin{aligned} B * \eta^3 * \exp(\eta * x) + \frac{P}{E * I_z} * A * \eta^2 * \exp(\eta * x) &= 0 \rightarrow (246) \\ (B * \eta + \frac{P}{E * I_z} * A) * \eta^2 * \exp(\eta * x) &= 0 \\ B * \eta^2 * \exp(\eta * x) + \frac{G * A_V}{E * I_z} * (A * \eta * \exp(\eta * x) - B * \exp(\eta * x)) &= 0 \rightarrow \\ [B * \eta^2 + \frac{G * A_V}{E * I_z} * (A * \eta - B)] * \exp(\eta * x) &= 0 \end{aligned}$$

and after algebraic manipulations:

$$\begin{aligned} (\frac{P}{E * I_z} * A + B * \eta) * \eta^2 * \exp(\eta * x) &= 0 \\ [(\frac{G * A_V}{E * I_z} * \eta) * A + (\eta^2 - \frac{G * A_V}{E * I_z}) * B] * \exp(\eta * x) &= 0 \end{aligned} \quad (247)$$

For the integration constant A and B to have solutions different than the trivial solution ($A = B = 0$) the *determinant* $\Omega(\eta)$ must be zero:

$$\Omega(\eta) = \begin{bmatrix} \frac{P}{E * I_z} & \eta \\ \frac{G * A_V}{E * I_z} * \eta & \eta^2 - \frac{G * A_V}{E * I_z} \end{bmatrix} = 0 \quad (248)$$

The characteristic equation of the determinant $\Omega(\eta)$ is:

$$G * P * A_V + E * I_z * (G * A_V - P) * \eta^2 = 0 \quad (249)$$

Solving equation (249) for η^2 an expression identical to expression (224), of k_m^2 , is obtained.

$$\begin{aligned}\eta^2 &= \frac{G * A_V * P}{E * I_z * (G * A_V - P)} = \frac{P}{E * I_z * (1 - \frac{P}{G * A_V})} = \\ &= \frac{P}{E * I_z * \beta} = k_m^2\end{aligned}\tag{250}$$

The general solutions for $v(x)$ and $\phi(x)$ are expressed as follows instead of (245):

$$v(x) = C_1 * \sin(k_m * x) + C_2 \cos(k_m * x) + C_3 * x + C_4\tag{251}$$

and

$$\phi(x) = \beta * C_1 * k_m * \cos(k_m * x) - \beta * C_2 * k_m * \sin(k_m * x) + C_3\tag{252}$$

where C_1 , C_2 , C_3 and C_4 are integration constants obtained imposing the boundary conditions at the ends of the column.

The expressions of the deflection $v(x)$ and rotation angle of the cross-section $\phi(x)$ first, second and third derivatives are:

$$v'(x) = \frac{d}{dx}v(x) = k_m * C_1 * \cos(k_m * x) - k_m * C_2 * \sin(k_m * x) + C_3\tag{253}$$

$$v''(x) = \frac{d^2}{dx^2}v(x) = -k_m^2 * C_1 * \sin(k_m * x) - k_m^2 * C_2 * \cos(k_m * x)\tag{254}$$

$$v'''(x) = \frac{d^3}{dx^3}v(x) = -k_m^3 * C_1 * \cos(k_m * x) + k_m^3 * C_2 * \sin(k_m * x)\tag{255}$$

$$\phi'(x) = \frac{d}{dx}\phi(x) = -\beta * C_1 * k_m^2 * \sin(k_m * x) - \beta * C_2 * k_m^2 * \cos(k_m * x)\tag{256}$$

$$\phi''(x) = \frac{d^2}{dx^2}\phi(x) = -\beta * C_1 * k_m^3 * \cos(k_m * x) + \beta * C_2 * k_m^3 * \sin(k_m * x) \quad (257)$$

$$\phi'''(x) = \frac{d^3}{dx^3}\phi(x) = \beta * C_1 * k_m^4 * \sin(k_m * x) + \beta * C_2 * k_m^4 * \cos(k_m * x) \quad (258)$$

The validity of the solutions (251).and (252).is verify by substituting them back into equations (244).

The boundary conditions are judge in a similar manner as these when the shear force is neglected. The novaly consists in the fact that the rotation of the cross-section is the angle $\phi(x)$ and not on $\theta(x)$. They are:

$$\begin{array}{llll} \circ & \text{fixed end} & v & = 0 & \phi = 0 \\ \circ & \text{pinned end} & v & = 0 & M = 0 \\ \circ & \text{free end} & M & = 0 & V = 0 \\ \circ & \text{fixed-sliding end} & \phi & = 0 & V = 0 \end{array} \quad (259)$$

The condition $M = 0$ implies throught relation (212) $\phi' = 0$, while $V = 0$ represents, in accordance to equation (47) a more complicated relation. The shear force V is expressed as $V = \frac{dM}{dx} + P*v' = E*I_z*\phi'' + P*v' = E*I_z*(\phi'' + \frac{P}{E * I'_z}*v') = E*I_z*(\phi'' + \beta*k_m^2*v')$ and consequently, the end condition $V = 0$ becomes $\phi'' + \beta * k_m^2 * v' = 0$. After algebraic manipulations the final expression is $k_m^2\beta C_3 = 0$.

To exemplify the application of the theoretical derivation, the case of the fixed-fixed column, shown in Figure 17.10.b is investigated. The integration constants are obtained enforcing the following end conditions:

- at point O ($x = 0$):

$$\begin{aligned} v(x = 0) &= 0 \rightarrow C_1 * \sin(k_m * 0) + C_2 \cos(k_m * 0) + C_3 * 0 + C_4 = 0 \rightarrow \\ &\rightarrow C_2 + C_4 = 0 \end{aligned} \quad (260)$$

$$\begin{aligned} \phi(x = 0) &= 0 \rightarrow \beta * C_1 * k_m * \cos(k_m * 0) - \beta * C_2 * k_m * \sin(k_m * 0) + C_3 = 0 \\ &\rightarrow \beta * C_1 * k_m + C_3 = 0 \end{aligned} \quad (261)$$

- at point A ($x = l$):

$$v(x = l) = 0 \rightarrow C_1 * \sin(k_m * l) + C_2 * \cos(k_m * l) + C_3 * l + C_4 = 0 \quad (262)$$

$$\phi(x = l) = 0 \rightarrow \beta * C_1 * k_m * \cos(k_m * l) - \beta * C_2 * k_m * \sin(k_m * l) + C_3 = 0 \quad (263)$$

The determinant $\Delta(k)$ is:

$$\Delta(k) = \begin{bmatrix} 0 & 1 & 0 & 1 \\ \beta * k_m & 0 & 1 & 0 \\ \sin(k_m * l) & \cos(k_m * l) & l & 1 \\ \beta * k_m * \cos(k_m * l) & -\beta * k_m * \sin(k_m * l) & 1 & 0 \end{bmatrix} = \quad (264)$$

$$= -l * k_m^2 * \beta^2 * \sin(k_m * l) + k_m * \beta * \cos^2(k_m * l) - 2 * k_m * \beta * \cos(k_m * l) + k_m \beta \sin^2 k_m l + k_m \beta + k_m * \beta * \sin^2(k_m * l) + k_m * \beta \quad (265)$$

The resulting characteristic equation is:

$$\begin{aligned} -l * k_m^2 * \beta^2 * \sin(k_m * l) - 2 * k_m * \beta \cos(k_m * l) + 2 * k_m * \beta &= 0 \rightarrow \\ k_m * \beta * [2 - 2 * \cos(k_m * l) - l * k_m * \beta * \sin(k_m * l)] &= 0 \rightarrow \\ 2 - 2 * \cos(k_m * l) - l * k_m * \beta * \sin(k_m * l) &= 0 \text{ and } k_m * \beta \neq 0 \end{aligned}$$

The solution of the characteristic equation is obtained graphically, by plotting the function located on the left side of the equation. The plot shown in Figure 17.35 contains a number of curves corresponding to $\beta = (1, 0.9, 0.5, 0.3)$.

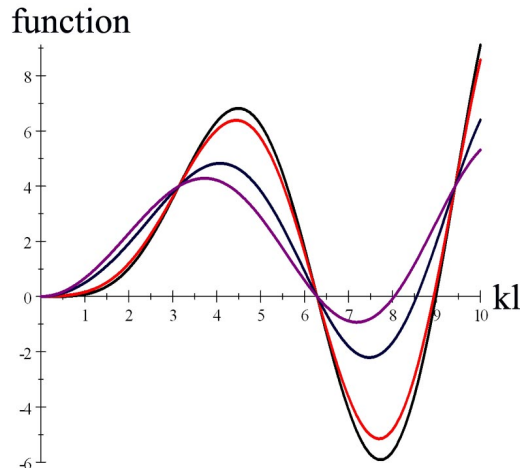


Figure 17.35

From the graph it can be seen that for all β the solutions coincide with:

$$k_m l = 2 * \pi \quad (266)$$

The first critical load P_{cr}^m is calculated from (250) as:

$$\begin{aligned} P_{cr}^m &= E * I_z * \beta * k_m^2 = E * I_z * \beta * \frac{4 * \pi^2}{l^2} = \\ &= \frac{P_{cr}^E}{1 + \frac{P_{cr}^E}{G * A_v}} \end{aligned} \quad (267)$$

where the critical load P_{cr}^E is the critical load calculated neglecting the shear force influence:

$$P_{cr}^E = E * I_z * \frac{\pi^2}{(\frac{l}{2})^2} = E * I_z * \frac{\pi^2}{l_b^2}$$

and the buckling length l_b is:

$$l_b = \frac{l}{2} = 0.5 * l \quad (268)$$

The critical normal stress σ_{cr}^m is calculated:

$$\sigma_{cr}^m = \frac{P_{cr}^m}{A} \quad (269)$$

Remark 50 (a) The expression (267) of the critical load is mathematically identical to the expression calculated for the Ideal Euler's Column (has different end conditions). Obviously the expression of the P_{cr}^E is different for each case, depending on the specific buckling length;

(b) Due to the mathematical identity, all the other conclusions reached during the Ideal Euler's Column investigation remain valid;

(c) The above conclusions must be checked for individual cases of end restrains.

1.5.3 Buckling of Columns Subjected to Inclined Loads

In the previous theoretical derivations the axial compressive load P always kept its vertical direction during the stability loss. Nevertheless, in some cases the compressive force P rotates during the lateral deflection taking place at the bifurcation time. To exemplify this aspect, the case of the fixed-free column subjected to compressive force P passing through a fixed point C , as shown in Figure 17.36.a, is considered. Practically, this case represents the situation of a stretched cable attached with one end to the cantilever tip A and the other to the fixed point C .

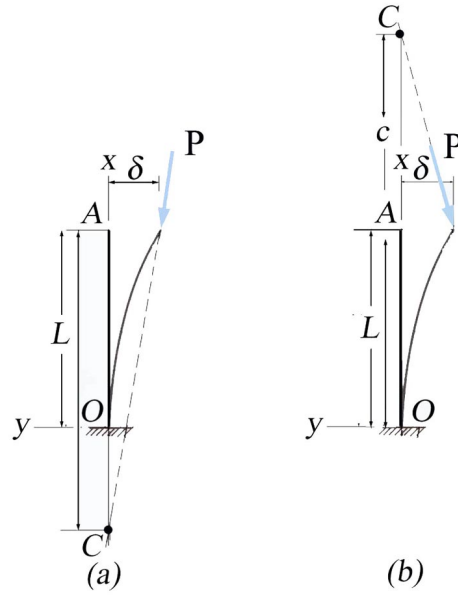


Figure 17.36 Buckling under Inclined Load

At the bifurcation point, the tip of the cantilever suffers a small lateral displacement δ . The main difference from the similar case analyzed before is the fact that the shear force V at the cantilever tip has a value, $P * \frac{\delta}{c}$, equal to the horizontal projection of the compressive force P . The integration constants C_1 , C_2 , C_3 and C_4 are obtained by imposing the boundary conditions at the cantilever ends. They are:

- at the fixed end point O ($x = 0$):

$$v(x = 0) = C_1 * \sin(k * 0) + C_2 \cos(k * 0) + C_3 * 0 + C_4 = 0 \rightarrow C_2 + C_4 = 0 \quad (270)$$

$$\theta(x = 0) = k * C_1 * \cos(k * 0) - k * C_2 * \sin(k * 0) + C_3 = 0 \rightarrow k * C_1 + C_3 = 0 \quad (271)$$

- at the free end A ($x = l$):

$$\begin{aligned}
-M(x = l) = 0 &\rightarrow E * I_z * v''(x = l) = 0 \rightarrow \\
&= -k^2 * C_1 * \sin(k * l) - k^2 * C_2 * \cos(k * l) = 0
\end{aligned} \tag{272}$$

$$\begin{aligned}
-V(x = l) + P * \frac{\delta}{c} &= 0 \rightarrow (E * I_z * v^{III}(x = l)) + P * v'(x = l) + P * \frac{\delta}{c} = 0 \\
&\rightarrow k^2 * E * I_z * C_3 = P * \frac{\delta}{c} \rightarrow P * C_3 = P * \frac{\delta}{c} \rightarrow C_3 = \frac{\delta}{c}
\end{aligned} \tag{273}$$

Combining the algebraic equations (270) through (273) an algebraic system of four equations is obtained:

$$\Delta(k) = \begin{bmatrix} 0 & 1 & 0 & 1 \\ k & 0 & 1 & 0 \\ -k^2 * \sin(k * l) & -k^2 * \cos(k * l) & 0 & 0 \\ 0 & 0 & 1 & 0 \end{bmatrix} \begin{bmatrix} C_1 \\ C_2 \\ C_3 \\ C_4 \end{bmatrix} = \begin{bmatrix} 0 \\ 0 \\ 0 \\ \frac{\delta}{c} \end{bmatrix} \tag{274}$$

, Solution is:
$$\begin{bmatrix} -\frac{1}{ck} \frac{\delta}{\cos kl} \sin kl \\ \frac{1}{ck} \frac{\delta}{\cos kl} \sin kl \\ -\frac{1}{ck} \frac{\delta}{\cos kl} \sin kl \end{bmatrix}$$

The solutions of the algebraic system (274) are:

$$\begin{bmatrix} C_1 \\ C_2 \\ C_3 \\ C_4 \end{bmatrix} = \begin{bmatrix} -\frac{\delta}{c * k} \\ \frac{\delta}{c * k} * \tan(k * l) \\ \frac{\delta}{c} \\ -\frac{\delta}{c * k} * \tan(k * l) \end{bmatrix} = -\frac{\delta}{c * k} * \begin{bmatrix} 1 \\ -\tan(k * l) \\ -k \\ \tan(k * l) \end{bmatrix} \tag{275}$$

Substituting the constants into the general solution (57) the expression of lateral displacement $v(x)$ and its superior derivatives are obtained:

$$\begin{aligned}
v(x) &= -\frac{\delta}{c * k} * \sin(k * x) + \frac{\delta}{c * k} * \tan(k * l) * \cos(k * x) + \frac{\delta}{c} * x - \frac{\delta}{c * k} * \tan(k * l) * \sin(k * x) \\
&= -\frac{\delta}{c * k} * [\sin(k * x) - \tan(k * l) * \cos(k * x) - k * x + \tan(k * l)]
\end{aligned} \tag{276}$$

$$\theta(x) = v'(x) = -\frac{\delta}{c * k} * [k * \cos(k * x) + k * \tan(k * l) * \sin(k * x) - k] \quad (277)$$

$$v''(x) = -\frac{\delta}{c * k} * [-k^2 * \sin(k * x) + k^2 * \tan(k * l) * \cos(k * x)] \quad (278)$$

$$v'''(x) = -\frac{\delta}{c * k} * [-k^3 * \cos(k * x) - k^3 * \tan(k * l) * \sin(k * x)] \quad (279)$$

The bending moment $M(x)$ and shear force $V_d(x)$ are:

$$M(x) = E * I_z * v''(x) = -\frac{\delta}{c * k} * E * I_z * [-k^2 * \sin(k * x) + k^2 * \tan(k * l) * \cos(k * x)] \quad (280)$$

$$V_d(x) = \frac{dM(x)}{dx} = E * I_z * v'''(x) = -\frac{\delta}{c * k} * E * I_z * [-k^3 * \cos(k * x) - k^3 * \tan(k * l) * \sin(k * x)] \quad (281)$$

The lateral displacement $v(x = l)$ has to be equal to the initially considered δ . Then, this condition is expressed as:

$$-\frac{\delta}{c * k} * [\sin(k * l) - \tan(k * l) * \cos(k * l) - k * l + \tan(k * l)] = \delta \quad (282)$$

After algebraic manipulations, the above equation becomes:

$$\begin{aligned} \tan(k * l) - k * l &= -c * k \rightarrow \tan(k * l) = -c * k + k * l \rightarrow \\ &\rightarrow \tan(k * l) = k * l * (1 - \frac{c}{l}) \rightarrow \\ &\rightarrow \tan(k * l) - k * l * (1 - \frac{c}{l}) = 0 \end{aligned} \quad (283)$$

Equation (283) is the *stability criterion*. The functional relation between $k * l$ and $\frac{c}{l} \in [0, \infty]$, represented by equation (283), is graphically depicted in Figure 17.37.

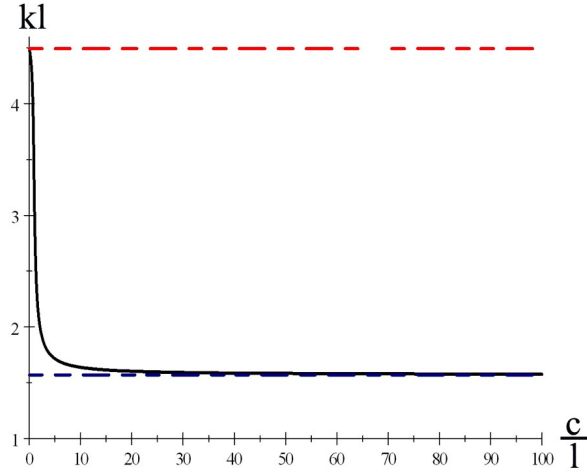


Figure 17.37

Remark 51 (a) The variation of $k * l$ with the ratio $\frac{c}{l}$ is a continuous decreasing function. The $k * l$ value abruptly decreases, almost linearly, from $\frac{c}{l} = 0$ through $\frac{c}{l} = 3.6$, followed by a slow variation and then, from $\frac{c}{l} = 10$ tends asymptotically towards the value 1.5709.

(b) for $\frac{c}{l} = 0$ the equation (283) reduces to $\tan(k * l) - k * l = 0$, the characteristic equation of the fixed-pinned column, and consequently $k * l = 4.493$. The corresponding buckling length is $l_b = 0.7 * l$;

(c) for $\frac{c}{l} = 3.6$ the solution, numerically obtained, is $k * l = 1.783$;

(d) for $\frac{c}{l} = 10$ the solution, numerically obtained, is $k * l = 1.6395$;

(e) for $\frac{c}{l} = \infty$ the solutions $k * l = 1.5709$, a value corresponding to fixed-free condition ($l_b = 2 * l$).

The buckling load P_{cr} and length l_b are both bounded:

$$0.25 * P_{cr}^E \leq P_{cr} \leq 2.07 * P_{cr}^E \quad (284)$$

$$0.7 * l \leq l_b \leq 2 * l \quad (285)$$

Remark 52 If the fixed point C is located below the tip of the cantilever an increase of the critical load P_{cr} in comparison to the critical load of the similar fixed-free column $0.25 * P_{cr}^E$ is recorded. The horizontal component plays the role of a horizontal spring and helps lowering the buckling length from $2 * l$ towards $0.7 * l$;

If the point C is located above the cantilever tip A , as shown in Figure 17.36.b, the direction of the force P horizontal projection changes the direction and the equation (283) transforms into:

$$\tan(k * l) - k * l * (1 + \frac{c}{l}) = 0 \quad (286)$$

The graphical representation of $k * l$ as function of $\frac{c}{l}$ the ratio, equation (286), is illustrated in Figure 17.38.

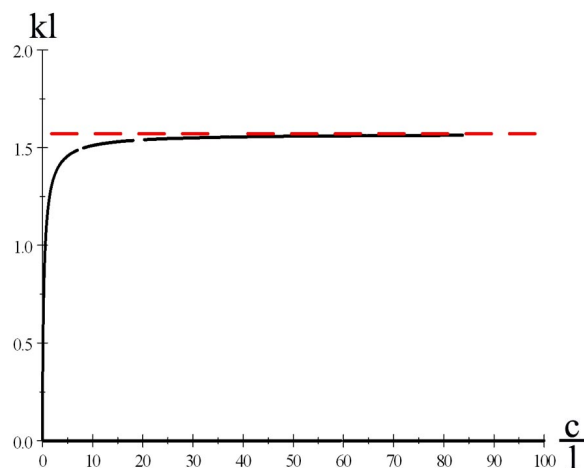


Figure 17.38

Remark 53 *If the fixed point C is located above the tip of the cantilever a decrease of the critical load P_{cr} in comparison to the critical load of the similar fixed-free column $0.25 * P_{cr}^E$ is noticed. The horizontal component increases the lateral deformation of the column, having an averse result on the buckling. For $\frac{c}{l} = 1$ the value of $k * l = 1.1656$, which corresponds to a buckling length $l_b \simeq 2.7 * l$ and critical load $P_{cr} = 0.139 * P_{cr}^E$.*

The buckling load P_{cr} and length l_b are both upper bounded:

$$P_{cr} \leq 0.25 * P_{cr}^E \quad (287)$$

$$l_b \leq 0.7 * l \quad (288)$$

1.5.4 Lateral Disturbing Loads

The assumption of the absence of the transversal, lateral, load considered until now it is just a theoretical idealization. The real columns are always subjected to lateral loads or

end applied moments caused by slightly eccentric application of the compressive force $P = \text{constant}$. The column under consideration is again the *Euler Idealized Column* loaded, this time, with a transversal distributed load $p_n(x)$ and two concentrated moments, M_O and M_A , acting at both ends of the column, in points O and A , respectively. The column and the loading are shown in Figure 17.39.

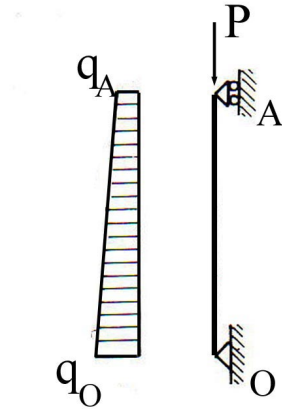


Figure 17.39 Lateral Disturbing Loads

Due to the existence of the lateral load $p_n(x)$, the deflection curve $v(x)$, the solution of the differential equation (52), is calculated accordingly to the general equation (426). This is not a trivial task, but the solution can be found using the methods of the general theory of ordinary differential equations. Where the analytical solution is impossible always the numerical solution is possible. For the case in point, a trapezoidal variation of the transversal load is considered. $p_n(x)$. This type of loading will serve the purpose to verify, for example, if the of Superimposition Principle remain valid in the presence of the compressive force. The load under consideration is expressed:

$$p_n(x) = q_A + \frac{q_O - q_A}{l}(l - x) \quad (289)$$

If the general solution $v(x) = v_0(x) + v_p(x)$ is replaced in the equation (52), a new form of the differential equation is obtained:

$$\left[\frac{d^4}{dx^4} v_0(x) + k^2 * \frac{d^2}{dx^2} v_0(x) \right] + \left[\frac{d^4}{dx^4} v_p(x) + k^2 * \frac{d^2}{dx^2} v_p(x) + \frac{p_n(x)}{E * I_z} \right] = 0 \quad (290)$$

The *first right parenthesis* is similar to the homogeneous differential equation previously solved and has as solution an expression similar to relation (57):

$$v_0(x) = C_1 * \sin(k * x) + C_2 \cos(k * x) + C_3 * x + C_4 \quad (291)$$

with the integration constants, C_1, C_2, C_3 , and C_4 , remained to be determined by imposing the boundary conditions. The solution $v_p(x)$ for *the second right parenthesis* has to be found. If a supplementary condition is imposed on the solution $v_p(x)$:

$$\frac{d^4}{dx^4}v_p(x) = 0 \quad (292)$$

then the expression of the particular solution is obtained by simple integration of:

$$k^2 * \frac{d^2}{dx^2}v_p(x) + \frac{p_n(x)}{E * I_z} = 0 \quad (293)$$

For the proposed load (289) the expression of the particular solution $v_p(x)$ is:

$$\begin{aligned} v_p(x) &= - \int \int \frac{p_n(x)}{k^2 * E * I_z} dx dx \\ &\rightarrow v_p(x) = - \frac{1}{k^2 * E * I_z} \int \int [q_A + \frac{q_O - q_A}{l}(l - x)] dx dx \\ &\rightarrow v_p(x) = - \frac{1}{k^2 * E * I_z} \int \int (q_O - \frac{\Delta q}{l}x) dx dx \\ &\rightarrow v_p(x) = - \frac{1}{k^2 * E * I_z} (\frac{q_O}{2}x^2 - \frac{\Delta q}{6l}x^3) \end{aligned} \quad (294)$$

where $\Delta q = q_O - q_A$.

Remark 54 (a) *The solution is a polynomial of third degree and consequently the condition (292) is verified. This condition can be verify only for polynomials of third order and this limitation considerably reduces the application of this modality of solving the general differential equation (52). For our study this method does the job*

(b) *the particular solution is obtained only by the undefined integrals missing the two generally required integration constants. Introducing these constants the total number will become six and there are available only four boundary conditions. For this reason the two additional integration constants are omitted.*

Combining the solutions (291) and (294) the general solution $v(x)$ is obtained:

$$v(x) = C_1 * \sin(k * x) + C_2 \cos(k * x) + C_3 * x + C_4 - \frac{1}{k^2 * E * I_z} (\frac{q_O}{2}x^2 - \frac{\Delta q}{6l}x^3) \quad (295)$$

The superior derivatives:

$$v'(x) = \frac{d}{dx}v(x) = k * C_1 * \cos(k * x) - k * C_2 * \sin(k * x) + C_3 - \frac{1}{k^2 * E * I_z} (q_O x - \frac{\Delta q}{2l} x^2) \quad (296)$$

$$v''(x) = \frac{d^2}{dx^2}v(x) = -k^2 * C_1 * \sin(k * x) - k^2 * C_2 * \cos(k * x) - \frac{1}{k^2 * E * I_z} (q_O - \frac{\Delta q}{l} x) \quad (297)$$

$$v'''(x) = \frac{d^3}{dx^3}v(x) = -k^3 * C_1 * \cos(k * x) + k^3 * C_2 * \sin(k * x) + \frac{1}{k^2 * E * I_z} \frac{\Delta q}{l} \quad (298)$$

The boundary conditions are:

- at the pined end O ($x = 0$):

$$v(x = 0) = C_1 * \sin(k * 0) + C_2 \cos(k * 0) + C_3 * 0 + C_4 + (0) = 0 \rightarrow C_2 + C_4 = 0 \quad (299)$$

$$M(x = 0) = -M_O \rightarrow E * I_z * v''(x = 0) = -M_O \quad (300)$$

$$\rightarrow E * I_z * [-k^2 * C_1 * \sin(k * 0) - k^2 * C_2 * \cos(k * 0) - \frac{1}{k^2 * E * I_z} (q_O - \frac{\Delta q}{l} 0)] = -M_O$$

$$\rightarrow -k^2 * C_1 * \sin(k * 0) - k^2 * C_2 * \cos(k * 0) - \frac{1}{k^2 * E * I_z} q_O = -\frac{M_O}{E * I_z}$$

$$\rightarrow k^2 * \sin(k * 0) * C_1 + k^2 * \cos(k * 0) * C_2 = \frac{M_O}{E * I_z} - \frac{1}{k^2 * E * I_z} q_O$$

$$\rightarrow k^2 * \sin(k * 0) * C_1 + k^2 * \cos(k * 0) * C_2 = \frac{1}{E * I_z} (M_O - \frac{q_O}{k^2})$$

$$\rightarrow k^2 * C_2 = \frac{1}{E * I_z} (M_O - \frac{q_O}{k^2})$$

- at the pinned end A ($x = l$):

$$v(x = l) = C_1 * \sin(k * l) + C_2 \cos(k * l) + C_3 * l + C_4 - \frac{1}{k^2 * E * I_z} (\frac{q_O}{2} l^2 - \frac{\Delta q}{6l} l^3) \quad (301)$$

$$\rightarrow C_1 * \sin(k * l) + C_2 \cos(k * l) + C_3 * l + C_4 = \frac{1}{k^2 * E * I_z} (\frac{q_O}{2} l^2 - \frac{\Delta q}{6} l^2)$$

$$\rightarrow C_1 * \sin(k * l) + C_2 \cos(k * l) + C_3 * l + C_4 = \frac{l^2}{2 * k^2 * E * I_z} (q_O - \frac{\Delta q}{3})$$

$$\rightarrow C_1 * \sin(k * l) + C_2 \cos(k * l) + C_3 * l + C_4 = \frac{l^2}{6 * k^2 * E * I_z} (2q_O + q_A)$$

$$\begin{aligned}
M(x = l) &= -M_A \rightarrow E * I_z * v''(x = l) = -M_A \rightarrow \\
&\rightarrow E * I_z * [-k^2 * C_1 * \sin(k * l) - k^2 * C_2 * \cos(k * l) - \frac{1}{k^2 * E * I_z} (q_O - \frac{\Delta q}{l} l)] = -M_A \\
&\rightarrow -k^2 * C_1 * \sin(k * l) - k^2 * C_2 * \cos(k * l) - \frac{1}{k^2 * E * I_z} (q_O - \Delta q) = -\frac{M_A}{E * I_z} \\
&\rightarrow -k^2 * C_1 * \sin(k * l) - k^2 * C_2 * \cos(k * l) = -\frac{M_A}{E * I_z} + \frac{1}{k^2 * E * I_z} (q_O - q_O + q_A) \\
&\rightarrow k^2 * C_1 * \sin(k * l) + k^2 * C_2 * \cos(k * l) = \frac{M_A}{E * I_z} - \frac{q_A}{k^2 * E * I_z} \\
&\rightarrow k^2 * C_1 * \sin(k * l) + k^2 * C_2 * \cos(k * l) = \frac{1}{E * I_z} (M_A - \frac{q_A}{k^2})
\end{aligned} \tag{302}$$

The equations (299) through (302) represent a algebraic system of four equations with four unknowns, the integration constants C_1 , C_2 , C_3 , and C_4 . The matricial representation of the system is:

$$\begin{bmatrix} 0 & 1 & 0 & 1 \\ 0 & k^2 & 0 & 0 \\ \sin(k * l) & \cos(k * l) & l & 1 \\ k^2 * \sin(k * l) & k^2 * \cos(k * l) & 0 & 0 \end{bmatrix} \begin{bmatrix} C_1 \\ C_2 \\ C_3 \\ C_4 \end{bmatrix} = \begin{bmatrix} 0 \\ \frac{1}{E * I_z} (M_O - \frac{q_O}{k^2}) \\ \frac{1}{l^2} (2q_O + q_A) \\ \frac{1}{E * I_z} (M_A - \frac{q_A}{k^2}) \end{bmatrix} \tag{303}$$

Solving the system (??) the four integration constants are obtained as:

$$\begin{bmatrix} C_1 \\ C_2 \\ C_3 \\ C_4 \end{bmatrix} = \frac{1}{k^4 E I_z} \begin{bmatrix} -\frac{1}{\sin kl} (q_A - \cos kl * q_O - k^2 M_A + k^2 \cos kl * M_O) \\ -(q_O - k^2 M_O) \\ \frac{1}{6l} ((6 + k^2 l^2) q_A - (6 - 2k^2 l^2) q_O - 6k^2 M_A + 6k^2 M_O) \\ (q_O - k^2 M_O) \end{bmatrix} \tag{304}$$

Replacing the integration constants (304) back into relations (295) and (297) the deflection curve $v(x)$ and bending moment $M(x)$ are calculated:

$$\begin{aligned}
v(x) &= \frac{1}{k^4 EI_z} \left(\left(-\frac{\sin kx}{\sin kl} + \frac{x}{6l} (6 + k^2 l^2) \right) * q_A + \left(\frac{\sin kx}{\sin kl} \cos kl - \cos kx - \frac{x}{6l} (6 - 2k^2 l^2) + 1 \right) * q_O + \right. \\
&\quad \left. + \left(\frac{\sin kx}{\sin kl} k^2 - \frac{x}{l} k^2 \right) * M_A + \left(-\frac{\sin kx}{\sin kl} k^2 \cos kl + k^2 \cos kx + \frac{x}{l} k^2 - k^2 \right) * M_O - k^2 x^2 \left(\frac{q_O}{2} - \frac{q_O - q_A}{6} \right) \right) \\
&= \frac{1}{k^4 EI_z} \left(\left(-\frac{\sin kx}{\sin kl} + \frac{x}{6l} (6 + k^2 l^2) - \frac{k^2}{6l} x^3 \right) * q_A + \left(\frac{\sin kx}{\sin kl} \cos kl - \cos kx - \frac{x}{6l} (6 - 2k^2 l^2) + 1 - \frac{k^2}{6l} x^3 \right) * q_O + \right. \\
&\quad \left. + \left(\frac{\sin kx}{\sin kl} k^2 - \frac{x}{l} k^2 \right) * M_A + \left(-\frac{\sin kx}{\sin kl} k^2 \cos kl + k^2 \cos kx + \frac{x}{l} k^2 - k^2 \right) * M_O \right)
\end{aligned}$$

$$\begin{aligned}
M(x) &= \frac{1}{k^4} \left(\left(k^2 \frac{\sin kx}{\sin kl} \right) * q_A + \left(-k^2 \frac{\sin kx}{\sin kl} \cos kl + k^2 \cos kx \right) * q_O + \left(-k^4 \frac{\sin kx}{\sin kl} \right) * M_A + \right. \\
&\quad \left. + \left(k^4 \frac{\sin kx}{\sin kl} \cos kl - k^4 \cos kx \right) * M_O - \left(k^2 q_O - k^2 x \frac{q_O - q_A}{l} \right) \right) \\
&= \frac{1}{k^4} \left(\left(k^2 \frac{\sin kx}{\sin kl} - \frac{k^2}{l} x \right) * q_A + \left(-k^2 \frac{\sin kx}{\sin kl} \cos kl + k^2 \cos kx - k^2 + \frac{k^2}{l} x \right) * q_O + \right. \\
&\quad \left. + \left(-k^4 \frac{\sin kx}{\sin kl} \right) * M_A + \left(k^4 \frac{\sin kx}{\sin kl} \cos kl - k^4 \cos kx \right) * M_O \right)
\end{aligned}$$

The verification of the boundary conditions is conducted by evaluating the expressions (305) and (306) successively for $x = 0$ and $x = l$.

The above derived expressions of the deflection curve and bending moment are used in the following pages to analyse a series of interesting phenomenon directly related to the structural engineering practice.

1.5.4.1 Lateral constant load If only a lateral constant load q , acts on a *Idealized Euler Column* the above calculated (305) and (306) can be particularized ($q_A = q_O = q$ and $M_A = M_O = 0$) as follows:

$$v(x) = -\frac{q}{2k^4 EI_z \sin kl} (2 \cos kx \sin kl - 2 \cos kl \sin kx - 2 \sin kl + 2 \sin kx + k^2 x^2 \sin kl - k^2 l x \sin kl) \quad (307)$$

$$\begin{aligned}
M(x) &= \frac{q}{k^2} (\cos kx - 1 + \frac{1 - \cos kl}{\sin kl} \sin kx) \\
&= \frac{ql^2}{8} \frac{8}{k^2 l^2} (\cos kx - 1 + \frac{1 - \cos kl}{\sin kl} \sin kx) \\
&= M_{\max}^0 \frac{8}{k^2 l^2} (\cos kx - 1 + \frac{1 - \cos kl}{\sin kl} \sin kx)
\end{aligned} \quad (308)$$

where $M_{\max}^0 = \frac{ql^2}{8}$ is the maximum bending moment calculated in the absence of the compressive force.

The location of the maximum bending moment, $x = \frac{l}{2}$, is determined calculating the point of stationarity of the bending moment $M(x)$ expression (308):

$$\frac{d}{dx}(\cos kx - 1 + \frac{1 - \cos kl}{\sin kl} \sin kx) = 0 \quad (309)$$

Substituting the location $x = \frac{l}{2}$ into the bending moment expression (308), the maximum value of the bending moment is calculated:

$$\begin{aligned} M_{\max} &= M(x = \frac{l}{2}) = M_{\max}^0 \frac{8}{k^2 l^2} (\cos k \frac{l}{2} - 1 + \frac{1 - \cos kl}{\sin kl} \sin k \frac{l}{2}) \\ &= M_{\max}^0 \frac{8}{(\pi \sqrt{\frac{P}{P_E}})^2} (\cos \frac{\pi}{2} \sqrt{\frac{P}{P_E}} - 1 + \frac{1 - \cos \pi \sqrt{\frac{P}{P_E}}}{\sin \pi \sqrt{\frac{P}{P_E}}} \sin \frac{\pi}{2} \sqrt{\frac{P}{P_E}}) \end{aligned} \quad (310)$$

where $kl = \pi \sqrt{\frac{P}{P_E}}$ and $P_E = \frac{\pi^2 EI_z}{l^2}$.

If transformation $y = \sqrt{\frac{P}{P_E}}$ is applied the expression (310) becomes:

$$\begin{aligned} M_{\max} &= M_{\max}^0 \frac{8}{(\pi y)^2} (\cos \frac{\pi}{2} y - 1 + \frac{1 - \cos \pi y}{\sin \pi y} \sin \frac{\pi}{2} y) \\ &= M_{\max}^0 \frac{8}{(\pi y)^2} \frac{1 - \cos(\frac{\pi}{2} y)}{\cos(\frac{\pi}{2} y)} \end{aligned} \quad (311)$$

The variation of the ratio $\frac{M_{\max}}{M_{\max}^0}$ with $\frac{P}{P_E}$ is illustrated in Figure 17.40.

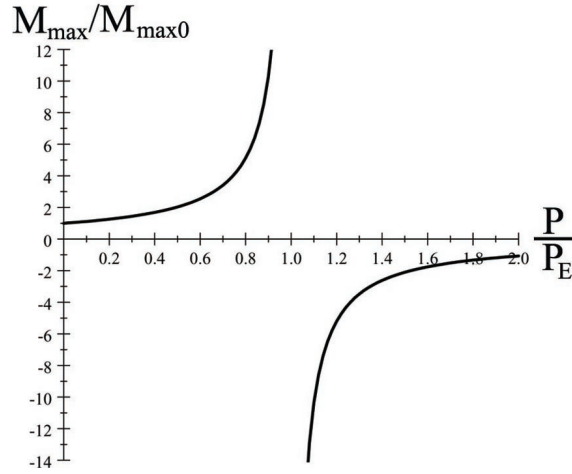


Figure 17.40

In the modern design codes the maximum bending moment M_{\max} is represented in a slightly different format, which is easily generalized for other loading cases and boundary conditions:

$$M_{\max} = M_{\max}^0 \frac{C_m}{1 - \frac{P}{P_E}} \quad (312)$$

where the coefficient C_m is called *magnification factor*:

$$C_m = (1 - y^2) \frac{8}{(\pi y)^2} \frac{1 - \cos(\frac{\pi}{2}y)}{\cos(\frac{\pi}{2}y)} \quad (313)$$

Obviously, the magnification factor C_m is also dependent on the ratio $\frac{P}{P_E}$. Its variation with ratio $\frac{P}{P_E}$ is pictured in Figure 17.41.

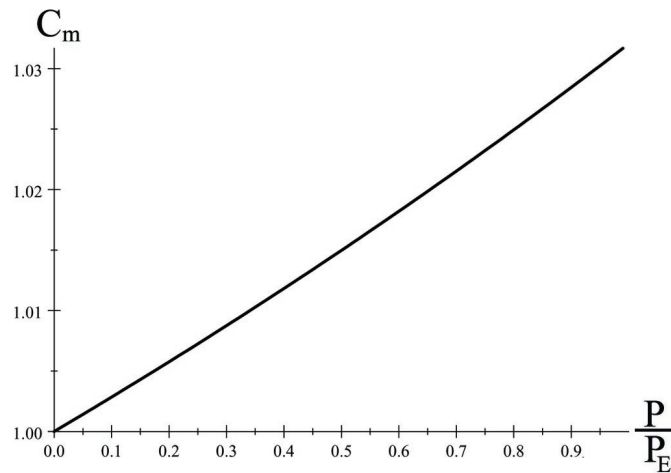


Figure 17.41 C_m Variation

Remark (a) The relation (311) indicates a continuous increased of the initial value of the maximum bending moment $M_{\max}^0 = \frac{ql^2}{8}$ for $\frac{P}{P_E} \in (0, 1)$. When the compressive force $P = P_E$ the maximum bending moment is ∞ .

(b) as it shown by the graph pictured in Figure 17.41, the magnification factor C_m varies slightly around the value 1, and consequently, the maximum bending moment can be represented as:

$$M_{\max} = M_{\max}^0 \frac{1}{1 - \frac{P}{P_E}} \quad (314)$$

1.5.4.2 Existing End Moments M_O and M_A Proceeding similar as in the previous section, the general relations (305) and (306) are particularized by setting $q_O = q_A = 0$ as:

$$v(x) = \frac{1}{k^2 EI_z} \left[\left(\frac{1}{\sin kl} \sin kx - \frac{1}{l} x \right) M_A + \left(\cos kx - 1 + \frac{1}{l} x - \frac{\cos kl}{\sin kl} \sin kx \right) M_O \right] \quad (315)$$

$$M(x) = -\frac{1}{\sin kl} \sin kx * M_A + \left(\frac{\cos kl}{\sin kl} \sin kx - \cos kx \right) M_O \quad (316)$$

The location of the cross-section x , where the bending moment $M(x)$ realizes its maximum, is obtained by solving:

$$\begin{aligned} \frac{d}{dx} M(x) &= 0 & (317) \\ \rightarrow \frac{d}{dx} \left(-\frac{1}{\sin kl} \sin kx * M_A + \left(\frac{\cos kl}{\sin kl} \sin kx - \cos kx \right) M_O \right) &= 0 \\ \rightarrow -\frac{1}{\sin kl} \cos kx * M_A + \left(\frac{\cos kl}{\sin kl} \cos kx + \sin kx \right) M_O &= 0 \\ \rightarrow -\frac{1}{\sin kl} * M_A + \left(\frac{\cos kl}{\sin kl} + \tan kx \right) M_O &= 0 \\ \rightarrow \tan kx &= \frac{1}{\sin kl} * \frac{M_A}{M_O} - \frac{\cos kl}{\sin kl} \\ \rightarrow \tan kx &= \frac{1}{\sin kl} * \alpha - \frac{\cos kl}{\sin kl} \end{aligned}$$

where $\alpha = \frac{M_A}{M_O}$ is the ratio of the end moments.

Expressing $\sin kx$ and $\cos kx$ as functions of $\tan kx$ and substituting them into the bending moment equation (316), the maximum bending moment is calculated as:

$$\begin{aligned}
M_{\max} &= -\frac{1}{\sin kl} \frac{\tan kx}{\sqrt{1 + \tan^2 kx}} * M_A + \left(\frac{\cos kl}{\sin kl} \frac{\tan kx}{\sqrt{1 + \tan^2 kx}} - \frac{1}{\sqrt{1 + \tan^2 kx}} \right) M_O \quad (318) \\
&= -\frac{\tan kx}{\sqrt{1 + \tan^2 kx}} M_O \left(\frac{1}{\sin kl} * \frac{M_A}{M_O} - \frac{\cos kl}{\sin kl} + \frac{1}{\tan kx} \right) = \\
&= -\frac{\tan kx}{\sqrt{1 + \tan^2 kx}} M_O \left(\tan kx + \frac{1}{\tan kx} \right) = -\frac{\tan^2 kx}{\sqrt{1 + \tan^2 kx}} M_O \left(1 + \frac{1}{\tan^2 kx} \right) = \\
&= -M_O \sqrt{1 + \tan^2 kx}
\end{aligned}$$

Substituting first equation (317) and further $kl = \pi \sqrt{\frac{P}{P_E}} = \pi \sqrt{\beta}$ into (318) the maximum bending moment M_{\max} becomes:

$$M_{\max} = -M_O \sqrt{1 + \left(\frac{1}{\sin \pi \sqrt{\beta}} * \alpha - \frac{\cos \pi \sqrt{\beta}}{\sin \pi \sqrt{\beta}} \right)^2} \quad (319)$$

where is the ratio $\beta = \frac{P}{P_E}$.

The maximum bending moment M_{\max} is then expressed using a magnification factor C_m as:

$$M_{\max} = M_O \frac{C_m}{1 - \frac{P}{P_E}} \quad (320)$$

where the magnification factor C_m is:

$$\begin{aligned}
C_m &= \left(1 - \frac{P}{P_E} \right) \sqrt{1 + \left(\frac{1}{\sin \pi \sqrt{\beta}} * \alpha - \frac{\cos \pi \sqrt{\beta}}{\sin \pi \sqrt{\beta}} \right)^2} = \\
&= (1 - \beta) \sqrt{1 + \left(\frac{1}{\sin \pi \sqrt{\beta}} * \alpha - \frac{\cos \pi \sqrt{\beta}}{\sin \pi \sqrt{\beta}} \right)^2}
\end{aligned} \quad (321)$$

The variation of the magnification factor depends on the two important ratios $\alpha = \frac{M_A}{M_O}$ and $\beta = \frac{P}{P_E}$. Considering that $M_O \geq M_A$ the limits of the ratios are established as:

$$-1 \leq \alpha \leq 1 \quad (322)$$

and

$$0 < \beta < 1 \quad (323)$$

Remark 55 The maximum bending moment M_{\max} , (320) tends to ∞ as $\beta = \frac{P}{P_E} \rightarrow 1$ and consequently, the ratio is limited to $\beta < 1$. This case corresponds to loss of stability.

The variation of the magnification factor C_m for various ratios $-1 \leq \alpha \leq 1$ and $\beta \in [0.1, 0.3, 0.5, 0.7, 0.9]$ is illustrated in Figure 17.42.

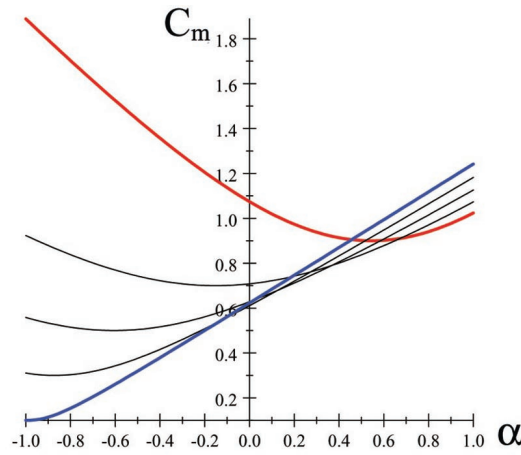


Figure 17.42 C_m Variation

1.5.4.3 Eccentric Loading. The Secant Formula In this section a new situation is considered. The ideal pinned-ended column is subjected to an *eccentric concentrated compressive force* P acting at both ends O and A as shown in Figure 17.43.a. The eccentricity e of the force P is measured from vertical axis x of the column. The *eccentrically applied force* P is replaced by a *centric compressive force* P and *two concentrated moments of equal magnitude* acting at both ends O and A of the column, as shown in Figure 17.9.b.

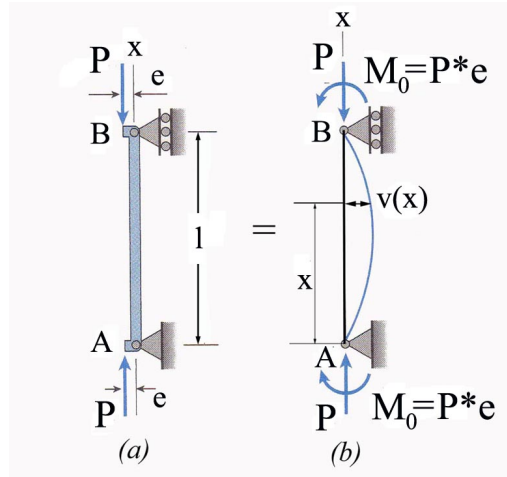


Figure 17.43 Eccentric Loaded Column

In the absence of a transversal distributed force, $p_n(x) = 0$, the lateral deflection $v(x)$ and the bending moment $M(x)$ obtained in the previously section, equations (315) and (315), remain valid and are employed herein..The end moments M_O and M_A are expressed:

$$M_O = -P * e \quad (324)$$

$$M_A = -P * e \quad (325)$$

and consequently the ratio α becomes:

$$\alpha = \frac{M_A}{M_O} = 1 \quad (326)$$

Substituting (324) and (325) into (??) the deflctive curve $v(x)$ is:

$$\begin{aligned} v(x) &= -\frac{Pe}{k^2 EI_z} \left[\left(\frac{1}{\sin kl} \sin kx - \frac{1}{l} x \right) + \left(\cos kx - 1 + \frac{1}{l} x - \frac{\cos kl}{\sin kl} \sin kx \right) \right] = \\ &= -\frac{Pe}{P} \left(\frac{1}{\sin kl} \sin kx - \frac{1}{l} x + \cos kx - 1 + \frac{1}{l} x - \frac{\cos kl}{\sin kl} \sin kx \right) = \\ &= -e \left(\frac{1 - \cos kl}{\sin kl} \sin kx + \cos kx - 1 \right) = \\ &= -e \left(\tan \frac{kl}{2} \sin kx + \cos kx - 1 \right) \end{aligned}$$

The location x of the maximum of the displacement function $v(x)$, is found at the middle of the column length l :

$$\begin{aligned}\frac{d}{dx}v(x) &= 0 \rightarrow \tan\left(\frac{kl}{2}\right) * \cos(k * x) - \sin(k * x) = 0 \\ &\rightarrow x = \frac{l}{2}\end{aligned}\tag{327}$$

and consequently:

$$\begin{aligned}v_{\max} &= -e * \left[\tan\left(\frac{kl}{2}\right) * \sin\left(k * \frac{l}{2}\right) + \cos\left(k * \frac{l}{2}\right) - 1\right] = \\ &= -e * \left[\sec\left(\frac{kl}{2}\right) - 1\right]\end{aligned}\tag{328}$$

A different format of equation (328) is obtained by substituting the product $k * l = \pi * \sqrt{\frac{P}{P_{cr}}}$:

$$v_{\max} = -e * \left[\sec\left(\frac{\pi}{2} \sqrt{\frac{P}{P_{cr}}}\right) - 1\right]\tag{329}$$

The load deflection diagram representing the variation of the ratio $\frac{P}{P_{cr}}$ function of the maximum displacement v_{\max} is illustrated in Figure 17.44 for few eccentricity values $e \in [0, 0.1, 0.5, 1]$.

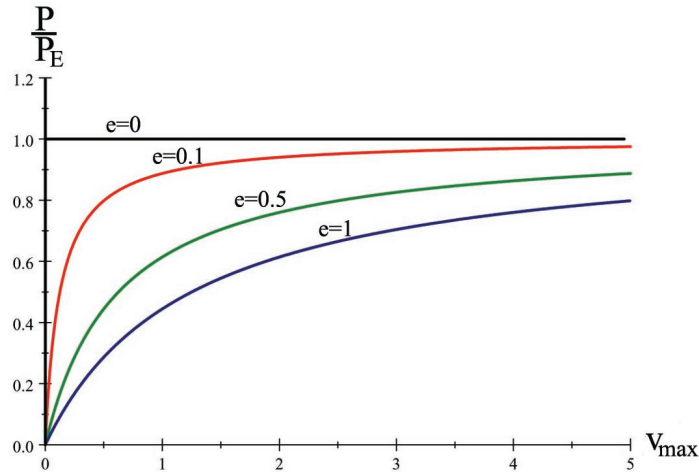


Figure 17.44 Load-Deflection Diagram

Remark 56 Analyzing the equation (329), representing the variation of the maximum displacement v_{\max} of the pinned-ended beam-column, few interesting conclusion can be emphasized:

(a) unlike the case when $e = 0$ of the ideal Euler column which deflects laterally only the axial compressive force equals or is greater than the critical load $P > P_{cr}$, the similar beam-column deflects for any value of P accordingly to expression (329);

(b) when $P = 0$ then $\sec(0) = 1$ and $v_{\max} = 0$ indifferent the value of e ;

(c) when $P \rightarrow P_{cr}$ then $\sec(\frac{\pi}{2}) = \infty$ and $v_{\max} \rightarrow \infty$ indifferent the value of e ;

(d) the transversal deflection v_{\max} is a non-linear function of P and linear function of e ;

Particularizing equation (317) for $\alpha = 1$ the location of the maximum bending moment M_{\max} is located at middle of the column length l :

$$\begin{aligned} \tan kx &= \frac{1}{\sin kl} - \frac{\cos kl}{\sin kl} = \tan \frac{k * l}{2} \\ \rightarrow kx &= \frac{k * l}{2} \rightarrow x = \frac{l}{2} \end{aligned} \quad (330)$$

Substituting equations (324) (330) into equation (318) the maximum bending moment M_{\max} is calculated:

$$\begin{aligned} M_{\max} &= P * e * \sqrt{1 + \left(\tan \frac{k * l}{2} \right)^2} = \\ &= P * e * \sec\left(\frac{k * l}{2}\right) \end{aligned} \quad (331)$$

The maximum normal stress σ_x^{\max} pertinent to the critical cross-section is obtained:

$$\begin{aligned} \sigma_x^{\max} &= \frac{P}{A} + \frac{M_{\max}}{I_z} * y_{\max} = \frac{P}{A} + \frac{P * e * \sec\left(\frac{k * l}{2}\right)}{A * r_z^2} * y_{\max} = \\ &= \frac{P}{A} * \left[1 + \frac{e * y_{\max}}{r_z^2} * \sec\left(\frac{k * l}{2}\right) \right] \end{aligned} \quad (332)$$

Substituting equation (??) into equation (332) the *Secant Formula* is obtained:

$$\begin{aligned}
\sigma_x^{\max} &= \frac{P}{A} * [1 + \frac{e * y_{\max}}{r_z^2} * \sec(\frac{\pi}{2} \sqrt{\frac{P}{P_{cr}}})] = \frac{P}{A} * [1 + \frac{e * y_{\max}}{r_z^2} * \sec(\frac{l}{2} \sqrt{\frac{P}{E * I_z}})] = \\
&= \frac{P}{A} * [1 + \frac{e * y_{\max}}{r_z^2} * \sec(\frac{l}{2} \sqrt{\frac{P}{E * A * r_z^2}})] = \frac{P}{A} * [1 + \frac{e * y_{\max}}{r_z^2} * \sec(\frac{l}{2 * r_z} * \sqrt{\frac{P}{E * A}})] = \\
&= \sigma_c * [1 + \frac{e * y_{\max}}{r_z^2} * \sec(\frac{\lambda}{2} * \sqrt{\frac{\sigma_c}{E}})]
\end{aligned} \tag{333}$$

where $\lambda = \frac{l}{r_z}$ and $\sigma_c = \frac{P}{A}$ are the slenderness of the column and the compressive normal stress for zero eccentricity ($e = 0$), respectively.

Considering that the beam-column member is made of structural steel, characterized by an elastic modulus $E = 200GPa$ and $\sigma_y^0 = 250MPa$, and the normal stress σ_x^{\max} in the critical cross-section reaches the proportionality limit value σ_y^0 then:

$$\begin{aligned}
\sigma_x^{\max} &= \sigma_y^0 \\
\rightarrow \sigma_c * [1 + \frac{e * y_{\max}}{r_z^2} * \sec(\frac{\lambda}{2} * \sqrt{\frac{\sigma_c}{E}})] &= \sigma_y^0
\end{aligned}$$

The ratio $\frac{\sigma_c}{\sigma_y^0}$ is plotted in Figure 17.45 function of the slenderness $\lambda \in [0, 200]$ and ratio

$\beta = \frac{e * y_{\max}}{r_z^2} \in [0, 0.1, 0.5, 1, 2]$, respectively, .

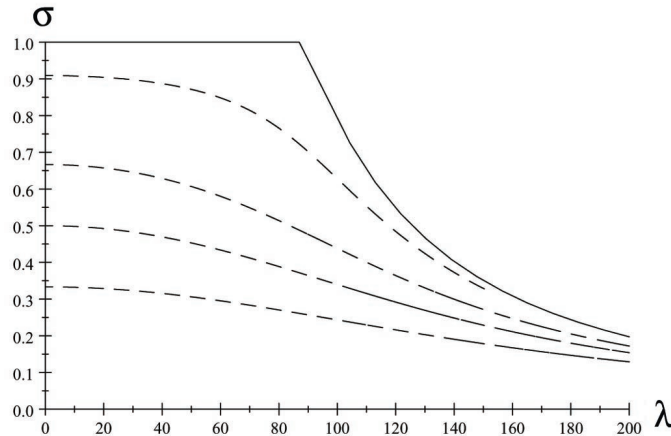


Figure 17.45 Variation of $\frac{\sigma_c}{\sigma_y^0}$

Remark 57 (a) *The Euler critical stress represents an upper-bound for the secant formula results and consequently:*

$$\sigma_x^{\max} < \sigma_{cr}$$

(b) *The Secant Formula represents a non-linear relation and the Superposition Principle does not apply;*

(c) *The Secant Formula applies to pin-ended ideal columns only, but similar expressions can be developed. This formula can be extended directly to the "cantilevered" columns by replacing the buckling length l with $2l$. The direct extension of the Secant Formula is not generally valid.*

1.5.5 Large Deflection

In *Lecture 7 of the volume I*, the relation between the cross-sectional bending moment $M(x)$ and the curvature $k(x)$ is established:

$$k(x) = \frac{1}{\rho(x)} = \frac{M(x)}{E * I_z} \quad (334)$$

where $E * I_z$ and $\rho(x)$ are the bending rigidity of the beam-column and the radius of curvature, respectively.

The geometrical differential expression, obtained at *Differential Geometry*, relating the cross-sectional transversal deflection $v(x)$ to the curvature $k(x)$ is:

$$k(x) = \frac{\frac{d^2v}{dx^2}}{\frac{3}{(1 + (\frac{dv}{dx})^2)^{\frac{3}{2}}}} = \frac{v''}{\frac{3}{(1 + (v')^2)^{\frac{3}{2}}}} \quad (335)$$

Combining the above two relations, (334) and (335), a new differential relation between the cross-sectional bending moment $M(x)$ and the deflection curve $v(x)$ is obtained:

$$M(x) = E * I_z * v'' * (1 + (v')^2)^{-\frac{3}{2}} \quad (336)$$

If the expression contained between the parenthesis located at the right-side of equation (336) is expanded in a *Taylor series*, the cross-sectional bending moment $M(x)$ becomes:

$$M(x) = E * I_z * v'' * \left(1 - \frac{3}{2}(v')^2 + \frac{15}{8}(v')^4 - \frac{35}{16}(v')^6 + \dots\right) \quad (337)$$

The *basic assumption 4*, extensively utilized in all previous sections, is mathematically expressed by:

$$M(x) \simeq E * I_z * v'' \quad (338)$$

a relation resulting from *the linearization of the expression (337)*.

The main scope of this section is to evaluate the error introduced in the calculation of the critical axial force sustained by a column when the linearized expression (338) is used instead of the exact expression (336).

A first indication of the error introduced in the evaluation of the cross-sectional bending moment $M(x)$ by linearization is obtained by plotting the variation of $(1 + (v')^2)^{-\frac{3}{2}}$ with first derivative of the deflection $v'(x)$. Additionally, different degrees of approximation offered by the Taylor series are superimposed on the graph. This suggestive evaluation is illustrated in Figure 17.46,

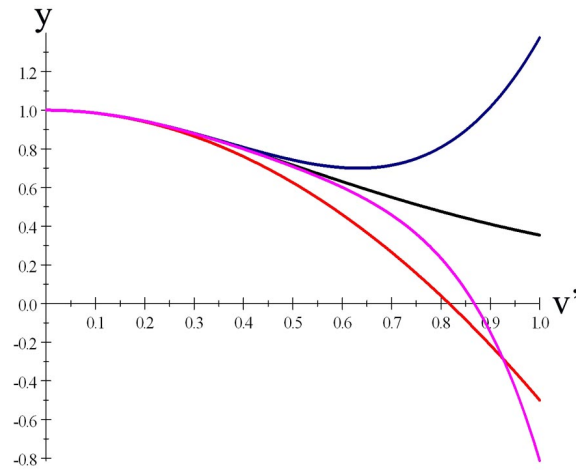
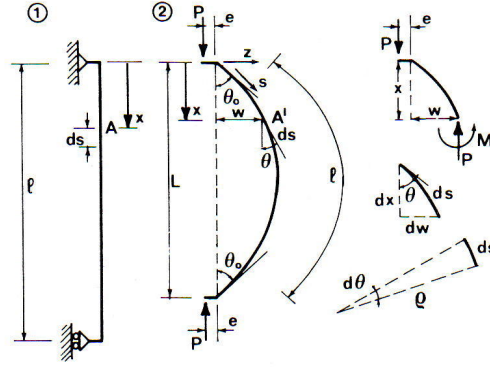


Figure 17.46 Degree of Approximation of $(1 + (v')^2)^{-\frac{3}{2}}$

Remark 58 *It is evident from the graph that the approximation is very good for the most simple approximation function $1 - \frac{3}{2}(v')^2$ until $v'(x) = 0.25$. The error is evaluated in the following table:*



▲ Beam-column under large deflections

Figure 2: Figure 17.47 Pin-Ended Column - Large Deformation

Case	$v'(x)$	$(1 + (v')^2)^{-\frac{3}{2}}$	$1 - \frac{3}{2}(v')^2$	% Error	Obs
1	0.05	0.996 26	0.996 25	1.0038×10^{-3}	< 1%
2	0.01	0.999 85	0.999 85	0.0	< 1%
3	0.02	0.999 99	0.999 4	5.9001×10^{-2}	< 1%
4	0.1	0.985 19	0.985	1.9286×10^{-2}	< 1%
5	0.13	0.975 18	0.974 65	5.4349×10^{-2}	< 1%
6	0.15	0.967 17	0.966 25	$9.512 3 \times 10^{-2}$	< 1%
7	0.2	0.942 87	0.94	3.0439×10^{-1}	< 1%
8	0.25	0.91308	0.906 25	0.748 02	< 1%
9	0.3	0.878 74	0.865	1.5636	> 1%

For $v'(x) \leq 0.25$, corresponding to an angle of 14° , the error obtained is less than 1%.

For a complete evaluation of the error induced by linearization the classical pin-ended column, shown in Figure 17.47, is reanalyzed.

The equilibrium equation (18) is re-written using equation (334) as:

$$\begin{aligned}
 M(x) + P * v(x) &= 0 \rightarrow \\
 \frac{E * I_z}{\rho(x)} + P * v(x) &= 0
 \end{aligned} \tag{339}$$

Substituting the geometrical expression of the radius of curvature $\rho(x) = \frac{ds}{d\theta}$ into equation (339) an equilibrium equation containing two unknown functions, θ and v , is obtained:

$$E * I_z * \frac{d\theta}{ds} + P * v = 0 \tag{340}$$

where θ is the rotation angle of the cross-section after the buckling deformation.

Remark 59 *The cross-sectional bending moment is expressed as:*

$$M(s) = E * I_z * \frac{d\theta}{ds} = E * I_z * \theta' \quad (341)$$

Differentiating equation (340) again about variable s , the location of the cross-section measured from the end O ($s = 0$) on the deflection curve:

$$E * I_z * \frac{d^2\theta}{ds^2} + P * \frac{dv}{ds} = 0 \quad (342)$$

From Figure 17.101, is observed that geometrically the derivative $\frac{dv}{ds} = \sin \theta$ and accordingly, the differential equation (342) is re-written as:

$$\theta'' + k^2 * \sin \theta = 0 \quad (343)$$

where $k^2 = \frac{P}{E * I_z}$.

The equation (343) is a *second order non-linear differential equation with constant coefficients*. In 1859, Kirchhoff found the solution and notice the striking mathematical similarity with the differential equation governing large oscillations of a pendulum. For this reason, in 1927, Love called the stability problem of the pin-ended column as the kinetic analogy of column.

Conclusion 60 *If the approximation $\sin \theta \simeq \theta - \frac{1}{6}\theta^3 + \frac{1}{120}\theta^5 + \dots$ is considered and only the first term is retained, equation (343) is transformed by linearization into previously obtained equation (21).*

First, multiplying by θ' equation (343) and then, recognizing the differential identities $\theta' * \theta'' = \frac{1}{2} * ((\theta')^2)'$ and $\theta' * \sin \theta = \theta' * \sin \frac{\theta}{2} * \cos \frac{\theta}{2} = \left(\left(\sin \frac{\theta}{2} \right)^2 \right)'$, the above differential equation is recast as:

$$\begin{aligned} \frac{1}{2} * ((\theta')^2)' + 2 * k^2 * \left(\left(\sin \frac{\theta}{2} \right)^2 \right)' &= 0 \rightarrow \\ \left(\frac{1}{2} * (\theta')^2 + 2 * k^2 * \left(\sin \frac{\theta}{2} \right)^2 \right)' &= 0 \end{aligned} \quad (344)$$

Integrating equation (344) the following differential equation is obtained:

$$\frac{1}{4 * k^2} * (\theta')^2 = - \left(\sin \frac{\theta}{2} \right)^2 + c^2 \quad (345)$$

where c is an integration constant determined using the initial conditions at end O :

$$\theta(s = 0) = \theta_0 \neq 0 \quad (346)$$

and

$$\begin{aligned} M(s = 0) &= 0 \rightarrow \\ E * I_z * \frac{1}{\rho(s = 0)} &= 0 \rightarrow E * I_z * \theta'_0 = 0 \rightarrow \\ &\rightarrow \theta'_0 = 0 \end{aligned} \quad (347)$$

The equation (345) is valid for any s including $s = 0$ and applying the boundary conditions (346) and (347) the constant c is calculated function of the initial rotation θ_0 :

$$\begin{aligned} \frac{1}{4 * k^2} * (\theta'_0)^2 &= - \left(\sin \frac{\theta_0}{2} \right)^2 + c^2 \rightarrow \\ 0 &= - \left(\sin \frac{\theta_0}{2} \right)^2 + c^2 \rightarrow \\ c &= \pm \sin \frac{\theta_0}{2} \end{aligned} \quad (348)$$

Replacing c into (345):

$$\frac{1}{4 * k^2} * (\theta')^2 = - \left(\sin \frac{\theta}{2} \right)^2 + \left(\sin \frac{\theta_0}{2} \right)^2 \quad (349)$$

and consequently,

$$\begin{aligned}
\theta' &= \pm 2 * k * \sqrt{\left(\sin \frac{\theta_0}{2}\right)^2 - \left(\sin \frac{\theta}{2}\right)^2} \rightarrow \\
\frac{d\theta}{ds} &= \pm 2 * k * \sqrt{\left(\sin \frac{\theta_0}{2}\right)^2 - \left(\sin \frac{\theta}{2}\right)^2} \rightarrow \\
ds &= - \frac{d\theta}{2 * k * \sqrt{\left(\sin \frac{\theta_0}{2}\right)^2 - \left(\sin \frac{\theta}{2}\right)^2}}
\end{aligned} \tag{350}$$

where \pm indicates that the deformation can be positive or negative.

Considered the assumption of the column inextensibility (*the original length l is preserved after the deformation*) and the deformation is symmetric ($\theta(s = \frac{l}{2}) = 0$) the following equality can be written:

$$\begin{aligned}
l &= 2 * \int_0^{\frac{l}{2}} ds = -\frac{1}{k} \int_{\theta_0}^0 \frac{d\theta}{\sqrt{\left(\sin \frac{\theta_0}{2}\right)^2 - \left(\sin \frac{\theta}{2}\right)^2}} = \\
&= \frac{1}{k} * \int_0^{\theta_0} \frac{d\theta}{\sqrt{\left(\sin \frac{\theta_0}{2}\right)^2 - \left(\sin \frac{\theta}{2}\right)^2}}
\end{aligned} \tag{351}$$

Considering the following variable change

$$\sin \frac{\theta}{2} = c * \sin \phi = \sin \frac{\theta_0}{2} * \sin \phi \tag{352}$$

one obtains by implicit differentiation:

$$\begin{aligned}
\frac{1}{2} * \cos \frac{\theta}{2} * \frac{d\theta}{d\phi} &= \sin \frac{\theta_0}{2} * \cos \phi \rightarrow \\
d\theta &= 2 * \frac{\sin \frac{\theta_0}{2} * \cos \phi}{\cos \frac{\theta}{2}} * d\phi
\end{aligned} \tag{353}$$

Replacing (352) and (353) into (351):

$$\begin{aligned}
l &= \frac{1}{k} * \int_0^{\frac{\pi}{2}} \frac{2 * \frac{\sin \frac{\theta_0}{2} * \cos \phi}{\cos \frac{\theta}{2}}}{\sqrt{\left(\sin \frac{\theta_0}{2}\right)^2 - \left(\sin \frac{\theta_0}{2} * \sin \phi\right)^2}} * d\phi = \frac{2}{k} * \int_0^{\frac{\pi}{2}} \frac{\sin \frac{\theta_0}{2} * \cos \phi}{\cos \frac{\theta}{2} * \sin \frac{\theta_0}{2} \sqrt{1 - (\sin \phi)^2}} * d\phi \quad (354) \\
&= \frac{2}{k} * \int_0^{\frac{\pi}{2}} \frac{\sin \frac{\theta_0}{2} * \cos \phi}{\cos \frac{\theta}{2} * \sin \frac{\theta_0}{2} * \cos \phi} * d\phi = \frac{2}{k} * \int_0^{\frac{\pi}{2}} \frac{1}{\cos \frac{\theta}{2}} * d\phi = \frac{2}{k} * \int_0^{\frac{\pi}{2}} \frac{1}{\sqrt{1 - \left(\sin \frac{\theta_0}{2} * \sin \phi\right)^2}} * d\phi
\end{aligned}$$

where the integration limits are obtained from (352): for $\theta = 0 \rightarrow \sin \phi = \frac{\sin \frac{\theta}{2}}{\sin \frac{\theta_0}{2}} = 0 \rightarrow$

$\phi = 0$ and for $\theta = \theta_0 \rightarrow \sin \phi = \frac{\sin \frac{\theta_0}{2}}{\sin \frac{\theta_0}{2}} = 1 \rightarrow \phi = \frac{\pi}{2}$.

From equation (354) an integral relation between the compressive force P and the initial rotation θ_0 is obtained by replacing $k = \frac{\pi}{l} * \sqrt{\frac{P}{P_E}}$:

$$\begin{aligned}
k &= \frac{2}{l} * \int_0^{\frac{\pi}{2}} \frac{1}{\sqrt{1 - \left(\sin \frac{\theta_0}{2} * \sin \phi\right)^2}} * d\phi \rightarrow \quad (355) \\
\frac{\pi}{l} * \sqrt{\frac{P}{P_E}} &= \frac{2}{l} * \int_0^{\frac{\pi}{2}} \frac{1}{\sqrt{1 - \left(\sin \frac{\theta_0}{2} * \sin \phi\right)^2}} * d\phi \rightarrow \\
\frac{\pi}{2} * \sqrt{\frac{P}{P_E}} &= \int_0^{\frac{\pi}{2}} \frac{1}{\sqrt{1 - \left(\sin \frac{\theta_0}{2} * \sin \phi\right)^2}} * d\phi
\end{aligned}$$

where $P_E = \frac{\pi^2 * E * I_z}{l^2}$.

The left-side of the equation (354) is called the *complete elliptic integral of first kind* and obviously depends on θ_0 . If the integrated function of the left-sided integral is expanded into a Taylor series

$$\frac{1}{\sqrt{1 - \left(\sin \frac{\theta_0}{2} * \sin \phi\right)^2}} \simeq \left(1 + \frac{1}{2} \left(\sin \frac{\theta_0}{2} \sin \phi\right)^2 + \dots\right) \quad (356)$$

and only the first to terms are retained the equation (355) becomes:

$$\begin{aligned} \frac{\pi}{2} * \sqrt{\frac{P}{P_E}} &\simeq \int_0^{\frac{\pi}{2}} \left(1 + \frac{1}{2} \left(\sin \frac{\theta_0}{2} \sin \phi\right)^2\right) d\phi \rightarrow \\ \frac{\pi}{2} * \sqrt{\frac{P}{P_E}} &\simeq \int_0^{\frac{\pi}{2}} d\phi + \frac{1}{2} * \left(\sin \frac{\theta_0}{2}\right)^2 * \int_0^{\frac{\pi}{2}} (\sin \phi)^2 d\phi \end{aligned} \quad (357)$$

and then, it can be easily integrated as:

$$\begin{aligned} \frac{\pi}{2} * \sqrt{\frac{P}{P_E}} &\simeq \frac{\pi}{2} + \frac{1}{2} * \left(\sin \frac{\theta_0}{2}\right)^2 * \frac{\pi}{4} \rightarrow \\ P &\simeq P_E * \left[1 + \frac{1}{2} * \left(\sin \frac{\theta_0}{2}\right)^2\right] \end{aligned} \quad (358)$$

If again the $\left(\sin \frac{\theta_0}{2}\right)^2$ is expanded in a Taylor series

$$\left(\sin \frac{\theta_0}{2}\right)^2 = \frac{1}{4}\theta_0^2 - \frac{1}{48}\theta_0^4 + \frac{1}{1440}\theta_0^6 + \dots$$

and only the first three terms are retained:

$$P \simeq P_E * \left(1 + \frac{1}{8}\theta_0^2 - \frac{1}{96}\theta_0^4 + \frac{1}{2880}\theta_0^6 \right) \quad (359)$$

As before, the graphical representation of relation (359) is a very expressive indicator of the approximation made. The variation of ratio $\frac{P}{P_E}$ with θ_0 , measured in degrees, is illustrated in Figure 17.48.

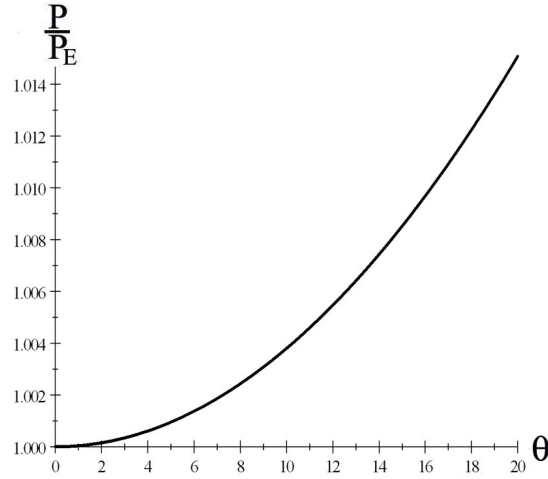


Figure 17.48 $\frac{P}{P_E}$ Variation

Conclusion 61 *It can be visualized from the graph that for rotation angles $\theta_0 \leq 17^\circ$*

$$P \leq 1.1 * P_E \quad (360)$$

and consequently, it can be concluded that for this range, covering majority of practical applications, *the error introduced by the utilization of the small deformation assumption (basic assumption 4) is acceptable.*

To complete the analysis of the large deformation influence two important geometrical characteristics are obtained and analyzed: the maximum lateral deflection v_{\max} and the total shortening of the column Δ .

The maximum lateral deflection v_{\max} is obtained by integration:

$$v_{\max} = \int_0^{\frac{l}{2}} dv \quad (361)$$

Knowing that:

$$dv = \sin \theta * ds \quad (362)$$

and replacing ds with relation (350) the maximum deflection v_{\max} is calculated:

$$\begin{aligned} v_{\max} &= \int_0^{\frac{l}{2}} dv = - \int_{\theta_0}^0 \sin \theta * \frac{d\theta}{2 * k * \sqrt{\left(\sin \frac{\theta_0}{2}\right)^2 - \left(\sin \frac{\theta}{2}\right)^2}} = \\ &= - \int_{\theta_0}^0 2 * \sin \frac{\theta}{2} * \cos \frac{\theta}{2} * \frac{d\theta}{2 * k * \sqrt{\left(\sin \frac{\theta_0}{2}\right)^2 - \left(\sin \frac{\theta}{2}\right)^2}} = \\ &= \int_0^{\theta_0} 2 * \sin \frac{\theta}{2} * \cos \frac{\theta}{2} * \frac{d\theta}{2 * k * \sqrt{\left(\sin \frac{\theta_0}{2}\right)^2 - \left(\sin \frac{\theta}{2}\right)^2}} \end{aligned} \quad (363)$$

The variable change between θ and ϕ is made by substituting equation (352) and (353) into (363):

$$\begin{aligned} v_{\max} &= \int_0^{\frac{\pi}{2}} \sin \frac{\theta_0}{2} * \sin \phi * \cos \frac{\theta}{2} * \frac{2 * \frac{\sin \frac{\theta_0}{2} * \cos \phi}{\cos \frac{\theta}{2}} * d\phi}{k * \sqrt{\left(\sin \frac{\theta_0}{2}\right)^2 - \left(\sin \frac{\theta_0}{2} * \sin \phi\right)^2}} = \\ &= \frac{2}{k} * \sin \frac{\theta_0}{2} * \int_0^{\frac{\pi}{2}} \frac{\sin \phi * \cos \phi * d\phi}{\sqrt{1 - (\sin \phi)^2}} = \frac{2}{k} * \sin \frac{\theta_0}{2} = \frac{2 * l}{\pi} * \sin \frac{\theta_0}{2} * \sqrt{\frac{P_E}{P}} \end{aligned} \quad (364)$$

Expanding $\sin \frac{\theta_0}{2}$ the in Taylor series and retaining the only first term the first approximation for v_{\max} is obtained:

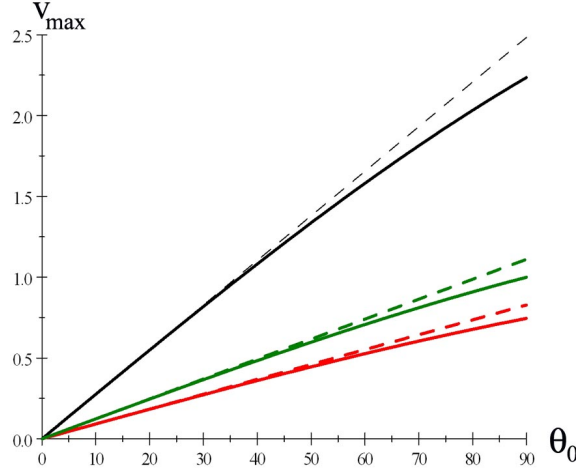


Figure 3: Figure 17.49 v_{\max}

$$v_{\max} = \frac{2 * l}{\pi} * \sqrt{\frac{P_E}{P}} * \left(\frac{\theta_0}{2} - \frac{1}{6} \left(\frac{\theta_0}{2} \right)^3 + .. \right) \simeq \frac{l}{\pi} * \sqrt{\frac{P_E}{P}} * \theta_0 \quad (365)$$

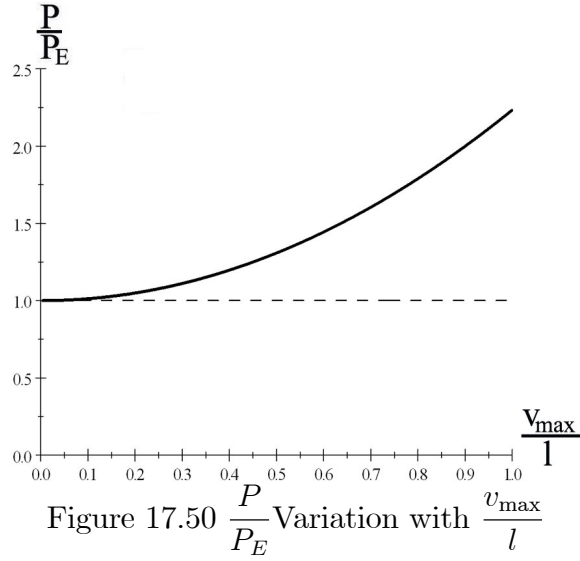
A graphical comparison of v_{\max} provided by the exact relation (364) and approximation (365) is illustrated in Figure 17.49 for $\frac{P}{P_E} \in [0.1, 0.5, 0.9]$:

Conclusion 62 *The value of v_{\max} obtained using the approximation (365) confers a good confidence for $\theta_0 \leq 40^\circ$.*

From equation (364) the axial compressive force P is calculated by replacing θ_0 with v_{\max} :

$$\begin{aligned} P &\simeq P_E * \left(1 + \frac{1}{8} \theta_0^2 \right) \simeq P_E * \left(1 + \frac{1}{8} \left(\frac{v_{\max}}{\frac{l}{\pi} * \sqrt{\frac{P_E}{P}}} \right)^2 \right) \rightarrow \\ \frac{P}{P_E} &\simeq 1 + \frac{\pi^2}{8 * l^2} * \frac{P}{P_E} * v_{\max}^2 \rightarrow \frac{P}{P_E} * \left(1 - \frac{\pi^2}{8 * l^2} * v_{\max}^2 \right) \simeq 1 \rightarrow \\ P &\simeq P_E * \frac{1}{1 - \frac{\pi^2}{8 * l^2} * v_{\max}^2} \rightarrow P \simeq P_E * \left(1 + \frac{\pi^2}{8 * l^2} * v_{\max}^2 \right) \end{aligned} \quad (366)$$

A graphical representation of the approximated value of the ratio $\frac{P}{P_E} \simeq 1 + \frac{\pi^2}{8} * \left(\frac{v_{\max}}{l} \right)^2$ provided by equation (366), is illustrated in Figure 17.50.



Conclusion 63 (a) Figure 17.104 indicates that for $\frac{v_{\max}}{l} \leq 0.1$

$$P \leq 1.01 * P_E \quad (367)$$

Conclusion 64 and consequently, the small deflection assumption can be employed;

(b) the axial force P increases with the deflection v_{\max} .

The total vertical displacement Δ , the shortening of the column under the axial compressive load P , is calculated in a similar manner as for v_{\max} . An approximation of the total shortening is obtained:

$$\Delta = \frac{\pi^2}{4 * l} * v_{\max}^2 \quad (368)$$

Remark 65 The vertical shortening of the column tip Δ is proportional to the square of the maximum lateral deflection v_{\max} .

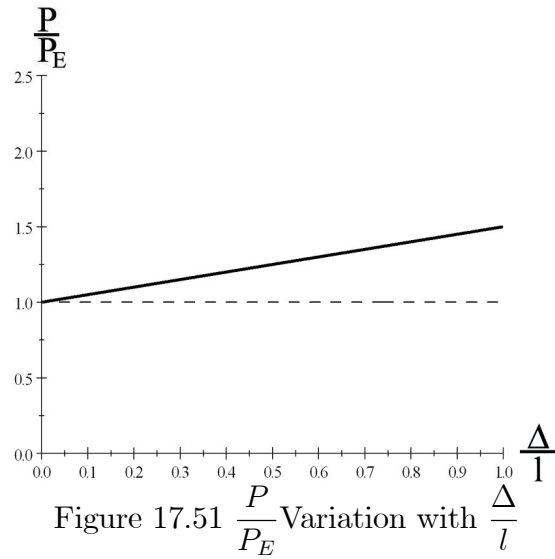
Substituting (368) into equation (366) the axial compressive force P is expressed function of Δ :

$$P \simeq P_E * \left(1 + \frac{1}{2 * l} * \Delta \right) \quad (369)$$

Remark 66 (a) The formula (369) is valid only after the bifurcation being dependent on Δ , which in turn is dependent, accordingly to (368), on v_{\max} ;

(b) The increase in the axial compressive force $P - P_E$ after the bifurcation is proportional to Δ or v_{\max}^2 .

The graphical representation of the ratio $\frac{P}{P_E}$ function of $\frac{\Delta}{l}$ is shown in Figure 17.51.



Remark 67 The normal stress σ is calculated dividing the compressive force P by the column area A :

$$\sigma \simeq \sigma_{cr} * \left(1 + \frac{1}{2} * \epsilon_{in}\right) \quad (370)$$

where $\epsilon_{in} = \frac{\Delta}{l}$ is the strain measured in the cross-section centroid.

Remark 68 The formula (370) is valid for an inextensible column.

To introduce the column flexibility an additional elastic strain ϵ_e has to be considered:

$$\epsilon_e = \frac{P - P_E}{E * A} = \frac{\sigma - \sigma_{cr}}{E} \quad (371)$$

The total strain ϵ_f is calculated:

$$\epsilon_f = \epsilon_{in} + \epsilon_e = 2 * \left(\frac{\sigma}{\sigma_{cr}} - 1 \right) + \frac{\sigma - \sigma_{cr}}{E} \quad (372)$$

Solving equation (372) for σ :

$$\begin{aligned} \sigma &= \sigma_{cr} + \frac{\sigma_{cr}}{2 + \frac{\sigma_{cr}}{E}} * \epsilon_f = \sigma_{cr} + \frac{\sigma_{cr}}{2 + \frac{\sigma_{cr}}{E}} * \frac{\Delta}{l} = \\ &= \sigma_{cr} + \frac{\sigma_{cr}}{2 + \left(\frac{\pi}{\lambda}\right)^2} * \frac{\Delta}{l} \end{aligned} \quad (373)$$

where $\Delta = 0$ at the bifurcation when $P = P_E$.

Multiplying equation (373) by A :

$$P = P_E + \frac{P_E}{2 + \frac{P_E}{E * A}} * \frac{\Delta}{l} \quad (374)$$

To account for the entire deformation the displacement existing at bifurcation has to be also added:

$$P(\Delta) = \begin{cases} P_E * \frac{\Delta}{\Delta_{cr}} & \text{if } \Delta \leq \Delta_{cr} \\ P_E + \frac{P_E}{2 + \frac{P_E}{E * A}} * \frac{\Delta - \Delta_{cr}}{l} & \text{if } \Delta > \Delta_{cr} \end{cases} \quad (375)$$

where $\Delta_{cr} = \frac{P_E * l}{E * A} = \sigma_{cr} * \frac{l}{E} = \frac{\pi^2 * E}{\lambda^2} * \frac{l}{E} = \left(\frac{\pi}{\lambda}\right)^2 * l$ is the shortening at bifurcation.

The normal stress σ calculated at the centroid position of the cross-section is:

$$\begin{aligned}
\sigma(\Delta) &= \begin{cases} \sigma_{cr} * \frac{\Delta}{\Delta_{cr}} & \text{if } \Delta \leq \Delta_{cr} \\ \sigma_{cr} + \frac{\sigma_{cr}}{2 + \frac{\sigma_{cr}}{E}} * \frac{\Delta - \Delta_{cr}}{l} & \text{if } \Delta > \Delta_{cr} \end{cases} = \\
&= \sigma_{cr} * \begin{cases} \frac{\Delta}{\Delta_{cr}} & \text{if } \Delta \leq \Delta_{cr} \\ 1 + \frac{1}{2 + \frac{\sigma_{cr}}{E}} * \left(\frac{\Delta}{l} - \frac{\sigma_{cr}}{E} \right) & \text{if } \Delta > \Delta_{cr} \end{cases} = \\
&= \sigma_{cr} * \begin{cases} \left(\frac{\lambda}{\pi} \right)^2 * \frac{\Delta}{l} & \text{if } \frac{\Delta}{l} \leq \left(\frac{\pi}{\lambda} \right)^2 \\ 1 + \frac{1}{2 + \left(\frac{\pi}{\lambda} \right)^2} * \left(\frac{\Delta}{l} - \left(\frac{\pi}{\lambda} \right)^2 \right) & \text{if } \frac{\Delta}{l} > \left(\frac{\pi}{\lambda} \right)^2 \end{cases}
\end{aligned} \tag{376}$$

Figure 17.52 illustrates the variation of the ratio $\frac{\sigma}{\sigma_{cr}}$ with $\frac{\Delta}{l}$ for $\lambda = 120$.

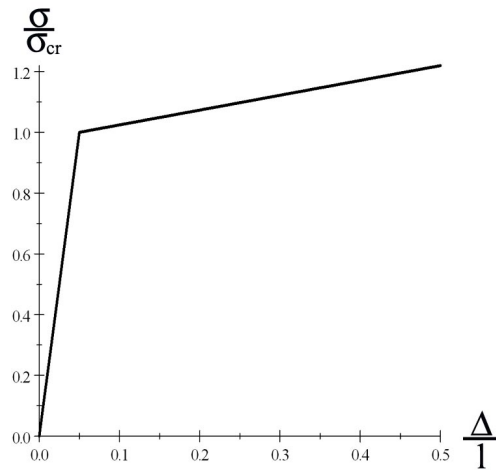


Figure 17.52 $\frac{\sigma}{\sigma_{cr}}$ Variation

1.6 Buckling of Simple Continuos Beams and Frames

In the previous sections the buckling of individual columns was discussed and mathematically characterized. In general the civil structures are composed from an ensemble of individual columns and beams, generically called frame, jointed at the ends.. The buckling of the frame is a very complex phenomenon and required a very extensive and in-depth theoretical approach, which without any doubt overpasses the scope of this lecture. In order for a student to understand and be ware of the differences existing between the buckling of individual member and the buckling of the same member being part of

a frame, two types of very simple plane structures are discussed: continuous beams and frames. For someone interested to explore the world of the structural stability the technical literature offers a large range of problems by considering different constitutive laws and dynamic nature of the loading.

1.6.1 Stiffness Matrix of Beam-Columns

The stiffness matrix K_{ff} is a mathematical expression relating the end reactions vector, moments and forces, R_{ff} of the member to its end degrees of freedom vector, rotations and translations, D_{ff} . In this section only the stiffness matrix K_{ff} of a plane member are developed. The mathematical transformation between the the end reactions vector R_{ff} and end degrees of freedom vector D_{ff} can be written as:

$$R_{ff} = K_{ff} * D_{ff} \quad (377)$$

where

$$R_{ff} = \begin{bmatrix} M_1 \\ V_1 \\ M_2 \\ V_2 \end{bmatrix} \quad (378)$$

$$D_{ff} = \begin{bmatrix} \theta_1 \\ v_1 \\ \theta_2 \\ v_2 \end{bmatrix} \quad (379)$$

and $\theta_1, \theta_2, v_1, v_2$ and $\Delta_{21} = v_2 - v_1$ are the rotations, displacements and the relative displacement of the member ends, respectively.

Each component of the stiffness matrix K_{ff} represents a reaction corresponding to a specific displacement having a unit value. If the degrees of freedom of a plane frame are considered fixed, one can observe that only two types of plane members, fixed-fixed and hinged-fixed, are comprised in the ensemble. Consequently, only the stiffness matrices for these two categories of beam-columns are developed and used in the following applications.

1.6.1.1 Fixed-Fixed Beam-Column (Figure 17.53) A fixed-fixed plane beam-column is characterized, *if the axial deformation is neglected*, by four degrees-of-freedom $\theta_1, \theta_2, v_1, v_2$ representing the rotation and the transversal displacement at ends 1 and 2, respectively.

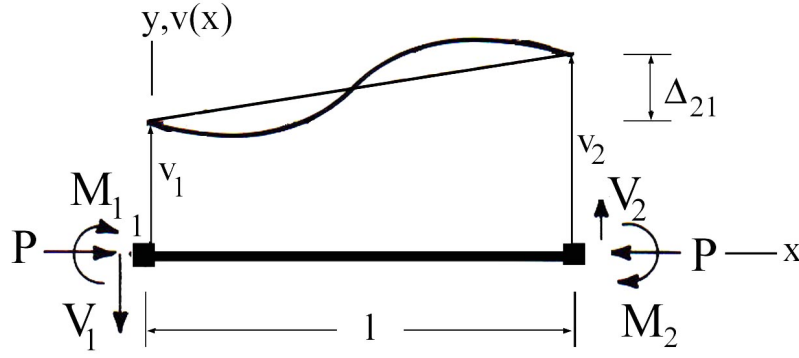


Figure 17.53

In order to obtain the relation between the reactions and the ends' degrees of freedom the integration constants C_1, C_2, C_3 and C_4 characterizing the general solution $v(x)$ expressed by equation (49) have to be calculated for the specific boundary conditions. They are:

- at the end 1 ($x = 0$):

$$v(x = 0) = v_1 \rightarrow C_1 * \sin(k * 0) + C_2 \cos(k * 0) + C_3 * 0 + C_4 = v_1 \rightarrow C_2 + C_4 = v_1 \quad (380)$$

$$\theta(x = 0) = -\theta_1 \rightarrow k * C_1 * \cos(k * 0) - k * C_2 * \sin(k * 0) + C_3 = -\theta_1 \rightarrow k * C_1 + C_3 = -\theta_1 \quad (381)$$

- at the end 2 ($x = l$)

$$v(x = l) = v_2 \rightarrow C_1 * \sin(k * l) + C_2 \cos(k * l) + C_3 * l + C_4 = v_2 \quad (382)$$

$$\theta(x = l) = -\theta_2 \rightarrow k * C_1 * \cos(k * l) - k * C_2 * \sin(k * l) + C_3 = -\theta_2 \quad (383)$$

Remark 69 *The minus signs are introduced in order to accommodate the general convention used in the structural analysis: the angles and moments are positive for a rotation in the clock direction.*

Equations (380) through (383) comprised a algebraic system, written in a matricial format, of for equations with constants coefficients:

$$\begin{bmatrix} 0 & 1 & 0 & 1 \\ k & 0 & 1 & 0 \\ \sin(k * l) & \cos(k * l) & l & 1 \\ k * \cos(k * l) & -k * \sin(k * l) & 1 & 0 \end{bmatrix} \begin{bmatrix} C_1 \\ C_2 \\ C_3 \\ C_4 \end{bmatrix} = \begin{bmatrix} v_1 \\ -\theta_1 \\ v_2 \\ -\theta_2 \end{bmatrix} \quad (384)$$

The constants are calculated solving the system (384):

$$C_1 = -\frac{\cos kl + kl \sin kl - 1}{2k \cos kl - 2k + k^2 l \sin kl} \theta_1 + \frac{\cos kl - 1}{2k \cos kl - 2k + k^2 l \sin kl} \theta_2 + k \frac{\sin kl}{2k \cos kl - 2k + k^2 l \sin kl} v_1 - k \frac{\sin kl}{2k \cos kl - 2k + k^2 l \sin kl} v_2 \quad (385)$$

$$C_2 = \frac{\sin kl - kl \cos kl}{2k \cos kl - 2k + k^2 l \sin kl} \theta_1 - \frac{\sin kl - kl}{2k \cos kl - 2k + k^2 l \sin kl} \theta_2 - \frac{k - k \cos kl}{2k \cos kl - 2k + k^2 l \sin kl} v_1 + \frac{k}{2k \cos kl - 2k + k^2 l \sin kl} v_2 \quad (386)$$

$$C_3 = -\frac{\cos kl - 1}{2 \cos kl + kl \sin kl - 2} \theta_1 - \frac{\cos kl - 1}{2 \cos kl + kl \sin kl - 2} \theta_2 - k \frac{\sin kl}{2 \cos kl + kl \sin kl - 2} v_1 + k \frac{\sin kl}{2 \cos kl + kl \sin kl - 2} v_2 \quad (387)$$

$$C_4 = -\frac{\sin kl - kl \cos kl}{2k \cos kl - 2k + k^2 l \sin kl} \theta_1 + \frac{\sin kl - kl}{2k \cos kl - 2k + k^2 l \sin kl} \theta_2 + \frac{k \cos kl - k + k^2 l \sin kl}{2k \cos kl - 2k + k^2 l \sin kl} v_1 - \frac{k}{2k \cos kl - 2k + k^2 l \sin kl} v_2 \quad (388)$$

The expression of the bending moment $M(x)$ is obtained as:

$$\begin{aligned} M(x) &= -k^2 * E * I_z * [C_1 * \sin(k * x) + C_2 * \cos(k * x)] = \\ &= -kEI_z \left(\frac{\sin(kl - kx) + \sin kx - kl \cos(kl - kx)}{2 \cos kl + kl \sin kl - 2} \theta_1 - \frac{\sin(kl - kx) + \sin kx - kl \cos kx}{2 \cos kl + kl \sin kl - 2} \theta_2 + \right. \end{aligned}$$

The end bending moments M_1 and M_2 are calculated particularizing equation (??):

$$\begin{aligned}
M_1 &= M(x=0) = -kEI_z \left(\frac{\sin kl - kl \cos kl}{2 \cos kl + kl \sin kl - 2} \theta_1 - \frac{\sin kl - kl}{2 \cos kl + kl \sin kl - 2} \theta_2 + k \frac{\cos kl - 1}{2 \cos kl + kl \sin kl - 2} \right) \\
&= EI_z \left(-\frac{1}{l} kl \frac{\sin kl - kl \cos kl}{2 \cos kl + kl \sin kl - 2} \theta_1 + \frac{1}{l} kl \frac{\sin kl - kl}{2 \cos kl + kl \sin kl - 2} \theta_2 - \frac{1}{l^2} k^2 l^2 \frac{\cos kl - 1}{2 \cos kl + kl \sin kl - 2} \right) \\
&= \frac{EI_z}{l} \left(-kl \frac{\sin kl - kl \cos kl}{2 \cos kl + kl \sin kl - 2} \theta_1 + kl \frac{\sin kl - kl}{2 \cos kl + kl \sin kl - 2} \theta_2 - \frac{1}{l} k^2 l^2 \frac{\cos kl - 1}{2 \cos kl + kl \sin kl - 2} \right) \\
&= \frac{EI_z}{l} \left(s(kl) \theta_1 + s(kl) c(kl) \theta_2 - \frac{1}{l} s(kl) (1 + c(kl)) v_1 + \frac{1}{l} s(kl) (1 + c(kl)) v_2 \right) = \frac{EI_z}{l} \left(s(kl) \theta_1 + s(kl) c(kl) \theta_2 - \frac{1}{l} s(kl) (1 + c(kl)) v_1 + \frac{1}{l} s(kl) (1 + c(kl)) v_2 \right)
\end{aligned}$$

$$\begin{aligned}
M_2 &= -M(x=l) = kEI_z \left(\frac{\sin kl - kl}{2 \cos kl + kl \sin kl - 2} \theta_1 - \frac{\sin kl - kl \cos kl}{2 \cos kl + kl \sin kl - 2} \theta_2 - k \frac{\cos kl - 1}{2 \cos kl + kl \sin kl - 2} \right) \\
&= EI_z \left(\frac{1}{l} kl \frac{\sin kl - kl}{2 \cos kl + kl \sin kl - 2} \theta_1 - \frac{1}{l} kl \frac{\sin kl - kl \cos kl}{2 \cos kl + kl \sin kl - 2} \theta_2 - \frac{1}{l^2} k^2 l^2 \frac{\cos kl - 1}{2 \cos kl + kl \sin kl - 2} \right) \\
&= EI_z \left(\frac{1}{l} kl \frac{\sin kl - kl}{2 \cos kl + kl \sin kl - 2} \theta_1 - \frac{1}{l} kl \frac{\sin kl - kl \cos kl}{2 \cos kl + kl \sin kl - 2} \theta_2 - \frac{1}{l^2} k^2 l^2 \frac{\cos kl - 1}{2 \cos kl + kl \sin kl - 2} \right) \\
&= \frac{EI_z}{l} \left(s(kl) c(kl) \theta_1 + s(kl) \theta_2 - \frac{1}{l} s(kl) (1 + c(kl)) v_1 + \frac{1}{l} s(kl) (1 + c(kl)) v_2 \right) = \frac{EI_z}{l} \left(s(kl) c(kl) \theta_1 + s(kl) \theta_2 - \frac{1}{l} s(kl) (1 + c(kl)) v_1 + \frac{1}{l} s(kl) (1 + c(kl)) v_2 \right)
\end{aligned}$$

where the notation stands for:

$$s(kl) = -\frac{kl(\sin kl - kl \cos kl)}{2 \cos kl + kl \sin kl - 2} = \frac{kl(\sin kl - kl \cos kl)}{2 - 2 \cos kl - kl \sin kl} \quad (393)$$

$$c(kl) = \frac{kl - \sin kl}{\sin kl - kl \cos kl} \quad (394)$$

The reaction forces, V_1 and V_2 are calculated from the member equilibrium, by writing the moment equation at the location of the end 2 and the projection of the forces on y axis:

$$-V_1 * l - P * (v_2 - v_1) + M_1 + M_2 = 0 \quad (395)$$

$$-V_1 + V_2 = 0 \quad (396)$$

Solving the first equilibrium equation and substituting the expressions of the end moments obtained above the reaction forces are:

$$\begin{aligned}
V_1 &= V_2 = V = \frac{M_1 + M_2 - P * (v_2 - v_1)}{l} = \\
&= \frac{\frac{EI_z}{l} \left(s(kl)\theta_1 + s(kl)c(kl)\theta_2 + \frac{1}{l}s(kl)(1 + c(kl))(v_2 - v_1) \right) + \frac{EI_z}{l} \left(s(kl)c(kl)\theta_1 + s(kl)\theta_2 + \frac{1}{l}s(kl)(1 + c(kl))(v_2 - v_1) \right)}{l} \\
&= \frac{\frac{EI_z}{l} \left(s(kl)\theta_1 + s(kl)c(kl)\theta_2 + \frac{1}{l}s(kl)(1 + c(kl))(v_2 - v_1) \right) + \left(s(kl)c(kl)\theta_1 + s(kl)\theta_2 + \frac{1}{l}s(kl)(1 + c(kl))(v_2 - v_1) \right)}{l} \\
&= \frac{EI_z}{l} \frac{(s(kl) + s(kl)c(kl))\theta_1 + (s(kl) + s(kl)c(kl))\theta_2 + \left(\frac{2}{l}s(kl)(1 + c(kl)) - k^2l \right)(v_2 - v_1)}{l} = \\
&= \frac{EI_z}{l} \left[\frac{s(kl)(1 + c(kl))}{l}\theta_1 + \frac{s(kl)(1 + c(kl))}{l}\theta_2 + \frac{2s(kl)(1 + c(kl)) - k^2l^2}{l^2}(v_2 - v_1) \right]
\end{aligned}$$

The expressions (391), (392) and (397) are employed to ensemble the stiffness matrix K_{ff} of the *fixed-fixed member* as follows:

$$\begin{bmatrix} M_1 \\ V_1 \\ M_2 \\ V_2 \end{bmatrix} = \frac{EI_z}{l} \begin{bmatrix} s(kl) & -\frac{s(kl)(1 + c(kl))}{l} & s(kl)c(kl) & \frac{s(kl)(1 + c(kl))}{l} \\ \frac{s(kl)(1 + c(kl))}{l} & -\frac{2s(kl)(1 + c(kl)) - k^2l^2}{l^2} & \frac{s(kl)(1 + c(kl))}{l} & \frac{2s(kl)(1 + c(kl)) - k^2l^2}{l^2} \\ s(kl)c(kl) & -\frac{s(kl)(1 + c(kl))}{l} & s(kl) & \frac{s(kl)(1 + c(kl))}{l} \\ \frac{s(kl)(1 + c(kl))}{l} & -\frac{2s(kl)(1 + c(kl)) - k^2l^2}{l^2} & \frac{s(kl)(1 + c(kl))}{l} & \frac{2s(kl)(1 + c(kl)) - k^2l^2}{l^2} \end{bmatrix} \quad (398)$$

where the matrix K_{ff} (4x4) is the *stiffness matrix of the fixed-fixed beam-column*:

$$K_{ff} = \frac{EI_z}{l} \begin{bmatrix} s(kl) & -\frac{s(kl)(1 + c(kl))}{l} & s(kl)c(kl) & \frac{s(kl)(1 + c(kl))}{l} \\ \frac{s(kl)(1 + c(kl))}{l} & -\frac{2s(kl)(1 + c(kl)) - k^2l^2}{l^2} & \frac{s(kl)(1 + c(kl))}{l} & \frac{2s(kl)(1 + c(kl)) - k^2l^2}{l^2} \\ s(kl)c(kl) & -\frac{s(kl)(1 + c(kl))}{l} & s(kl) & \frac{s(kl)(1 + c(kl))}{l} \\ \frac{s(kl)(1 + c(kl))}{l} & -\frac{2s(kl)(1 + c(kl)) - k^2l^2}{l^2} & \frac{s(kl)(1 + c(kl))}{l} & \frac{2s(kl)(1 + c(kl)) - k^2l^2}{l^2} \end{bmatrix} \quad (399)$$

The variation of the stiffness coefficients where $kl = \pi\sqrt{\frac{P}{P_E}}$ is illustrated in Figure 17.54.

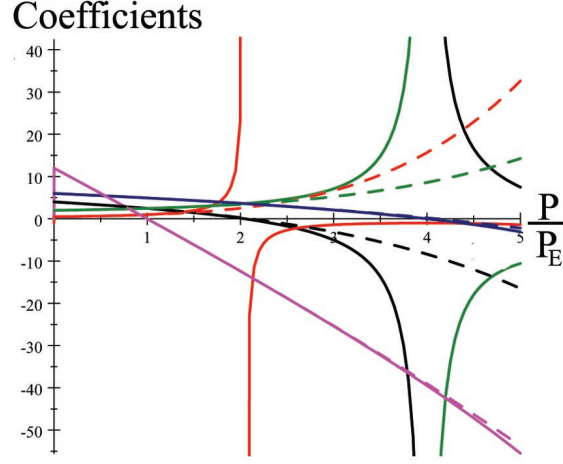


Figure 4: Figure 17.54 Stiffness Matrix Coefficients Variation

If the functions $s(kl)$ and $c(kl)$ are expanded in a *truncated Taylor series with five terms* around the value $kl = 0$ the expressions of the stiffness matrix coefficients become:

$$\begin{aligned}
 s(kl) &\simeq 4 - \frac{2}{15}(kl)^2 - \frac{11}{6300}(kl)^4 - \frac{1}{27000}(kl)^6 - \frac{509}{582120000}(kl)^8 = \\
 &= 4 - \frac{2}{15}\left(\pi\sqrt{\frac{P}{P_E}}\right)^2 - \frac{11}{6300}\left(\pi\sqrt{\frac{P}{P_E}}\right)^4 - \frac{1}{27000}\left(\pi\sqrt{\frac{P}{P_E}}\right)^6 - \frac{509}{582120000}\left(\pi\sqrt{\frac{P}{P_E}}\right)^8
 \end{aligned} \quad (400)$$

$$\begin{aligned}
 c(kl) &\simeq \frac{1}{2} + \frac{1}{40}(kl)^2 + \frac{11}{8400}(kl)^4 + \frac{67}{1008000}(kl)^6 + \frac{2579}{776160000}(kl)^8 = \\
 &= \frac{1}{2} + \frac{1}{40}\left(\pi\sqrt{\frac{P}{P_E}}\right)^2 + \frac{11}{8400}\left(\pi\sqrt{\frac{P}{P_E}}\right)^4 + \frac{67}{1008000}\left(\pi\sqrt{\frac{P}{P_E}}\right)^6 + \frac{2579}{776160000}\left(\pi\sqrt{\frac{P}{P_E}}\right)^8
 \end{aligned} \quad (401)$$

the expressions of the stiffness matrix coefficients become:

$$s(kl)c(kl) \simeq 2 + \frac{1}{30}(kl)^2 + \frac{13}{12600}(kl)^4 + \frac{11}{378000}(kl)^6 + \frac{907}{1164240000}(kl)^8 \quad (402)$$

$$s(kl)(c(kl) + 1) \simeq 6 - \frac{1}{10}(kl)^2 - \frac{1}{1400}(kl)^4 - \frac{1}{126000}(kl)^6 - \frac{37}{388080000}(kl)^8 \quad (403)$$

$$2s(kl)(c(kl) + 1) - k^2 l^2 \simeq 12 - \frac{6}{5}(kl)^2 - \frac{1}{700}(kl)^4 - \frac{1}{63000}(kl)^6 - \frac{37}{194040000}(kl)^8 \quad (404)$$

In order to substantiate the error make by the usage of the truncated Taylor series, substitute $kl = \pi\sqrt{\frac{P}{P_E}}$ in the expressions of the stiffness matrix coefficients and superimposed them over the exact expressions drawn in Figure 17.54. Because the functions $s(kl)$ and $c(kl)$ are the main components of the stiffness coefficients it is instructive to plot them together with various degrees of approximation as shown in Figure 17.55.

Figure 17.55 Degrees of Approximation for $s(\frac{P}{P_E})$ and $c(\frac{P}{P_E})$ Functions

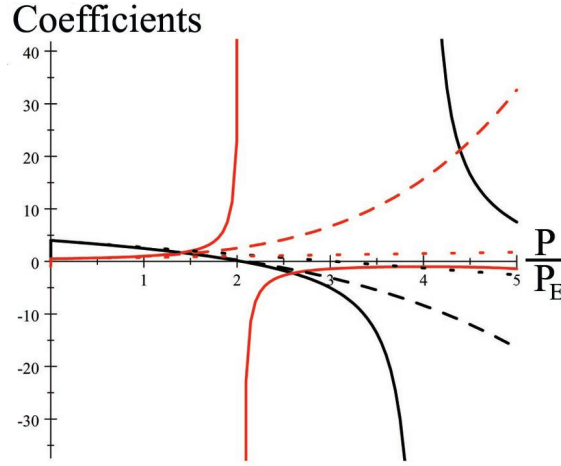


Figure 17.55 Functions $s(kl)$ and $c(kl)$

Remark 70 From Figure 17.55 can be infer that the approximation with only two terms closely follows the exact function for the interval $\frac{P}{P_E} \in [0, 1.5]$. Outside of this interval for $\frac{P}{P_E} > 1.5$ the error significantly increases and the exact function has to be used. The approximations with more terms reduce somehow the error, but the difference remain noticeable. It can be concluded that just the approximation with two terms is enough for the interval $\frac{P}{P_E} \in [0, 1.5]$.

Using the above coefficients to express the stiffness matrix K_{ff} (4x4) an interesting approximation is obtained:

$$\begin{aligned}
 K_{ff} &\simeq \frac{EI_z}{l} \begin{bmatrix} 4 & -\frac{6}{l} & 2 & \frac{6}{l} \\ 6 & -\frac{12}{l^2} & 6 & \frac{12}{l^2} \\ \frac{6}{l} & -\frac{12}{l^2} & \frac{6}{l} & \frac{12}{l^2} \\ 2 & -\frac{6}{l} & 4 & \frac{6}{l} \end{bmatrix} + \frac{EI_z}{l} \begin{bmatrix} -\frac{2}{15} & \frac{1}{10l} & \frac{1}{30} & -\frac{1}{10l} \\ -\frac{1}{10l} & \frac{1}{5l^2} & -\frac{1}{10l} & -\frac{1}{5l^2} \\ \frac{1}{30} & \frac{1}{10l} & -\frac{1}{15} & -\frac{1}{10l} \\ -\frac{1}{10l} & \frac{1}{5l^2} & -\frac{1}{10l} & -\frac{1}{5l^2} \end{bmatrix} k^2 l^2 + \dots \quad (405) \\
 &= K_{ff}^0 + K_{ff}^1 k^2 l^2 + \dots = K_{ff}^0 + K_{ff}^1 * (\pi\sqrt{\frac{P}{P_E}})^2 + \dots \quad (406)
 \end{aligned}$$

Remark 71 (a) The matrix K_{ff}^0 is the stiffness matrix for a fixed-fixed member when the compressive force is absent or negligible;

$$K_{ff}^0 = \frac{EI_z}{l} \begin{bmatrix} 4 & -\frac{6}{l} & 2 & \frac{6}{l} \\ \frac{6}{l} & \frac{12}{l^2} & \frac{6}{l} & \frac{12}{l^2} \\ 2 & -\frac{6}{l} & 4 & \frac{6}{l} \\ \frac{6}{l} & \frac{12}{l^2} & \frac{6}{l} & \frac{12}{l^2} \end{bmatrix} \quad (407)$$

Remark 72 (b) The matrix K_{ff}^1 represents the first correction when the compressive force is present;

$$\begin{aligned} K_{ff}^1 &= \frac{EI_z}{l} \begin{bmatrix} -\frac{2}{15} & \frac{1}{10l} & \frac{1}{30} & -\frac{1}{10l} \\ -\frac{1}{10l} & \frac{5l^2}{1} & -\frac{10l}{2} & -\frac{5l^2}{1} \\ \frac{1}{30} & \frac{10l}{6} & -\frac{15}{1} & -\frac{10l}{6} \\ -\frac{1}{10l} & \frac{5l^2}{1} & -\frac{10l}{2} & -\frac{5l^2}{1} \end{bmatrix} (\pi \sqrt{\frac{P}{P_E}})^2 \\ &= \frac{\pi^2 EI_z}{l} \frac{EI_z}{l} \begin{bmatrix} -\frac{2}{15} & \frac{1}{10l} & \frac{1}{30} & -\frac{1}{10l} \\ -\frac{1}{10l} & \frac{5l^2}{1} & -\frac{10l}{2} & -\frac{5l^2}{1} \\ \frac{1}{30} & \frac{10l}{6} & -\frac{15}{1} & -\frac{10l}{6} \\ -\frac{1}{10l} & \frac{5l^2}{1} & -\frac{10l}{2} & -\frac{5l^2}{1} \end{bmatrix} \frac{P}{P_E} \end{aligned} \quad (408)$$

To assess the error made by using the two term approximation in calculating the stiffness matrix a comparison is made for few ratios $\frac{P}{P_E}$:

-for $\frac{P}{P_E} = 0.5$

$$K_{ff} = \frac{EI_z}{l} \begin{bmatrix} 3.2945 & 2.936 & \frac{5.881}{l} \\ 2.936 & 3.2945 & \frac{5.881}{l} \\ \frac{5.881}{l} & \frac{5.881}{l} & \frac{6.044}{l^2} \end{bmatrix} \quad (409)$$

$$K_{ff}^{app} = \frac{EI_z}{l} \begin{bmatrix} 3.342 & 2.1645 & \frac{5.5065}{l} \\ 2.1645 & 3.342 & \frac{5.5065}{l} \\ \frac{5.5065}{l} & \frac{5.5065}{l} & \frac{6.0782}{l^2} \end{bmatrix} \quad (410)$$

max_error =

-for $\frac{P}{P_E} = 1$

??

1.6.1.2 Fixed-Hinged Column (Figure 17.56) A fixed-hinged plane beam-column is characterized, if the axial deformation is neglected, by three degrees-of-freedom θ_2, v_1, v_2 representing the rotation at end 1 and the transversal displacement at ends 1 and 2, respectively.

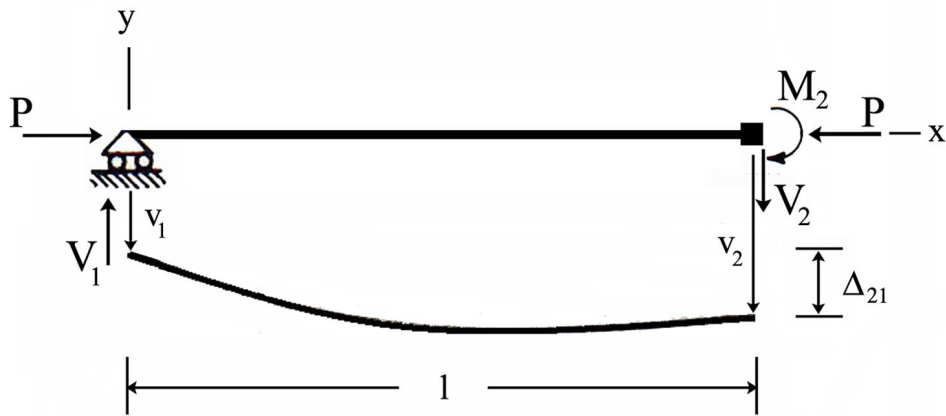


Figure 17.56 Fixed- Pined Column

To obtain the relation between the reactions and the ends' degrees of freedom the integration constants C_1, C_2, C_3 and C_4 characterizing the general solution $v(x)$ expressed by equation (49) are calculated for the specific boundary conditions They are:

- at the end 1 ($x = 0$)

$$v(x = 0) = -v_1 \rightarrow C_1 * \sin(k * 0) + C_2 \cos(k * 0) + C_3 * 0 + C_4 = v_1 \rightarrow C_2 + C_4 = -v_1 \quad (411)$$

$$\begin{aligned} M(x = 0) &= 0 \rightarrow -k^2 * E * I_z * [C_1 * \sin(k * 0) + C_2 * \cos(k * 0)] = 0 \\ &\rightarrow -k^2 * E * I_z * C_2 = 0 \end{aligned} \quad (412)$$

- at the end 2 ($x = l$)

$$v(x = l) = -v_2 \rightarrow C_1 * \sin(k * l) + C_2 \cos(k * l) + C_3 * l + C_4 = -v_2 \quad (413)$$

$$\theta(x = l) = -\theta_2 \rightarrow k * C_1 * \cos(k * l) - k * C_2 * \sin(k * l) + C_3 = -\theta_2$$

Remark 73 *The minus signs are introduced in order to accommodate the general convention used in the structural analysis: the angles and moments are positive for a rotation in the clock direction. Equations (411) through (??) comprised an algebraic system, written in a matricial format, for equations with constants coefficients:*

$$\begin{bmatrix} 0 & 1 & 0 & 1 \\ 0 & -k^2 * E * I_z & 0 & 0 \\ \sin(k * l) & \cos(k * l) & l & 1 \\ k * \cos(k * l) & -k * \sin(k * l) & 1 & 0 \end{bmatrix} \begin{bmatrix} C_1 \\ C_2 \\ C_3 \\ C_4 \end{bmatrix} = \begin{bmatrix} -v_1 \\ 0 \\ -v_2 \\ -\theta_2 \end{bmatrix} \quad (414)$$

The constants are calculated solving the system (414):

$$C_1 = \frac{l}{\sin kl - kl \cos kl} \theta_2 + \frac{1}{\sin kl - kl \cos kl} v_1 - \frac{1}{\sin kl - kl \cos kl} v_2 \quad (415)$$

$$C_2 = 0 \quad (416)$$

$$C_3 = -\frac{\sin kl}{\sin kl - kl \cos kl} \theta_2 - k \frac{\cos kl}{\sin kl - kl \cos kl} v_1 + k \frac{\cos kl}{\sin kl - kl \cos kl} v_2 \quad (417)$$

$$C_4 = -v_1 \quad (418)$$

The expression of the bending moment $M(x)$ is obtained as:

$$\begin{aligned} M(x) &= -k^2 * E * I_z * [C_1 * \sin(k * x) + C_2 * \cos(k * x)] = \\ &= -k^2 * E * I_z * \left(\frac{l \sin(k * x)}{\sin kl - kl \cos kl} \theta_2 + \frac{\sin(k * x)}{\sin kl - kl \cos kl} v_1 - \frac{\sin(k * x)}{\sin kl - kl \cos kl} v_2 \right) \end{aligned} \quad (419)$$

The end bending moments M_2 is calculated by particularizing equation (419) for $x = l$:

$$\begin{aligned}
M_2 &= -M(x = l) = k^2 EI_z \left(l \frac{\sin kl}{\sin kl - kl \cos kl} \theta_2 + \frac{\sin kl}{\sin kl - kl \cos kl} v_1 - \frac{\sin kl}{\sin kl - kl \cos kl} v_2 \right) \quad (420) \\
&= EI_z \left(k^2 l \frac{\sin kl}{\sin kl - kl \cos kl} \theta_2 + k^2 \frac{\sin kl}{\sin kl - kl \cos kl} v_1 - k^2 \frac{\sin kl}{\sin kl - kl \cos kl} v_2 \right) = \\
&= EI_z \left(\frac{1}{l} k^2 l^2 \frac{\sin kl}{\sin kl - kl \cos kl} \theta_2 + \frac{1}{l^2} k^2 l^2 \frac{\sin kl}{\sin kl - kl \cos kl} v_1 - \frac{1}{l^2} k^2 l^2 \frac{\sin kl}{\sin kl - kl \cos kl} v_2 \right) = \\
&= \frac{EI_z}{l} \left(k^2 l^2 \frac{\sin kl}{\sin kl - kl \cos kl} \theta_2 + \frac{1}{l} k^2 l^2 \frac{\sin kl}{\sin kl - kl \cos kl} v_1 - \frac{1}{l} k^2 l^2 \frac{\sin kl}{\sin kl - kl \cos kl} v_2 \right) = \\
&= \frac{EI_z}{l} \left(k^2 l^2 \frac{\sin kl}{\sin kl - kl \cos kl} \theta_2 - \frac{1}{l} k^2 l^2 \frac{\sin kl}{\sin kl - kl \cos kl} (v_2 - v_1) \right) = \\
&= \frac{EI_z}{l} \left(k^2 l^2 \frac{\sin kl}{\sin kl - kl \cos kl} \theta_2 - \frac{1}{l} k^2 l^2 \frac{\sin kl}{\sin kl - kl \cos kl} \Delta_{21} \right) = \\
&= \frac{EI_z}{l} \left(d(kl) \theta_2 - \frac{1}{l} d(kl) \Delta_{21} \right)
\end{aligned}$$

where the notation stands for:

$$d(kl) = k^2 l^2 \frac{\sin kl}{\sin kl - kl \cos kl} \quad (421)$$

and Δ_{21} is the relative displacement between the ends 1 and 2, respectively.

$$\Delta_{21} = v_2 - v_1 \quad (422)$$

The reaction forces, V_1 and V_2 are calculated from the member equilibrium, by writing the moment equation at the location of the end 2 and the projection of the forces on y axis:

$$V_1 * l + P * (v_2 - v_1) + M_2 = 0 \quad (423)$$

$$V_1 - V_2 = 0 \quad (424)$$

Solving the first equilibrium equation and substituting the expression of the end moment M_1 obtained above the reaction forces are

$$\begin{aligned}
V_1 &= V_2 = V = -\frac{M_2}{l} - \frac{P * (v_2 - v_1)}{l} = \\
&= -\frac{1}{l} \left(\frac{EI_z}{l} \left(d(kl)\theta_2 - \frac{1}{l}d(kl)\Delta_{21} \right) \right) - \frac{P * \Delta_{21}}{l} = \\
&= \frac{EI_z}{l^2} \left(-d(kl)\theta_2 + \frac{1}{l}d(kl)\Delta_{21} \right) - \frac{k^2 EI_z * \Delta_{21}}{l} = \\
&= \frac{EI_z}{l^2} \left(-d(kl)\theta_2 + \frac{1}{l}(d(kl) - k^2 * l^2)\Delta_{21} \right)
\end{aligned} \tag{425}$$

The expressions (420) and (425) are employed to ensemble the stiffness matrix of the *fixed-hinged member*:

$$\begin{bmatrix} M_2 \\ V \end{bmatrix} = \frac{EI_z}{l} \begin{bmatrix} d(kl) & -\frac{d(kl)}{l} \\ -\frac{d(kl)}{l} & \frac{d(kl) - k^2 l^2}{l^2} \end{bmatrix} \begin{bmatrix} \theta_2 \\ \Delta_{21} \end{bmatrix} \tag{426}$$

where the matrix K_{ff} (2×2) is the *stiffness matrix of the fixed-hinged beam-column*:

$$K_{ff} = \frac{EI_z}{l} \begin{bmatrix} d(kl) & -\frac{d(kl)}{l} \\ -\frac{d(kl)}{l} & \frac{d(kl) - k^2 l^2}{l^2} \end{bmatrix} \tag{427}$$

Remark 74 *The number of degrees of freedom is reduced to only two for the case of the fixed-hinged beam-column and consequently, the sizes of the stiffness matrix K_{ff} (2×2), reaction vector $R_{ff}(2, 1)$ and displacement end vector $D_{ff}(2, 1)$ are accordingly reduced.*

A similar discussion can be made relatively to the approximation of the function and stiffness matrix by expanding them in a truncated Taylor series with five terms.

1.6.1.3 Stability of Simple Continuos Column (Figure 17.57) A simple example of a continuous beam-column characterized by a constant cross-section is illustrated in Figure 17.57.a.

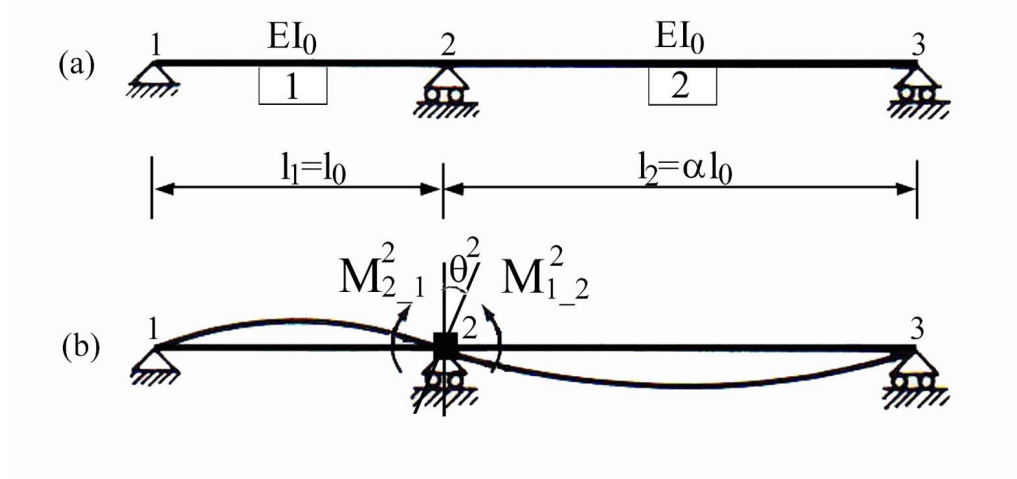


Figure 17.57

By fixing the rotation of the node 2, θ^2 (the upperscript indice refers at the node number of continuous beam, in this case node number 2), as illustrated in Figure 17.57.b, the system is divided into two fixed-hinged beams. If a clock-wise rotation θ^2 is applied to the fixity of node, in each member reactions will appear at the ends. A kinematic analysis of the possibilities of motion of the ends, followed by the reaction determination in accordance to equation (426), is evaluated for each individual member:

- member 1 : $(\frac{EI_z}{l} = \frac{EI_0}{l_1}, kl = k_1 l_1)$

kinematic analysis: $\theta_2 = \theta^2 \quad v_1 = 0 \quad v_2 = 0 \quad \Delta_{21} = 0$

reactions calculation accordingly to equation (426):

$$\begin{bmatrix} M_{2-1} \\ V_{-1} \end{bmatrix} = \frac{EI_0}{l_1} \begin{bmatrix} d(k_1 l_1) & -\frac{d(k_1 l_1)}{l_1} \\ -\frac{d(k_1 l_1)}{l_1} & \frac{d(k_1 l_1)}{l_1^2} - k_1^2 l_1^2 \end{bmatrix} \begin{bmatrix} \theta_2 = \theta^2 \\ \Delta_{21} = 0 \end{bmatrix} = \quad (428)$$

$$\begin{bmatrix} M_{2-1} \\ V_{-1} \end{bmatrix} = \frac{EI_0}{l_1} \begin{bmatrix} d(k_1 l_1) \theta^2 \\ -\frac{d(k_1 l_1)}{l_1} \theta^2 \end{bmatrix} \quad (429)$$

- member 2 : $(\frac{EI_z}{l} = \frac{EI_0}{l_2}, kl = k_2 l_2)$

kinematic analysis: $\theta_2 = \theta^2 \quad v_1 = 0 \quad v_2 = 0 \quad \Delta_{21} = 0$

reactions calculation adapting equation (426) to the beam position in the system:

$$\begin{bmatrix} M_{2_2} \\ V_{_2} \end{bmatrix} = \frac{EI_0}{l_2} \begin{bmatrix} d(k_2 l_2) & -\frac{d(k_2 l_2)}{l_2} \\ -\frac{d(k_2 l_2)}{l_2} & \frac{d(k_2 l_2) - k_2^2 l_2^2}{l_2^2} \end{bmatrix} \begin{bmatrix} \theta_2 = \theta^2 \\ \Delta_{21} = 0 \end{bmatrix} = \quad (430)$$

$$\begin{bmatrix} M_{2_2} \\ V_{_2} \end{bmatrix} = \frac{EI_0}{l_2} \begin{bmatrix} d(k_2 l_2) \theta^2 \\ -\frac{d(k_2 l_2)}{l_2} \theta^2 \end{bmatrix} \quad (431)$$

The total moment M^2 is artificially induced by the imposed rotation θ^2 is zero in reality:

$$M^2 = 0 \rightarrow M_{2_1} + M_{2_2} = 0 \quad (432)$$

Substituting the expressions of the moments, M_{2_1} and M_{2_2} , calculated in equations (428) and (430) into equation (432) the following equilibrium equation is obtained:

$$\begin{aligned} \frac{EI_0}{l_1} d(k_1 l_1) \theta^2 + \frac{EI_0}{l_2} d(k_2 l_2) \theta^2 &= 0 \rightarrow \\ \left[\frac{EI_0}{l_1} d(k_1 l_1) + \frac{EI_0}{l_2} d(k_2 l_2) \right] \theta^2 &= 0 \end{aligned} \quad (433)$$

Equation (433) imposes for $\theta^2 \neq 0$ that :

$$\frac{EI_0}{l_1} d(k_1 l_1) + \frac{EI_0}{l_2} d(k_2 l_2) = 0 \quad (434)$$

Equation (434) represents the *stability equation* of the beam-column.

To solve this equation a number of cosmetic arrangements has to be conducted, by unifying some of the parameters involved:

$$\begin{aligned} l_1 &= l_0 \\ l_2 &= \alpha l_0 \\ k_1 l_1 &= l_1 \sqrt{\frac{P_1}{EI_1}} = l_0 \sqrt{\frac{P}{EI_0}} = kl \\ k_2 l_2 &= l_2 \sqrt{\frac{P_2}{EI_2}} = \alpha l_0 \sqrt{\frac{P}{EI_0}} = \alpha kl \end{aligned} \quad (435)$$

Substituting parameters expressed by equations (435) into equation (434) the following *stability equation* is obtained:

$$\frac{EI_0}{l_0}d(kl) + \frac{EI_0}{\alpha l_0}d(\alpha kl) = 0 \quad (436)$$

At this point, the explicit expressions of the functions $d(kl)$ type has to be substituted into equation (436) and after algebraic manipulations:

$$(kl)^2 \frac{\sin kl}{\sin kl - kl \cos kl} + \alpha(kl)^2 \frac{\sin \alpha kl}{\sin \alpha kl - \alpha kl \cos \alpha kl} = 0 \quad (437)$$

The trigonometric equation (437) is solved graphically and the representative functional relation between α and kl is shown in Figure 17.58

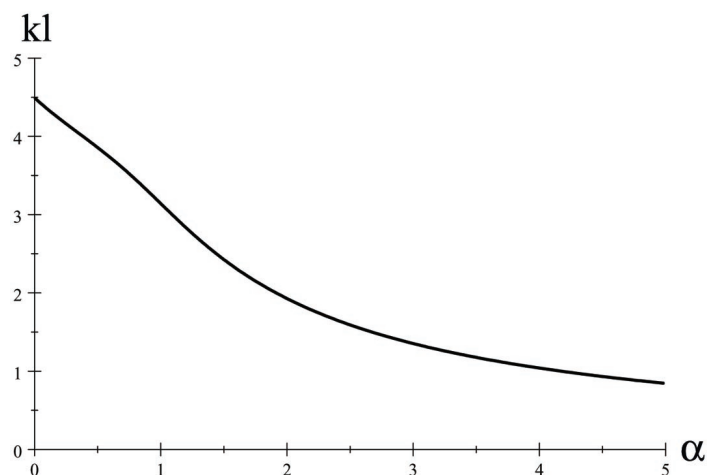


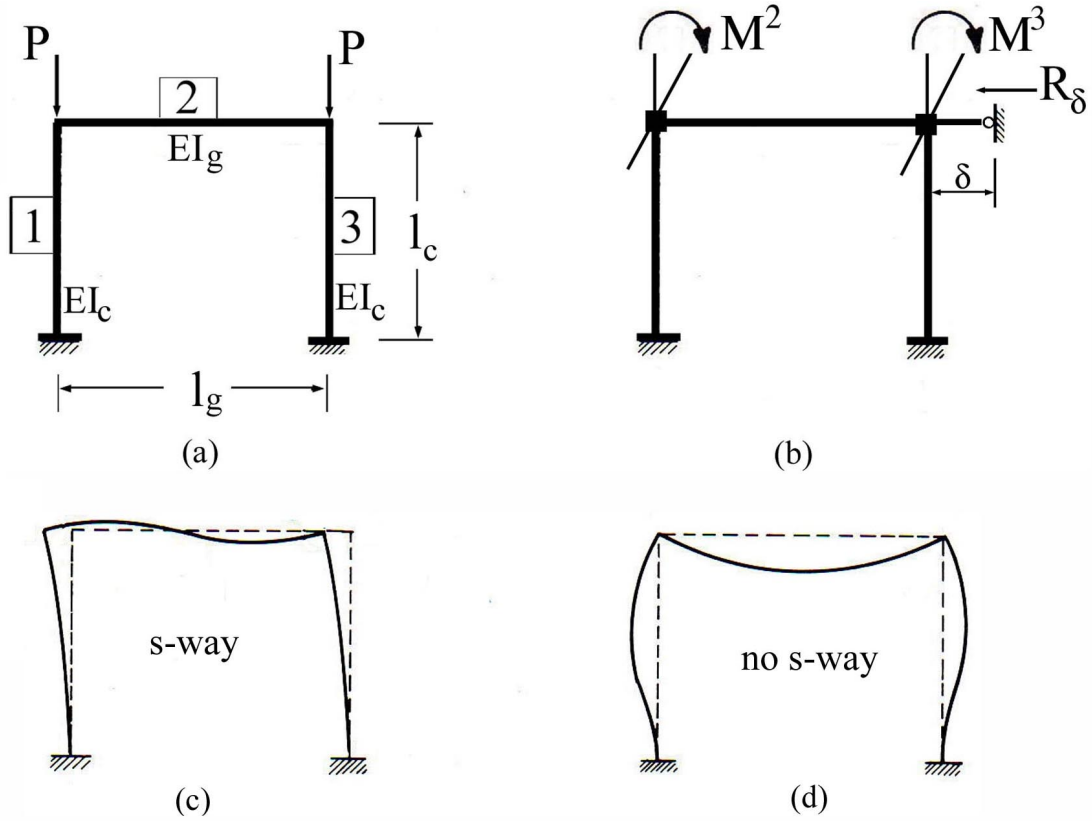
Figure 17.58

Some of the results obtained from the the graph illustrated in Figure 17.58 are presented in the following table:

$\alpha = l_2/l_1$	kl	$l_b/l = \pi/kl$	$P/P_E = (kl/\pi)^2$
0.05	4.4208	0.71064	1.9802
1.0	3.1416	1.00000	1.0000
2.0	1.9283	1.6292	0.3767
3.0	1.3533	2.3214	0.1856
4.0	1.0403	3.0199	0.1097
5.0	0.8446	3.7196	0.0723

(438)

1.6.1.4 Stability of Simple Frame (Figure 17.59) The simple case of the planar frame shown in Figure 17.59.a.



The frame has three possibilities of movement: the rotations of nodes 2 and 3, θ_1 and θ_2 , and the horizontal displacement, δ of the girder 23. *The reduced number of movement possibilities, the number of degrees of freedom, which in general are equal to the number of free nodes, 2 in this case, multiplied by 3, is due to the assumption the beam-columns are considered rigid along their longitudinal axis.* As was proceed in the previous example, the three degrees of freedom are blocked and the resulting structure, illustrated in Figure 17.59.b, made of tree fixed-fixed beam-columns results. Because the configuration of the structure does not have a clear path to follow and orientate each member, the path used is shown by arrows indicated on Figure 17.59.b. Using the stiffness matrices pertinent to each member, the corresponding moments and shear forces are calculated:

- member 1 ($\frac{EI_z}{l} = \frac{EI_c}{l_c}$, $kl = k_c l_c$) represents the columns (2 – 3):

$$\text{kinematic analysis:} \quad \theta_{1_1} = 0 \quad v_{1_1} = 0 \quad \theta_{2_1} = \theta^2 \quad v_{2_1} = -\delta$$

reactions calculation:

$$\begin{bmatrix} M_{1_1} = M_{-1}^1 \\ V_{1_1} = V_{-1}^1 \\ M_{2_1} = M_{-1}^2 \\ V_{2_1} = V_{-1}^2 \end{bmatrix} = \frac{EI_c}{l_c} \begin{bmatrix} \frac{s(k_cl_c)}{l_c} & -\frac{s(k_cl_c)(1+c(k_cl_c))}{l_c} & \frac{s(k_cl_c)c(k_cl_c)}{l_c} & \frac{s(k_cl_c)(1+c(k_cl_c))}{l_c} \\ \frac{s(k_cl_c)(1+c(k_cl_c))}{l_c} & -\frac{2s(k_cl_c)(1+c(k_cl_c))-k_c^2l_c^2}{l_c^2} & \frac{s(k_cl_c)(1+c(k_cl_c))}{l_c} & \frac{2s(k_cl_c)(1+c(k_cl_c))-k_c^2l_c^2}{l_c^2} \\ s(k_cl_c)c(k_cl_c) & -\frac{s(k_cl_c)(1+c(k_cl_c))}{l_c} & s(k_cl_c) & \frac{s(k_cl_c)(1+c(k_cl_c))}{l_c} \\ \frac{s(k_cl_c)(1+c(k_cl_c))}{l_c} & -\frac{2s(k_cl_c)(1+c(k_cl_c))-k_c^2l_c^2}{l_c^2} & \frac{s(k_cl_c)(1+c(k_cl_c))}{l_c} & \frac{2s(k_cl_c)(1+c(k_cl_c))-k_c^2l_c^2}{l_c^2} \end{bmatrix} \quad (439)$$

Remark 75 The first subscript, 1 or 2, of the reaction vector components represent the end number of the typical beam-column corresponding to the notation in the section where the stiffness matrix has been developed. The second subscript of the reaction vector components preceded by a underscore line indicates the number of the member in the structure (1)

- member 2 ($\frac{EI_z}{l} = \frac{EI_g}{l_g}, k_g l_g = 0$) noaxial load represents the girder (2 – 3):

kinematic analysis: $\theta_{1_2} = \theta^2 \quad v_{1_2} = 0 \quad \theta_{2_2} = \theta^3 \quad v_{2_2} = 0$ (the columns are finite rigid axially)

reactions calculation:

$$\begin{bmatrix} M_{1_2} = M_{-2}^2 \\ V_{1_2} = V_{-2}^2 \\ M_{2_2} = M_{-2}^3 \\ V_{2_2} = V_{-2}^3 \end{bmatrix} = \frac{EI_g}{l_g} \begin{bmatrix} \frac{s(0)}{l_g} & -\frac{s(0)(1+c(0))}{l_g} & \frac{s(0)c(0)}{l_g} & \frac{s(0)(1+c(0))}{l_g} \\ \frac{s(0)(1+c(0))}{l_g} & -\frac{2s(0)(1+c(0))-0^2}{l_g^2} & \frac{s(0)(1+c(0))}{l_g} & \frac{2s(0)(1+c(0))-0^2}{l_g^2} \\ s(0)c(0) & -\frac{s(0)(1+c(0))}{l_g} & s(0) & \frac{s(0)(1+c(0))}{l_g} \\ \frac{s(0)(1+c(0))}{l_g} & -\frac{2s(0)(1+c(0))-0^2}{l_g^2} & \frac{s(0)(1+c(0))}{l_g} & \frac{2s(0)(1+c(0))-0^2}{l_g^2} \end{bmatrix} \quad (440)$$

$$\begin{bmatrix} M_{1_2} = M_{-2}^2 \\ V_{1_2} = V_{-2}^2 \\ M_{2_2} = M_{-2}^3 \\ V_{2_2} = V_{-2}^3 \end{bmatrix} = \frac{EI_g}{l_g} \begin{bmatrix} 4 & -\frac{6}{l} & 2 & \frac{6}{l} \\ \frac{6}{l} & -\frac{12}{l^2} & \frac{6}{l} & \frac{12}{l^2} \\ 2 & -\frac{6}{l} & 4 & \frac{6}{l} \\ \frac{6}{l} & -\frac{12}{l^2} & \frac{6}{l} & \frac{12}{l^2} \end{bmatrix} \begin{bmatrix} \theta_{1_2} = \theta^2 \\ v_{1_2} = 0 \\ \theta_{2_2} = \theta^3 \\ v_{2_2} = 0 \end{bmatrix}$$

- member 3 ($\frac{EI_z}{l} = \frac{EI_c}{l_c}, kl = k_cl_c$) represents the column (3 – 4):

kinematic analysis: $\theta_{1_3} = \theta^3 \quad v_{1_3} = \delta \quad \theta_{2_3} = 0 \quad v_{2_3} = 0$

reactions calculation:

$$\begin{bmatrix} M_{1_3} = M^3_3 \\ V_{1_3} = V^3_3 \\ M_{2_3} = M^4_3 \\ V_{2_3} = V^4_3 \end{bmatrix} = \frac{EI_c}{l_c} \begin{bmatrix} \frac{s(k_cl_c)}{l_c} & -\frac{s(k_cl_c)(1+c(k_cl_c))}{l_c} & \frac{s(k_cl_c)c(k_cl_c)}{l_c} & \frac{s(k_cl_c)}{l_c} \\ \frac{s(k_cl_c)(1+c(k_cl_c))}{l_c} & -\frac{2s(k_cl_c)(1+c(k_cl_c))-k_c^2l_c^2}{l_c^2} & \frac{s(k_cl_c)(1+c(k_cl_c))}{l_c} & \frac{2s(k_cl_c)}{l_c} \\ s(k_cl_c)c(k_cl_c) & -\frac{s(k_cl_c)(1+c(k_cl_c))}{l_c} & s(k_cl_c) & \frac{s(k_cl_c)}{l_c} \\ \frac{s(k_cl_c)(1+c(k_cl_c))}{l_c} & -\frac{2s(k_cl_c)(1+c(k_cl_c))-k_c^2l_c^2}{l_c^2} & \frac{s(k_cl_c)(1+c(k_cl_c))}{l_c} & \frac{2s(k_cl_c)}{l_c} \end{bmatrix} \begin{bmatrix} \theta^3 \\ \delta \\ 0 \\ 0 \end{bmatrix} \quad (441)$$

Remark 76 *The rotations of the nodes 2 and 3, θ^2 and θ^3 , and the lateral displacement δ of the real structure are not prevented. The induced blockages generate artificial reaction at these locations, which are in reality zero.*

Using the finding of the above remark, the moment reactions, M^2 and M^3 , and the horizontal force reaction R_δ generated around the fixity blocks of the nodes 2 and 3 and in the horizontal restraint of the lateral displacement three equations of equilibrium are written:

$$\begin{aligned} M^2 &= 0 \\ M^3 &= 0 \\ R_\delta &= 0 \end{aligned} \quad (442)$$

Substituting into equation (442) the expressions of the corresponding moments and reactions of individual members, equations (439) through (??), results:

$$\begin{aligned} M^2_{-1} + M^2_{-2} &= 0 \\ M^3_{-2} + M^3_{-3} &= 0 \\ V^2_{-1} + V^3_{-3} &= 0 \end{aligned} \quad (443)$$

and explicitly after algebraic manipulations the system (443) becomes:

$$\begin{bmatrix} M_{2_1} = M_{-1}^2 \\ V_{2_1} = V_{-1}^2 \end{bmatrix} = \frac{EI_c}{l_c} \begin{bmatrix} s(k_cl_c)\theta^2 - \frac{s(k_cl_c)(1+c(k_cl_c))}{l_c}\delta \\ \frac{s(k_cl_c)(1+c(k_cl_c))}{l_c}\theta^2 - \frac{2s(k_cl_c)(1+c(k_cl_c)) - k_c^2 l_c^2}{l_c^2}\delta \end{bmatrix}$$

$$\begin{bmatrix} M_{1_2} = M_{-2}^2 \\ M_{2_2} = M_{-2}^3 \end{bmatrix} = \frac{EI_g}{l_g} \begin{bmatrix} 4\theta^2 + 2\theta^3 \\ 2\theta^2 + 4\theta^3 \end{bmatrix} = \frac{EI_c}{l_c} \begin{bmatrix} 4\alpha\theta^2 + 2\alpha\theta^3 \\ 2\alpha\theta^2 + 4\alpha\theta^3 \end{bmatrix}$$

$$\begin{bmatrix} M_{1_3} = M_{-3}^3 \\ V_{1_3} = V_{-3}^3 \end{bmatrix} = \frac{EI_c}{l_c} \begin{bmatrix} s(k_cl_c)\theta^3 - \frac{s(k_cl_c)(1+c(k_cl_c))}{l_c}\delta \\ \frac{s(k_cl_c)(1+c(k_cl_c))}{l_c}\theta^3 - \frac{2s(k_cl_c)(1+c(k_cl_c)) - k_c^2 l_c^2}{l_c^2}\delta \end{bmatrix}$$

$$\begin{aligned} (s(k_cl_c) + 4\alpha)\theta^2 + 2\alpha\theta^3 - \frac{s(k_cl_c)(1+c(k_cl_c))}{l_c}\delta &= 0 \quad (444) \\ 2\alpha\theta^2 + (s(k_cl_c) + 4\alpha)\theta^3 - \frac{s(k_cl_c)(1+c(k_cl_c))}{l_c}\delta &= 0 \\ -\frac{s(k_cl_c)(1+c(k_cl_c))}{l_c}\theta^2 - \frac{s(k_cl_c)(1+c(k_cl_c))}{l_c}\theta^3 + 2\frac{2s(k_cl_c)(1+c(k_cl_c)) - k_c^2 l_c^2}{l_c^2}\delta &= 0 \end{aligned}$$

where $\alpha = \frac{EI_g}{l_g} * \frac{l_c}{EI_c} = \frac{I_g}{I_c} * \frac{l_c}{l_g}$. (Attention $s(k_cl_c)$ and $c(k_cl_c)$ are functions of kl !!!!!)

In matricial format the system (443) is re-written as:

$$\begin{bmatrix} s(k_cl_c) + 4\alpha & 2\alpha & -\frac{s(k_cl_c)(1+c(k_cl_c))}{l_c} \\ 2\alpha & s(k_cl_c) + 4\alpha & -\frac{s(k_cl_c)(1+c(k_cl_c))}{l_c} \\ -\frac{s(k_cl_c)(1+c(k_cl_c))}{l_c} & -\frac{s(k_cl_c)(1+c(k_cl_c))}{l_c} & 2\frac{2s(k_cl_c)(1+c(k_cl_c)) - k_c^2 l_c^2}{l_c^2} \end{bmatrix} \begin{bmatrix} \theta^2 \\ \theta^3 \\ \delta \end{bmatrix} = \begin{bmatrix} 0 \\ 0 \\ 0 \end{bmatrix} \quad (445)$$

The system (444) is homogeneous and to have non-trivial solutions, different of the trivial solution is required that the determinant of the coefficients to be zero:

$$\begin{vmatrix} s(k_cl_c) + 4\alpha & 2\alpha & -\frac{s(k_cl_c)(1+c(k_cl_c))}{l_c} \\ 2\alpha & s(k_cl_c) + 4\alpha & -\frac{s(k_cl_c)(1+c(k_cl_c))}{l_c} \\ -\frac{s(k_cl_c)(1+c(k_cl_c))}{l_c} & -\frac{s(k_cl_c)(1+c(k_cl_c))}{l_c} & 2\frac{2s(k_cl_c)(1+c(k_cl_c)) - k_c^2 l_c^2}{l_c^2} \end{vmatrix} = 0 \quad (446)$$

Expanding the determinant located in the left side of equation (446) the following characteristic equation results:

$$[1-c(k_cl_c)^2]s(k_cl_c)^3+[12\alpha c(k_cl_c)-2\alpha c(k_cl_c)^2-y^2+14\alpha]s(k_cl_c)^2+8[3\alpha^2+3c(k_cl_c)\alpha^2-y^2\alpha]s(k_cl_c)-12y^2\alpha^2=0 \quad (447)$$

The calculation of finding the exact solution of kl function from the equations (447) is an impossibility and consequently, the *graphical implicit method* is employed again. Substituting the expression of the functions $s(k_cl_c)$ and $c(k_cl_c)$ into equations (447) the equations of the following plane curve is obtained:

$$\begin{aligned} & \left(1 - \left(\frac{y - \sin y}{\sin y - y \cos y}\right)^2\right) \left(\frac{y(\sin y - y \cos y)}{2 - 2 \cos y - y \sin y}\right)^3 + \\ & + \left(12x \left(\frac{y - \sin y}{\sin y - y \cos y}\right) - 2x \left(\frac{y - \sin y}{\sin y - y \cos y}\right)^2 - y^2 + 14x\right) \left(\frac{y(\sin y - y \cos y)}{2 - 2 \cos y - y \sin y}\right)^2 - \\ & + \left(24x^2 + 24 \left(\frac{y - \sin y}{\sin y - y \cos y}\right) x^2 - 8xy^2\right) \left(\frac{y(\sin y - y \cos y)}{2 - 2 \cos y - y \sin y}\right) + \\ & - 12x^2y^2 = 0 \end{aligned} \quad (448)$$

where $y = k_cl_c$ and $x = \alpha$.

The curve representing the functional relation between kl function α is illustrated in Figure 17.60.

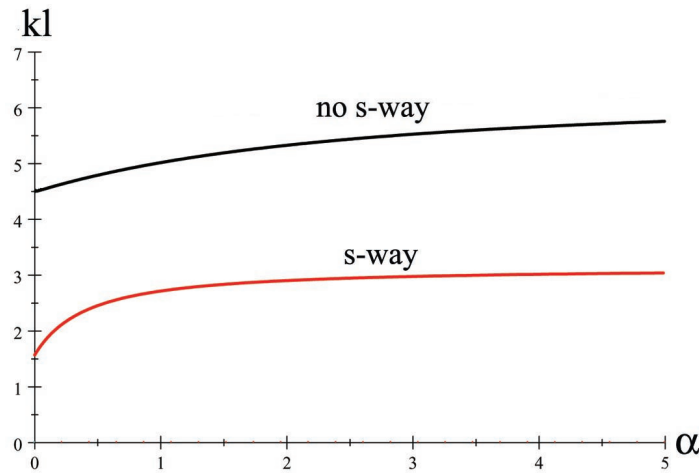


Figure 17.60 Functional Relation $kl - \alpha$

Some of the results plotted on Figure 17.60 are also numerically obtained by solving equation (448) for different values. They are presented in the following table:

$\alpha = l_2/l_1$	kl	$l_b/l = \pi/kl$	$P/P_E = (k_c l_c/\pi)^2$
0.0	1.5708	2.00000	0.25000
1.0	2.7165	1.15649	0.74768
2.0	2.9041	1.08178	0.85452
3.0	2.9777	1.05504	0.89838
4.0	3.0166	1.04143	0.92202
5.0	3.0406	1.03321	0.93675
100.0	3.1364	1.00166	0.99669

(449)

Remark 77 Analyzing the functional relation $\alpha - kl$ illustrated by the graph shown in Figure 17.60 it can be concluded:

(a) the buckling length l_b and minimum critical load P_{cr} of the columns varies $1 \leq l_b \leq 2$ and $0.25P_E \leq P_{cr} \leq P_E$ respectively;

(b) for $I_g \rightarrow 0$ the parameter $\alpha = \frac{I_g}{I_c} * \frac{l_c}{l_g} \rightarrow 0$ and $kl \rightarrow 1.57$, value corresponding to a buckling length $l_b = 2 * l$ and a minimum critical load $P_{cr} = 0.25P_E$;

(c) for $I_g \rightarrow \infty$ the parameter $\alpha = \frac{I_g}{I_c} * \frac{l_c}{l_g} \rightarrow \infty$ and $kl \rightarrow 3.14$, value corresponding to a buckling length $l_b = l$ and a minimum critical load $P_{cr} = P_E$ where $P_E = \frac{\pi^2 EI_c}{l_c}$;

(d) the buckling is an antisymmetric buckling (sway) This conclusion can be easily substantiated if considering a value for the lateral displacement $\delta \neq 0$ the system (445) reduces to a symmetrical system with two unknowns θ^2 and θ^3 and equal free terms proportional to δ . Solving this system for any kl results that $\theta^2 = \theta^3$

(e) a symmetric buckling (no-sway) required $\delta = 0$, a condition requiring the existence of the lateral fixity blockage of the frame and consequently the stability condition (445) reduces to:

$$\begin{bmatrix} s(k_c l_c) + 4\alpha & 2\alpha \\ 2\alpha & s(k_c l_c) + 4\alpha \end{bmatrix} \begin{bmatrix} \theta^2 \\ \theta^3 \end{bmatrix} = \begin{bmatrix} 0 \\ 0 \end{bmatrix} \quad (450)$$

Then, the corresponding characteristic equation is:

$$(s(k_c l_c) + 4\alpha)^2 - 4\alpha^2 = 0 \quad (451)$$

Proceeding in a similar manner as for the antisymmetric buckling the implicit curve is superimposed plotted on Figure 17.58. A table containing representative results is presented below:

$\alpha = l_2/l_1$	kl	$l_b/l = \pi/kl$	$P/P_E = (k_c l_c/\pi)^2$
0.0	4.4934	0.6992	2.0455
1.0	5.1330	0.6120	2.6699
2.0	5.4361	0.5779	2.9943
3.0	5.6134	0.5596	3.1933
4.0	5.7297	0.5483	3.3263
5.0	5.8118	0.5406	3.4217
100.0	6.2523	0.5025	3.9603

(452)

It can be concluded that for no-sway case, the symmetric buckling, the buckling length l_b and minimum critical load P_{cr} of the columns varies as:

$$0.5 \leq l_b \leq 0.7 \text{ and } 2P_E \leq P_{cr} \leq 4P_E, \text{ respectively;}$$

1.7 Inelastic Buckling of the Ideal Column

The inelastic buckling of a column is also exemplified by investigating the Euler ideal column which is characterized by hinged-pinned end constraints. The behavior of the ideal columns subjected to an compressive force P is characterized by the value of its slenderness $\lambda = \frac{l}{r_z}$ in three categories:

- (a) if $\lambda_0 \leq \lambda = \frac{l}{r_z} \leq 200$, where $\lambda_0 = \pi * \sqrt{\frac{E}{\sigma_y^0}}$ the column is called *long column* and its buckling behavior is governed by the Euler formulae (35), (39) and (40) previously established. For this type of buckling the material is constrained to the elastic range;
- (b) if $20 < \lambda = \frac{l}{r_z} \leq \lambda_0$ the column is called *intermediate column* and represents the material behavior between the on-set yielding stress σ_y^0 and the ultimate stress σ_u ;
- (c) if $0 < \lambda = \frac{l}{r_z} \leq 20$ the column is called *short column* and the buckling does not occurs. The material loses its capacity in pure compression.

The first and the last categories, the *long and short column*, were in-depth analyzed, but the buckling phenomenon related to the *intermediate column* needs additional consideration. This type of buckling is called *inelastic buckling*. The behavior of the ideal Euler column subjected to centric compressive force is illustrated in Figure 17.61.

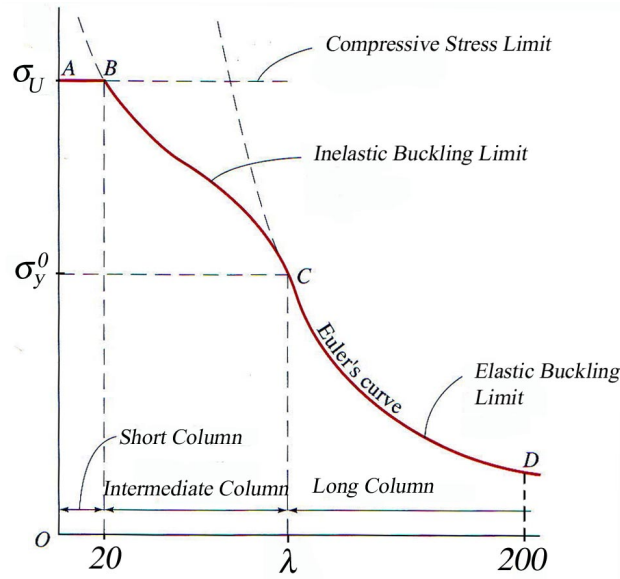


Figure 17.61 Buckling Behavior of a Column

It is assumed that when the column is just on the verge of buckling the average normal compressive stress σ_x on its cross-section reaches, as illustrated in Figure 17.62, a value σ_x^B greater than the on-set yielding value σ_y^0 :

$$\sigma_x = \sigma_x^B = \frac{P}{A} > \sigma_y^0 \quad (453)$$

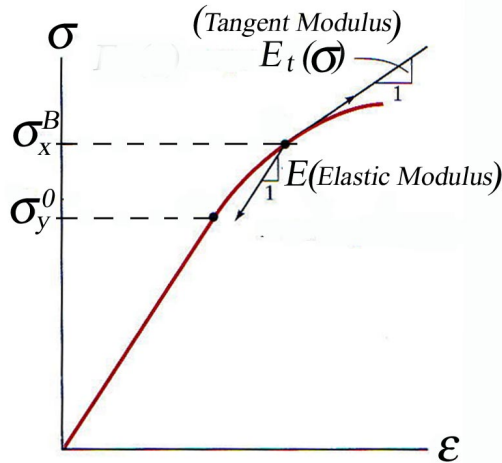


Figure 17.62 Compressive Stress-Strain Diagram

There are three principal theories predicting the value of σ_x^B at which the column will buckle inelastically: (a) the *Tangent Modulus Theory*, (b) the *Reduced Modulus Theory* and (c) *Shanley Theory*.

1.7.1 The Tangent Modulus Theory

In 1889, two scientists, Considere and Engeser, independently had suggested that the column strength in the inelastic range might be obtained simply by substituting E_t , the *tangent modulus*, instead of E in the Euler formula. *This conclusion is based on the assumption that the column retains its linear equilibrium configuration until the compressive force reaches its critical value ($P = P_{cr}$) and only after that the lateral flexion of the column, the curved equilibrium configuration, takes place without any change in the magnitude of the compressive force P .* This assumption implies that the member is in a *neutral equilibrium*. Under this assumption the theoretical development is conducted in a similar manner with that used for the investigation of the previously treated elastic buckling of the Euler's ideal column. The equation (18) $M_z(x) = -P * v(x)$ remains valid, but in the equation (19)

the elastic modulus E is replaced by the tangent modulus E_t . The tangent modulus, as illustrated in Figure 17.62, represents the slope of the compressive stress-strain curve at σ_x^B . The new differential equation, valid only for the case of small deformations, is:

$$\frac{dv(x)^2}{dx^2} = \frac{M_z(x)}{E_t * I_z} \quad (454)$$

where I_z is the moment of inertia.

Combining equations (18) and (454) the following *second-order homogeneous differential equation* is obtained:

$$E_t * I_z * v(x)'' + P * v(x) = 0 \quad (455)$$

The equation (455) is mathematically identical to equation (20) and consequently, the critical load is written as:

$$P_{cr}^t = \frac{\pi^2 * E_t(\sigma_x) * I_z}{l^2} = \alpha(\sigma_x) * P_{cr}^E \quad (456)$$

and

$$\sigma_{cr}^t(\sigma, \lambda) = \frac{\pi^2 * E_t(\sigma_x)}{\lambda^2} = \alpha(\sigma_x) * \sigma_{cr}^E \quad (457)$$

where $\alpha(\sigma_x) = \frac{E_t(\sigma_x)}{E}$ and $E_t(\sigma_x) = \frac{d\sigma}{d\epsilon}(\sigma = \sigma_x^B)$.

Remark 78 (a) *The calculation of P_{cr} is conducted using an iterative procedure.*

(b) *The Tangent-Modulus Theory, as shown in equations (456) and (457) considers in the calculation of the critical load P_{cr} only an unique value, the tangent modulus $E_t(\sigma_x)$, fact which conducts to some difference when the comparison with laboratory tests is made;*

(c) *The experimental results indicate a slightly greater value for the critical load than the value P_{cr}^t calculated by the Tangent Modulus Theory. This fact is explained by the error introduced by the assumption that is no variation in the value of the axial load during the configurations change.*

1.7.2 The Reduced Modulus Theory

In 1895, Engeser proceeded to develop a new general formula for inelastic buckling of the columns by introducing the concept of the *reduced modulus* E_r . He stated that the reduced modulus E_r depends not only on the values of E_t and E_c , but also on the shape of the column cross-section. Later, in 1910, Theodor von Karman, explicitly derived the expressions of the reduced modulus pertinent to rectangular and idealized H (the web is considered of zero area) cross-sections.

The reduced modulus E_r , also called *the double modulus*, is calculated considering as the starting point two important observations:

(a) *When the critical load P_{cr} is attained, the column changes its original linear configuration with a curved configuration. The result of the change in the column geometrical configuration is the fact that the stress condition also changes from the pure compression stress distribution $\sigma_x = -\sigma_{cr} > \sigma_y^0$ to a more complicated stress distribution $\sigma_x = -\sigma_{cr} \pm \sigma_x^M > \sigma_y^0$ induced by newly created eccentric compression. It can be noticed the change in the normal stress distribution σ_x from $\sigma_x = -\sigma_x^P$ to $\sigma_x = -\sigma_x^P \pm \sigma_x^M$, when $P = P_{cr}$, correspond to the two possible equilibrium configurations, the straight or curved equilibrium configuration configurations. Because the axial compressive $P = P_{cr}$ remain constant the *equilibrium is neutral* ;*

(b) *The cross-section of the column subjected to eccentric compression is divided into two areas characterized by different stress behavior due to the fact that the material is in the plastic range. The zone where $\sigma_x = -\sigma_{cr} - \sigma_x^M > -\sigma_{cr}$ a plastic loading takes place and consequently, the deformation is controlled by the tangent modulus $E_t(\sigma_x)$, while in the zone where the stress is $\sigma_x = -\sigma_{cr} + \sigma_x^M < -\sigma_{cr}$ the material suffers a plastic unloading and the deformation is controlled by modulus of elasticity E . In the case under scrutiny, the Euler ideal column, following the physical deformation of the column, the loading plastic zone is always located in the proximity of the axial compressive force P , on the inside face of the deformed member, while the unloading plastic zone is located on the opposite side, on the outside face of the member.*

Considering that the cross-section of the column has an axis of symmetry, axis y_c , and consequently, the buckling manifests in the plane of this axis, the stress distribution on the current column cross-section is illustrated in Figure 17.63.

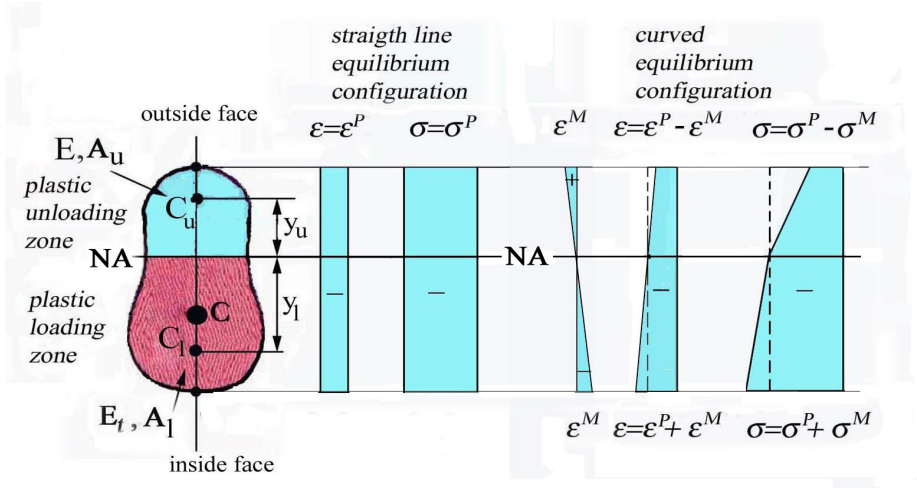


Figure 17.63 Reduce Modulus Theory

Remark 79 (a) The change in the stress distribution when the curved equilibrium configuration is considered is due entirely to the appearance on the column cross-section of the bending moment $M = -P * v$, while the compressive axial force P remains $P = P_{cr}$ constant. The equilibrium is neutral.

(b) The compression is treated as an initial condition and only the bending produced by the buckling is of interest.

The existence of two material behavior zones resembles the bending theory of the nonhomogeneous beam developed in Lecture 11. Consequently, some of the previously obtained results, the equations (11.97) and (11.101), are used in this section by accommodating the notation to the existing situation. It has to be noticed that in the studied case the position of the neutral axis NA also represents the border line between the two areas, A_u and A_l , with different material behavior.

The position of the neutral axis and the equivalent rigidity are obtained from the following equations:

$$E_t * S_z^{A_l} + E * S_z^{A_u} = 0 \quad (458)$$

and

$$y_u + y_l = f(h) \quad (459)$$

where A_u and A_l are the areas of the unloading and loading zones, respectively. The distances $y_u > 0$ and $y_l > 0$ are the distances from the centroids of the two areas measured from the neutral axis. The $f(h)$ is a function of the cross-section height h .

Using the equations (458) and (459) the unknown position of the NA is calculated as fraction of the cross-section height h .

The equivalent *weighted flexural rigidity* K_{eqv} is then obtained as:

$$K_{eqv} = E_t * I_z^{A_l} + E * I_z^{A_u} = E_r * I_z \quad (460)$$

where the moments of inertia $I_z^{A_l}$ and $I_z^{A_u}$ are calculated relatively to the position of the neutral axis (NA).

The reduced modulus E_r is expressed as:

$$E_r = \frac{E_t * I_z^{A_l} + E * I_z^{A_u}}{I_z} \quad (461)$$

where I_z is the moment of inertia of the *entire cross-section* calculated for the centroidal axis Z_c .

Accepting the small deformation assumption, the differential equation (11.102) is then re-written as:

$$\frac{dv(x)^2}{dx^2} = \frac{1}{\rho(x)} = \frac{M_z(x)}{K_{eqv}(x)} = \frac{M_z(x)}{E_r * I_z} \quad (462)$$

Combining equation (462) and (18) a *second order differential equation*, similar with that employed in the investigation of the elastic buckling of the Euler ideal column, is obtained:

$$E_r * I_z * v(x)'' + P * v(x) = 0 \quad (463)$$

Using the mathematical analogy between the equations (462) and (20), the critical load is calculated as:

$$P_{cr}^r = \frac{\pi^2 * E_r * I_z}{l^2} \quad (464)$$

and

$$\sigma_{cr}^r(\lambda) = \frac{\pi^2 * E_r}{\lambda^2} \quad (465)$$

The reduced modulus pertinent to the *rectangular cross-section*, shown in Figure 17.25, is obtained following the above described formulation.

Figure 17.24

The formulae (458) and (459) are re-written as:

$$E * b * (2 * y_u) * y_u - E_t * b * (2 * y_l) * y_l = 0 \quad (466)$$

$$2 * y_u + 2 * y_l = h \quad (467)$$

Solving equations (466) and (467) the distances y_u and y_l and implicitly position of the neutral axis NA are calculated:

$$\begin{aligned} y_u &= \frac{1}{2} h \frac{\sqrt{E_t}}{(\sqrt{E_t} + \sqrt{E})} \\ y_l &= \frac{1}{2} h \frac{\sqrt{E}}{(\sqrt{E_t} + \sqrt{E})} \end{aligned} \quad (468)$$

Substituting the results (468) into equation (461) the reduced modulus E_r pertinent to a rectangular cross-section is obtained:

$$\begin{aligned} E_r &= \frac{E_t * I_z^{A_l} + E * I_z^{A_u}}{I_z} = \frac{E_t * \frac{b * (2 * y_l)^3}{3} + E * \frac{b * (2 * y_u)^3}{3}}{\frac{b * h^3}{12}} \\ &= 4 \frac{E * E_t}{(\sqrt{E} + \sqrt{E_t})^2} \end{aligned} \quad (469)$$

If a ration $\alpha = \frac{E_t}{E}$ is defined then, the equations (468) and (469) are recasted as:

$$\begin{aligned} y_u &= \frac{1}{2}h \frac{\sqrt{\alpha}}{(1 + \sqrt{\alpha})} \\ y_l &= \frac{1}{2}h \frac{1}{(1 + \sqrt{\alpha})} \end{aligned} \quad (470)$$

and

$$E_r = 4 * E * \frac{\alpha}{(1 + \sqrt{\alpha})^2} \quad (471)$$

The ratio $\frac{E_r}{E}$ is plotted in Figure 17.64

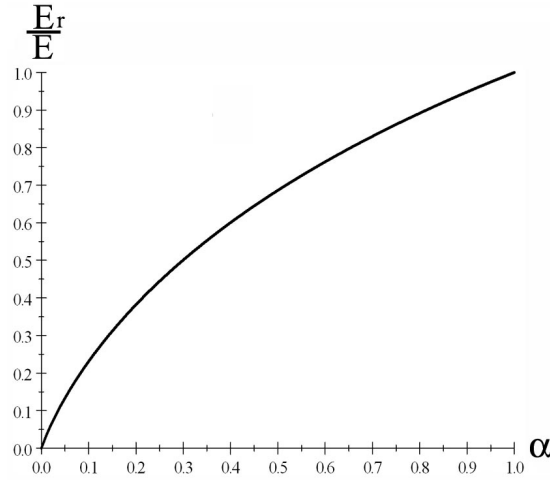


Figure 17.64 Variation of E_r/E

Remark 80 (a) The critical load P_{cr}^r is obtained from an iterative process;

(b) The value of the reduced modulus E_r is difficult to calculate and depends on the shapes of the stress-strain curve and the cross-section, respectively;

(c) The usage of this theory implies that the bending must be present on the cross-section for the change in stress distribution to take place and consequently, a reduced modulus E_r to be possible to manifest. The experimental results confirm that the bending moment appears only after change in configurations, from the straight line to curved, and therefore, in reality, the axial load P never reaches the value of the calculated critical load P_{cr}^r . From laboratory testing always critical loads inferior to the calculated P_{cr}^r are obtained.

1.7.3 The Shanley Theory

In 1946, the American professor F.R. Shanley, in an one-page paper, explained the shortcomings of the previously exposed theories used in the evaluation of the inelastic buckling of columns and proposed a new theoretical approach. This approach, known in the technical literature, as the *Shanley' Theory*, is able to solve the theoretical nonconcordances of the *Tangent Modulus* and *Reduced Modulus Theories*. He follows five months later with a second paper containing additional theoretical explanations pertinent of newly proposed theory and experimental test results in support of the theoretical findings.

The *Shanley Theory* departs from the previously exposed theories of the inelastic buckling, the *Tangent Modulus Theory* and *Reduced Modulus Theory*, by recognizing the physical impossibility of the analogy between the elastic (elastic range) and inelastic (plastic range) buckling of a column. *In the case of the elastic buckling, the Euler approach, the critical load P_{cr} is reached with the column in a neutral equilibrium, by considering that the change in the equilibrium configurations does not produced any change in the magnitude of the axial loading P . If this assumption is rejected and the increase of the axial load P during the change in the equilibrium configurations is allowed, then, the modification of the normal stress on the cross-section, as shown in Figure 17.64, is less dramatic due to the increase of normal stress σ_x^P induced by the axial force P . Accordingly to Shanley Theory, when the load P reaches the the load corresponding to P_{cr}^t the change in the equilibrium configuration (the bending) starts and the load P continues to increased until the new equilibrium is obtained.*

Remark 81 (a) *The Shanley Theory assumption invalidates the main assumption used in the elastic buckling calculation that the equilibrium is neutral at the bifurcation point;*

(b) *The values of the maximum and minimum normal stresses, illustrated in Figure 17.64, are increased and, respectively decreased by comparison with the similar situation expressed by the Reduced Modulus Theory, due to the increase of the axial force P from P_{cr}^t to P_{cr}^r . Consequently, the a new reduced modulus E_s is calculated. Its value is bordered by the previously calculated value of E_t and E_r , respectively;*

$$E_t \leq E_s \leq E_r \quad (472)$$

(c) *The differential equation (54) repeatedly employed in the elastic evaluation of the ideal column buckling is forth order ordinary differential equation with constant coefficients (P is constant at the bifurcation). In the case of the inelastic buckling of a column, accordingly to Shanley Theory, this equation becomes nonlinear in nature and a functional relation between the axial load P and lateral displacement $v(x)$ is established. It is obvious that an iterative procedure is required to determine the inelastic critical load P_{cr}^s .*

$$P_{cr}^t \leq P_{cr}^s \leq P_{cr}^r \quad (473)$$

An informative illustration of the comparison between the critical load obtained for the elastic and inelastic behavior consideration is shown in Figure 17.65.

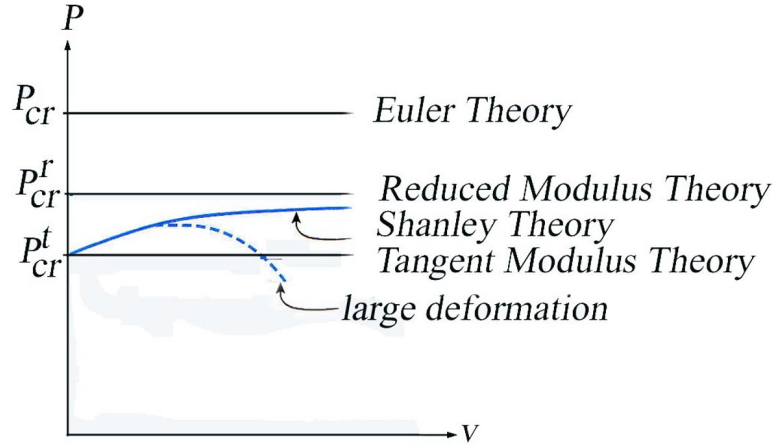


Figure 17.65 Load-Deflection Diagram for Elastic and Inelastic Behavior

The curves shown in Figure 17.65 are valid only for the case of "small deformations". In reality, if the lateral deformation increases the "small deformation" assumption has to be replaced and consequently, the *exact formula of the curvature* has to be employed. The results obtained in that case are schematically shown with dashed line, indicating a reduction of the critical load value with the increase in the lateral displacement.

Remark 82 (a) The critical load P_{cr}^s calculated using Shanley Theory is bounded, under the assumption of "small deformations", by critical loads, P_{cr}^t and P_{cr}^r , calculated employing the Tangent Modulus Theory and Reduced modulus Theory, respectively.

$$P_{cr}^t \leq P_{cr}^s \leq P_{cr}^r \quad (474)$$

(b) Due to the complexity of the calculation involved in the determination of the inelastic critical load P_{cr}^s using Shanley Theory and from the observation that under the assumption of "small deformations" this critical load is not considerably greater than the critical load calculated using the Tangent Modulus P_{cr}^t , it is reasonable to accept the later as the practical critical load.

The theoretical results of the *Shanley Theory* were intensely verified by numerous experiments. Today, this theory is universally accepted and employed by the majority of the structural steel codes.

1.8 Practical Evaluation of the Columns

1.8.1 Summary of Ideal Column Theoretical Cases

The theoretical cases of an ideal column characterized by different boundary conditions, in-depth treated in the previous sections, are summarized in the Table 1. These are the most commonly boundary conditions encountered in the structural practice and are

used by the structural engineers in judging the buckling characteristics of the designed columns. Table 1 contains the buckling coefficient α which is used in the estimation of the buckling length $l_f = \alpha * l$.


Buckling Modes of an Ideal Column	(a)	(b)	(c)	(d)	(e)	(f)
Buckling Coefficient α	0.5	0.7	1.0	2.0	1.0	2.0
Legend	 Fixed Rotation and Lateral Translation Free Rotation and Fixed Lateral Translation Fixed Rotation and Free Lateral Translation Free Rotation and Lateral Translation					

Table 1 - Theoretical Buckling Coefficients